Asymptotic models for surface waves in coated elastic solids

Ali Mohammed A Mubaraki

Submitted in partial fulfilment of the requirements of the degree of Doctor of Philosophy

Keele University
School of Computing and Mathematics

Keele UNIVERSITY

June 2021

Declaration of Authorship

I certify that this thesis submitted for the degree of Doctor of Philosophy is the result of my own research, except where otherwise acknowledged, and that this thesis (or any part of the same) has not been submitted for a higher degree to any other university or institution.

Signed: Ali Mubuaraki

Date: June 8, 2021

Presentations

- The asymptotic model for surface elastic waves on an isotropic half-plane coated by a thin orthotropic layer, the British Applied Mathematics Colloquium, the School of Mathematics and Statistics, St Andrews University, March 2018.

- Asymptotic theory for surface wave on coated solid, the European-Latin-American Conference of Theoretical and Applied Mechanics (ELACTAM-2019), University of Havana, February 2019.

- Explicit model for surface waves on a multi-layered elastic half-space, the British Applied Mathematics Colloquium, the School of Mathematics and Statistics, University of Bath, May 2019.

- Explicit model for surface waves on an elastic half-space coated by a thin vertically inhomogeneous layer, Dynamical Systems -Theory and Applications Conference of (DST-2019), University of Lodz, Poland, December 2019.

- Moving load on an elastic half-space coated with a thin vertically inhomogeneous layer, the European conference (EURODYN-2020) in Athens, Greece, November 2020.

Acknowledgements

First and foremost, I thank God for awarding me all the help, ability, volition and determination to complete this thesis.

I extend my personal gratitude to my supervisors Dr Danila Prikazchikov and Professor Julius Kaplunov, for their overall guidance as they consistently contributed their time and ideas towards my progress at achieving this project. I am genuinely grateful; your support has been the most profitable experience for me. Your mentoring and encouragement have been a considerable source of strength to me.

I am also grateful to Dr Saad Althobaiti from Taif University in Saudi Arabia and Dr Vladimir Bratov from Saint-Petersburg State University in Russia for fruitful discussions and sharing ideas.

I would also like to acknowledge the aid of the Royal Embassy of Saudi Arabia Cultural Bureau in London and Taif university on granting me the opportunity to continue for achieving this work.

I am truly grateful to my family, friends and colleagues for their continuous prayers and encouragement throughout my research.

May the Almighty God richly bless all of you.

Abstract

This thesis deals with surface wave propagation in elastic solids. It develops further the methodology of asymptotic hyperbolic-elliptic models for the surface elastic waves, aiming at two main areas, namely, accounting for the effects of a thin coating layer, as well as incorporating the influence of gravity.

The derived model for surface waves on a coated elastic half-space subject to prescribed surface stresses reflects the physical nature of elastic surface waves, for which the decay over the interior is described by a "pseudo-static" elliptic equation, whereas wave propagation along the boundary is governed by a singularly perturbed hyperbolic equation, with the perturbation in the form of a pseudo-differential operator. This perturbative term originates from the effect of a thin coating layer, which is modelled in terms of effective boundary conditions, derived within the long-wave limit approximation of the corresponding problem in linear elasticity.

Various types of coatings are studied in this thesis, including anisotropic and vertically inhomogeneous thin layers. The analysis reveals a qualitatively similar hyperbolic equation, singularly perturbed by a pseudo-differential operator, with the appropriate coefficient incorporating the overall effect of the material properties of the coating and the substrate.

The established methodology is then illustrated for approximate treatment of several rather technical problems in elastodynamics, in particular, analysis of moving loads on a coated half-plane. The implementation of the hyperbolic-elliptic model allows a

natural classification of scenarios and elegant approximations of the exact solution, with clear physical interpretation of the associated numerical illustrations of near-surface dynamics for several types of vertical inhomogeneity.

Finally, the effect of gravity is embedded into the developed methodology of hyperbolic-elliptic asymptotic models for surface waves. As a result, the wave equation on the surface is regularly perturbed by a pseudo-differential operator, accounting for the effect of the gravitational field.

Contents

List of Figures

List of Tables

Introduction

Coated and layered structures have numerous applications in advanced engineering and technology. In particular, coatings are predominantly utilised to protect the material surface from corrosion caused by chemical and physical exterior agents, improve fatigue and fire resistance, wettability, adhesion, etc., see e.g. Bose [2017], Chattopadhyay and Raju [2007], Datta [1993], Padture et al. [2002], Pawlowski [2008] and Veprek and Veprek-Heijman [2008]. We also mention important biological applications, for example, implantation of biomaterials in human body to rehabilitate biological and mechanical functions for raising the quality of life. In this case, coatings are widely used to reduce the mechanical loads on the implant surface, see e.g. Hauert [2003], Li et al. [2014] and Tiainen [2001]. Also, we refer to applications in nanoindentation tests, used to determine the mechanical properties of materials, depth-sensing, etc. see e.g. Argatov and Mishuris [2018], Argatov and Sabina [2016] and Borodich [2014].

Coated solids are particular types of layered structures, widely used in civil, aerospace and marine engineering, see. e.g. Brigatti and Mottana [2011]. Manufacturing of layered structures is generally performed through combining/blending two or more materials. In particular, the materials with high-contrasting properties (for instance,

density, geometrical parameters and stiffness) are often connected to create unique materials, see e.g. Aßmus et al. [2016], Kaplunov et al. [2021]. Therefore, by selectively picking the convenient combination of materials, the desirable properties of layered structures can be accomplished, providing a strong motivation for studying the mechanics of layered elastic solids.

One type of important dynamic problems for layered elastic solids is related to wave propagation in such structures. This area has received considerable attention in the last few decades. We refer in particular, to studies of harmonic wave propagation in an elastic sandwich plate, see e.g. Berdichevsky [2010], Kaplunov et al. [2017], Lee and Chang [1979], Prikazchikova et al. [2020], Rogerson and Sandiford [2000], Ryazantseva and Antonov [2012], Morozov et al. [2020], as well as related studies of composite materials in engineering structures, see e.g. Mikhasev and Altenbach [2019], Reddy [2003] and references therein.

Among elastic waves, considerable attention has been drawn to surface waves. They have a rich history, being studied since the late 19^{th} century, starting from the classical contribution by Lord Rayleigh [1885], giving the name to a wave propagating along the surface of an elastic half-space and decaying over the interior, presently known as the Rayleigh wave. In addition to conventional applications of surface waves in seismology, e.g. Takeuchi and Saito [1972], there are also more recent applications, within the context of telecommunications, acoustics and material science, see e.g. Adams et al. [2007], Campbell [1998] and Royer and Dieulesaint [1999]. Surface waves are also used in non-destructive evaluation, in order to detect the mechanical and structural properties of the material under test, such as the presence of cracking,

see e.g. Cho [2003] and Hevin et al. [1998]. In addition, prominent applications in engineering and technology are noted, embracing on particular areas of seismic protection, increasing the quality of highways and railway transport, etc., see e.g. Krylov [2001], Palermo et al. [2016]. Analysis of surface wave propagation in an elastic half-space is among the most exciting research areas in linear elastodynamics. Recently, a lot of interest has been on the so-called "seismic meta-surfaces", see e.g. Colombi et al. [2017], Colquitt et al. [2017], De Ponti et al. [2020], Wootton et al. [2019], as well as attempts of cloaking for elastic waves Quadrelli et al. [2021], Wootton [2020].

The issues of the existence and uniqueness of surface elastic waves were addressed in Barnett and Lothe [1974], Chadwick [1976a], Kamotskii and Kiselev [2009], Lothe and Barnett [1976]. There has been a lot of contributions, studying surface wave propagation in anisotropic solids, see e.g. Chadwick and Smith [1977], Destrade [2001a,b] and Fu and Mielke [2002] to name a few. We also mention contributions focused on surface waves in pre-stressed media, see e.g. Chadwick and Jarvis [1979], Dowaikh and Ogden [1990], Prikazchikov and Rogerson [2004], as well as incorporating the effect of gravity, starting from the original work Bromwich [1898], followed by influential results of Biot [1940, 1965], and a number of more recent contributions, see Nath and Sengupta [1999], Sethi et al. [2012], Sharma [2020], Vinh [2009], Vinh and Seriani [2009]. Surface waves in vertically inhomogeneous solids were studied in Alenitsyn [1967], Argatov and Iantchenko [2019] and Balogun and Achenbach [2012].

The problem of surface wave propagation in coated elastic solids has received substantial attention of researchers, see e.g. Achenbach and Keshava [1967], Glushkov

et al. [2012], Zhou et al. [2017], to name a few. Often, the asymptotic modelling is used to simplify the problem, see e.g. Cai and Fu [1999], Dai et al. [2010], Shuvalov and Every [2008]. Related results for the Rayleigh-type dispersive bending edge wave on a stiffened plate have been recently reported in Alzaidi et al. [2019b,a]. Indeed, the existence of a thin coating layer naturally motivates an asymptotic approach, relying on a small geometric parameter, namely the ratio of the thickness of the coating layer to a typical wavelength.

The asymptotic methods in elasticity, were rapidly developing for static problems for thin plates and shells see Goldenveizer [1976] and references therein. Asymptotic methods have proved to be a powerful tool for justification of *adhoc* engineering theories Goldenveizer [1966], Goldenveizer et al. [1993]. The method of direct asymptotic integration, developed by A.L. Goldenveizer, see also Goldenveizer [1980], has been extensively applied in dynamic problems, associated with high-frequency approximations, in both short and long-wave ranges, see Kaplunov et al. [1998, 2016a]. The approach has been extended to anisotropic and pre-stressed solids Kaplunov et al. [2000, 2002a,b], Nolde et al. [2004], Pichugin and Rogerson [2002], Rogerson and Prikazchikova [2009]. Various boundary conditions have been treated Erbaş et al. [2011], Kaplunov [1995], Kaplunov and Nolde [2002], Lashhab et al. [2015]. We also mention delicate treatments of initial value problems, see Kaplunov et al. [2006a], Nolde [2007]. Recent results also include treatment of high contrast Kaplunov et al. [2018, 2019a], nonlocally elastic plates Chebakov et al. [2017], as well high-order theory for rectangular beams Nolde et al. [2018] and refined dynamic equations for a thin elastic annulus Ege et al. [2021].

A popular approach to modelling surface waves propagating on an elastic half-space, covered with a thin coating layer, is related to the so-called effective boundary conditions on the interface between the layer and the half-space, essentially replacing the mechanical effect of the coating. These conditions have appeared first in Tiersten [1969], as a result of *adhoc* approach. The results were later criticised in Bövik [1996], suggesting a refined formulation with the approach extended in Niklasson et al. [2000] for anisotropic coating. However, the results of Bövik [1996] were demonstrated to be erroneous in Dai et al. [2010], and the consistency of original conditions formulated by Tiersten [1969] was confirmed, also matching the result of the two-term expansion of the exact dispersion relation within the long-wave limit which was obtained by Shuvalov and Every [2008]. Additionally, the validity of Tiersten [1969] results has been discussed by many other publications e.g. see Godoy et al. [2012], Kaplunov et al. [2019b], Malischewsky and Scherbaum [2004]. We also mention high-order approximations for coating layers developed by Zakharov [2006, 2010].

The method of "effective boundary conditions" has been applied account for anisotropy Pham and Vu [2016], Vinh and Linh [2012], various types of contact scenarios Vinh and Anh [2014], Vinh et al. [2014], as well as for weak inhomogeneity Vinh and Anh [2015]. We also cite a recent contribution of Vinh et al. [2019] focused on the horizontal-to-vertical displacement ratio of surface waves in a layered half-space.

One of the notable achievements in theoretical analysis of surface wave propagation in an isotropic half-space is related to consideration of surface waves of arbitrary profile, relying on the theory of harmonic functions. It has seemingly first appeared as an additional chapter by Sobolev et al. [1937] in translation, however, this contribution was

seemingly unnoticed by the "western" academic community until recently. The same idea appears again in Friedlander [1948], and then has been developed in Chadwick [1976b] for both Rayleigh and Stoneley waves. The approach has been generalised further to 3D formulation in Kiselev and Parker [2010], as well as to anisotropy and pre-stress Achenbach [1998], Parker [2013], Prikazchikov [2013], see also results for surface waves with transverse structure Kiselev [2004, 2015] and Parker and Kiselev [2008].

Most of the above-cited contributions on surface waves are dealing with a homogeneous wave, that is assuming traction-free boundary conditions on the surface, with a few exceptions as seen in Dai et al. [2010] and Şahin [2020], treating the 3D problem for a coated half-space, subject to prescribed vertical and tangential loading, respectively. Indeed, the eigensolutions for the Rayleigh wave can be perturbed and expressed in terms of a single harmonic function Chadwick [1976b], which leads to a hyperbolic-elliptic asymptotic model for Rayleigh waves excited due to specified surface stresses, involving a wave equation for one of the Lamé potentials that govern the propagation of surface disturbances, serving as a boundary condition for the elliptic equation describing the behaviour over the inner of the elastic half-space.

The hyperbolic-elliptic asymptotic model of surface waves on elastic half-space was first derived in Kaplunov and Kossovich [2004] using the symbolic operator approach, followed by further development in Kaplunov et al. [2006b], based on a slow-time perturbation procedure. The approach was developed to incorporate the effects of 3D in Dai et al. [2010], Ege et al. [2015], mixed boundary conditions in Erbaş et al. [2013], anisotropy in Fu et al. [2020] and Nobili and Prikazchikov [2018], and pre-stress in

Khajiyeva et al. [2018] and Prikazchikov [2020]. The methodology has been summarised in Kaplunov and Prikazchikov [2013, 2017]. A parabolic-elliptic formulation for the dispersive Rayleigh-type bending edge wave has been developed in Kaplunov et al. [2016b]. We also mention the explicit second-order model of a wave propagating on the surface of elastic half-space, presented by Wootton et al. [2020]. The asymptotic formulation for transient Love waves was derived by Ahmad et al. [2011]. Recent results also include consideration of surface wave on a coated half-space with a clamped surface Kaplunov et al. [2019c], inspired by a rigorous mathematical analysis in Cherednichenko and Cooper [2015]. We also note the composite wave models for elastic plates and shells, combining both the appropriate long-wave behaviour and short-wave approximation associated with Rayleigh front, see Erbaş et al. [2018, 2019], as well as application of the model for energy harvesting Chaplain et al. [2020].

The elliptic-hyperbolic model provides a simplified framework for evaluating the Rayleigh wave contribution to the overall dynamic response for a general class of surface loading. Since the model extracts the contribution of the Rayleigh wave to the overall dynamic response, it is highly relevant for situations when surface wave dominates, in particular, for the near-resonant regimes of the moving load, see Kaplunov and Prikazchikov [2017]. Analysis of elastodynamics of a half-space subject to action of moving loads have been a subject of numerous investigations, including the classical works of Cole [1958], Gakenheimer and Miklowitz [1969], Freund [1972, 1973], Payton [1967], as well as revisits of Bakker et al. [1999], Georgiadis and Barber [1993], de Hoop [2002]. This is a rather active area, with recent contributions focussed on ground vibrations induced by high-speed trains Cao et al. [2012], Feng

et al. [2017], Sun et al. [2016], response of layered half-space Sun et al. [2019], You et al. [2019, 2020], Zhenning et al. [2016], beams on foundations Froio et al. [2018], Dimitrovová [2019], Zhen et al. [2020], as well as studying effect of porosity Ba and Liang [2017], Wang et al. [2020], Zhang and Liu [2020].

Implementation of the explicit model for the Rayleigh wave in Dai et al. [2010] allowed a number of approximate solutions in terms of elementary functions to problems considered previously, e.g. see Cole [1958], Goldshtein [1965], and also led to a number of novel approximate solutions. The hyperbolic-elliptic model was first utilized for a transient 2D moving load problem in Kaplunov et al. [2010]. Then, the 3D explicit solution of the steady-state problem for a moving force on an elastic half-space, was presented by Kaplunov et al. [2013], and then extended to 3D analysis of the near-resonant regimes of a moving point load on a coated elastic half-space in Erbaş et al. [2017]. A distributed moving load on the surface of a coated half-space was analysed by Şahin and Ege [2017].

This thesis aims at further developments of the methodology of hyperbolic-elliptic models for Rayleigh waves and derivation of asymptotic formulations for surface waves on a coated half-space excited by prescribed surface loadings, as well as for surface waves on a homogeneous half-space with effect of gravity.

The outline of this thesis is as follows.

Chapter 1 introduces the governing relations of a linear elastodynamics, formulated in terms of the Lamé potentials. Next, we present a brief derivation of the Rayleigh wave

equation, as well as the eigensolution of arbitrary profile, followed by the hyperbolic-elliptic model for the Rayleigh wave excited by surface stresses. Then, the propagation of a surface wave on a coated isotropic elastic half-space is considered. First, an exact dispersion relation is derived. Then, an explicit model for a surface wave is constructed, including the previously known formulation for vertical loading Dai et al. [2010], and novel results for tangential loading, involving a pseudo-differential equation on the interface for Lamé potential, having not only the vertical loading in the right hand side, but also a Hilbert transform of the horizontal component.

Chapter 2 extends upon the explicit model for surface wave propagation on a coated elastic half-space presented in Chapter 1 to the case of an orthotropic coated half-space, generalising further result in Nobili and Prikazchikov [2018]. The effect of a thin orthotropic layer can be replaced by the effective boundary conditions, allowing the derivation of the hyperbolic-elliptic formulation for surface wave. The model is formulated in terms of the auxiliary harmonic function, containing an elliptic equation governing the behaviour over the half-space, along with the singularly perturbed wave equation on the interface between the coating and the substrate, involving surface stresses in the right hand side. In the case of reduction to isotropy this harmonic function becomes a derivative of the Lamé elastic potential. Various particular cases of the obtained model are discussed.

In Chapter 3, the propagation of surface waves on an elastic isotropic half-space covered by a thin, vertically inhomogeneous layer is considered. The derived effective boundary conditions for modelling the inhomogeneous coating layer are also specified for a particular case of multi-layered coatings. Explicit analytical results are then

obtained. Next, we analyse the pseudo-differential equation at the interface between the coating and the substrate. A special case related to a possible zero group velocity within the long-wave limit, having an interesting physical interpretation of energy not propagating in the coating layer, is studied. Finally, an illustrative example of impact loading on a coated elastic half-space is considered, demonstrating the smoothing effect of the coating.

In Chapter 4, the near-resonant regimes of moving steadily along the surface of a coated half-space are analysed, for the case of the vertically inhomogeneous coating, see Althobaiti et al. [2020]. Both cases of a point and distributed loads are considered. The analysis begins by adapting the hyperbolic-elliptic formulation for the Rayleigh wave for the prescribed a vertical surface loading, which contain an elliptic equation for the elastic potential over the interior, and a singularly perturbed wave equation on the boundary between the substrate and the layer. In order to incorporate the effect of poles, the method of fictitious absorption is implemented see e.g. Schulenberger and Wilcox [1971], revealing the ranges of problem parameters, for which the radiation of energy from the moving source occurs. Lastly, numerical illustrations of the near-surface dynamics are presented.

Chapter 5 is aimed at generalising an explicit asymptotic model for the Rayleigh wave in order to incorporate the influence of gravity. First, the exact dispersion relation is derived. The problem demonstrates the weak coupling between the Lamé potentials in the equations of motion, hence suggesting a natural small parameter. The approximate secular equation is then obtained, being valid within the short-wave region. Therefore, the Rayleigh-type behaviour is found at leading order, allowing

the derivation of the explicit formulation for surface waves on a coated half-space. The model contains an elliptic equation governing the behaviour within the elastic half-space, with boundary value given on the surface by a perturbed wave equation. Similarly, to the case of a coated half-space the perturbation is in the form of a pseudo-differential operator, however, this is now a regular perturbation, not a singular one, accounting for the effect of the coating.

Finally, the conclusion and bibliography are presented at the end of this thesis.

Chapter 1

Basic equations of linear elastodynamics

This chapter necessitates the narration of some required basic equations for the thesis, in conjunction with original details of their derivations, found in Achenbach [2012], Graff [2012] and Kaplunov and Prikazchikov [2017] collectively with some references which are mentioned below.

First, constitutive relations are introduced in Section 1.1, and then equations of motion for wave propagation in linear elasticity are given in Section 1.2. Elastic Lamé potentials are presented in Section 1.3. Rayleigh waves on an elastic half-space are discussed in Section 1.4, along with the asymptotic hyperbolic-elliptic formulation for the Rayleigh wave induced by prescribed surface loading. Finally, the dispersion relation for a coated elastic half-space is derived in Section 1.5.

1.1 Constitutive relations in elastic solids

In this section, we discuss briefly the relationship between stress (σ) and strain (ε) components for a homogeneous linearly elastic solid. Let us start from the stress-strain curve, taking the form as $\sigma = g(\varepsilon)$ of elastic materials subjected to prescribed uniaxial stress forcing conditions, see Fig. 1.1.

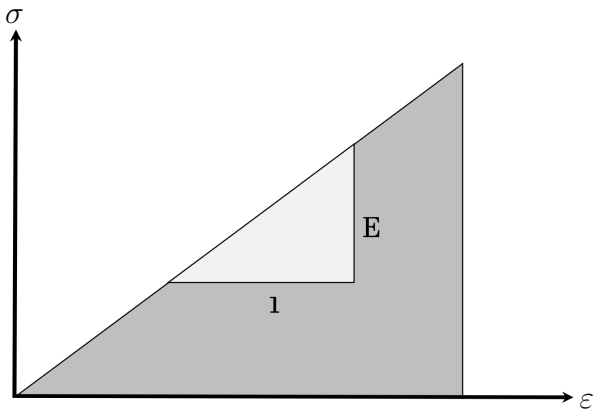

Figure 1.1: Stress-strain diagram in linear elasticity (uniaxial tension).

The first part of the stress-strain diagram for most materials utilized in engineering is a straight line. For a model subjected to a uniaxial load, we get

$$\sigma = E\,\varepsilon, \tag{1.1}$$

which is known as the Hooke's Law.

In 3D linear elasticity, Hooke's Law can be generalised for homogeneous elastic materials as

$$\sigma_{kl} = C_{klmn}\,\varepsilon_{mn}, \tag{1.2}$$

where C_{klmn}, $(k, l, m, n = 1, 2, 3)$ are components of the fourth-order stiffness tensor or the elastic moduli, σ_{kl} are stress tensor components and ε_{mn} are the components of infinitesimal strain tensor, determined through the displacements u_k as

$$\varepsilon_{mn} = \frac{1}{2}\left(u_{m,n} + u_{n,m}\right), \tag{1.3}$$

where a comma in the subscript denotes differentiation with respect to the corresponding spatial variable. Note that the Einstein summation convention is assumed in (1.2).

The fourth-order stiffness tensor includes eighty one components for the 3D problems. However, due to symmetries of the stiffness tensor, for most general anisotropy the number of independent stiffness components is twenty one.

Let us now discuss the orthotropic material briefly, having mechanical properties that differ in three perpendicular directions, and each direction has double rotational symmetry (see, Slaughter [2012], pp. 206). Due to the symmetry properties, the number of independent stiffness components reduces to nine. Thus, the stress-strain relations can be summarised as

$$\begin{bmatrix} \sigma_{11} \\ \sigma_{22} \\ \sigma_{33} \\ \sigma_{12} \\ \sigma_{13} \\ \sigma_{23} \end{bmatrix} = \begin{bmatrix} c_{11} & c_{12} & c_{13} & 0 & 0 & 0 \\ & c_{22} & c_{23} & 0 & 0 & 0 \\ & & c_{33} & 0 & 0 & 0 \\ & & & c_{44} & 0 & 0 \\ & symm & & & c_{55} & 0 \\ & & & & & c_{66} \end{bmatrix} \begin{bmatrix} \varepsilon_{11} \\ \varepsilon_{22} \\ \varepsilon_{33} \\ \varepsilon_{12} \\ \varepsilon_{13} \\ \varepsilon_{23} \end{bmatrix}, \tag{1.4}$$

where $c_{11}, c_{22}, ..., c_{66}$ are stiffness constants in the Voigt notation, within which the pairs of indices for the elastic moduli C_{klmn} are combined, recasting as $11 \Rightarrow 1$, $22 \Rightarrow 2$, $33 \Rightarrow 3$, $23 \Rightarrow 4$, $13 \Rightarrow 5$ and $12 \Rightarrow 6$ with a small letter c, for more details see Slaughter [2012].

In the case of elastic isotropic materials, the number of material constants reduces to two, namely

$$c_{11} = c_{22} = c_{33} = \lambda + 2\mu, \qquad c_{12} = c_{13} = c_{23} = \lambda, \qquad c_{44} = c_{55} = c_{66} = \mu, \tag{1.5}$$

where λ and μ denote the Lamé elastic moduli. These may be expressed through the Young's elastic modulus E and the Poisson's ratio ν as

$$\mu = \frac{E}{2\,(1+\nu)} \qquad \text{and} \qquad \lambda = \frac{\nu\, E}{(1+\nu)\,(1-2\nu)}. \tag{1.6}$$

The constitutive relations for isotropic elastic solids follow from (1.4) - (1.5) as

$$\sigma_{kl} = \lambda\, \delta_{kl}\, (u_{1,1} + u_{2,2} + u_{3,3}) + \mu\, (u_{k,l} + u_{l,k})\,, \tag{1.7}$$

where δ_{kl} is Kronecker's delta, defined by

$$\delta_{kl} = \begin{cases} 1 & k = l, \\ 0 & k \neq l. \end{cases} \tag{1.8}$$

Finally, for the plane strain problem of a linearly elastic half-space in (x_1, x_3) plane, the strain tensor components satisfy

$$\varepsilon_{m2} = 0, \quad m = 1, 2, 3. \tag{1.9}$$

1.2 Dynamic equations of motion

In this section, the 3D equations of motion of a linearly elastic medium are summarised.

Let us consider the traction components (stresses) acting on the faces of an infinitesimal cuboid located along the three coordinates axis, see Fig. 1.2. Assume that the stress specified at the center of the face represents the average stress on each face of the cube. The stress σ_{11} is located at the center of the back infinitesimal face, whereas at the center front face in Ox_1 direction it may be approximated as $\sigma_{11} + \sigma_{11,1}\, dx_1$. The same procedure may be carried out for other stresses, see Fig. 1.2, (see e.g. Graff [2012], Kramer [1996]).

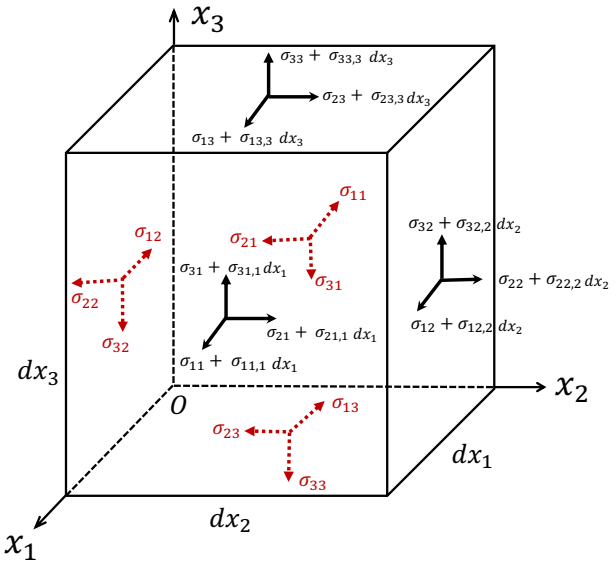

Figure 1.2: Stresses on infinitesimal cube.

Therefore, it is now possible to evaluate the stresses along the Ox_1, Ox_2 and Ox_3 directions. Based on the Newton's Second Law, in absence of body forces, along the

Ox_1 direction we get

$$\begin{aligned}
&(\sigma_{11} + \sigma_{11,1}\, dx_1)\, dx_2\, dx_3 - \sigma_{11}\, dx_2\, dx_3 \\
&+ (\sigma_{21} + \sigma_{21,2}\, dx_2)\, dx_1\, dx_3 - \sigma_{21}\, dx_1\, dx_3 \\
&+ (\sigma_{31} + \sigma_{31,3}\, dx_3)\, dx_1\, dx_2 - \sigma_{31}\, dx_1\, dx_2 = \rho\, dx_1\, dx_2\, dx_3\, u_{1,tt},
\end{aligned} \tag{1.10}$$

which simplifies as

$$\sigma_{11,1} + \sigma_{21,2} + \sigma_{31,3} = \rho\, u_{1,tt}, \tag{1.11}$$

where ρ is volume mass density.

Operating in the same manner for the Ox_2 and Ox_3 directions, we deduce

$$\sigma_{12,1} + \sigma_{22,2} + \sigma_{32,3} = \rho\, u_{2,tt}, \tag{1.12}$$

and

$$\sigma_{13,1} + \sigma_{23,2} + \sigma_{33,3} = \rho\, u_{3,tt}. \tag{1.13}$$

Equations (1.11)-(1.13) represent the equations of motion in 3D elastic solids, known as the Cauchy equations of motion.

From (1.4), the latter equations of motion can be expressed in terms of the displacement components u_k $(k = 1, 2, 3)$ for an orthotropic media as (see e.g, Chadwick [1976a]),

$$\begin{aligned}
&c_{11}\, u_{1,11} + c_{66}\, u_{1,22} + c_{55}\, u_{1,33} + (c_{12} + c_{66})\, u_{2,12} + (c_{13} + c_{55})\, u_{3,13} = \rho u_{1,tt}, \\
&c_{66}\, u_{2,11} + c_{22}\, u_{2,22} + c_{44}\, u_{2,33} + (c_{12} + c_{66})\, u_{1,12} + (c_{23} + c_{44})\, u_{3,23} = \rho u_{2,tt}, \\
&c_{55}\, u_{3,11} + c_{44}\, u_{3,22} + c_{33}\, u_{3,33} + (c_{13} + c_{55})\, u_{1,13} + (c_{23} + c_{44})\, u_{2,23} = \rho u_{3,tt}.
\end{aligned} \tag{1.14}$$

In the case of isotropic elastic material, equations in (1.14) reduce to the conventional Navier equations of motion, see e.g. Goncharov and Brekhovskikh [1985], Graff [2012] and Lanckau [1984]

$$(\lambda + \mu)\,\mathrm{grad}\,\mathrm{div}\,\mathbf{u} + \mu\,\nabla^2\,\mathbf{u} = \rho\,\mathbf{u}_{,tt}, \tag{1.15}$$

in which $\mathbf{u} = (u_1, u_2, u_3)$ is the displacement vector, and ∇^2 is the 3D Laplace operator in spatial coordinates.

1.3 Elastic Lamé potentials

Let us employ the Helmholtz decomposition, see Achenbach [2012], expressing the displacement vector $\mathbf{u}$ as

$$\mathbf{u} = \mathrm{grad}\,\phi + \mathrm{curl}\,\Psi, \tag{1.16}$$

with a conventional assumption

$$\mathrm{div}\,\Psi = 0, \tag{1.17}$$

where ϕ is a scalar longitudinal potential and $\Psi = (\psi_1, \psi_2, \psi_3)$ is a vector transverse potential. It follows from (1.16) that

$$\mathrm{div}\,\mathbf{u} = \nabla^2\,\phi. \tag{1.18}$$

Plugging equations (1.16) and (1.18) into equation (1.15) yields

$$\mathrm{grad}(c_1^2\,\nabla^2\,\phi - \phi_{,tt}) + \mathrm{curl}(c_2^2\,\nabla^2\,\Psi - \Psi_{,tt}) = 0, \tag{1.19}$$

where c_1 and c_2 are the longitudinal and transverse wave speeds, respectively, defined by

$$c_1 = \sqrt{\frac{\lambda + 2\mu}{\rho}}, \qquad \text{and} \qquad c_2 = \sqrt{\frac{\mu}{\rho}}. \tag{1.20}$$

Equation (1.19) leads to uncoupled wave equations

$$\nabla^2 \phi - \frac{1}{c_1^2}\, \phi_{,tt} = 0, \qquad \text{and} \qquad \nabla^2 \Psi - \frac{1}{c_2^2}\, \Psi_{,tt} = 0. \tag{1.21}$$

In the case of the plane strain setup in (x_1, x_3) plane (1.9) the vector potential Ψ is taken as $\Psi = (0, -\psi, 0)$, hence the equations (1.9) and (1.16) give

$$u_1 = \phi_{,1} - \psi_{,3}, \qquad \text{and} \qquad u_3 = \phi_{,3} + \psi_{,1}. \tag{1.22}$$

The equations of motion in (1.21) are then reduced to

$$\phi_{,11} + \phi_{,33} - \frac{1}{c_1^2}\, \phi_{,tt} = 0, \qquad \text{and} \qquad \psi_{,11} + \psi_{,33} - \frac{1}{c_2^2}\, \psi_{,tt} = 0. \tag{1.23}$$

Furthermore, the constitutive relations for the plane strain problem can be expressed in terms of the elastic Lamé potentials as

$$\begin{aligned} \sigma_{11} &= \mu \left[\kappa^2\, \phi_{,11} + \left(\kappa^2 - 2\right)\, \phi_{,33} - 2\, \psi_{,13}\right], \\ \sigma_{33} &= \mu \left[\left(\kappa^2 - 2\right)\, \phi_{,11} + \kappa^2\, \phi_{,33} + 2\, \psi_{,13}\right], \\ \sigma_{13} &= \mu \left(2\phi_{,13} + \psi_{,11} - \psi_{,33}\right), \end{aligned} \tag{1.24}$$

where $\kappa^2 = c_1^2 \,/\, c_2^2$.

1.4 Rayleigh waves on an elastic half-space

In this section, the derivation of the classical Rayleigh wave equation is introduced. Then, the Rayleigh waves of the sinusoidal profile are generalised to those of arbitrary profile. Finally, an explicit hyperbolic-elliptic model for the Rayleigh wave induced by prescribed surface loading is presented.

1.4.1 Elementary Derivation

We start from equations of motion (1.21), subject to free boundary conditions on the surface $x_3 = 0$

$$\sigma_{k3} = 0, \quad k = 1, 2, 3, \tag{1.25}$$

which may be expressed through the elastic Lamé potentials as

$$\begin{aligned} 2\phi_{,13} - \psi_{1,12} + \psi_{2,11} - \psi_{2,33} + \psi_{3,23} &= 0, \\ 2\phi_{,23} - \psi_{1,12} + \psi_{1,33} + \psi_{2,12} - \psi_{3,13} &= 0, \\ \kappa^2\,\phi_{,33} + \left(\kappa^2 - 2\right)\left(\phi_{,11} + \phi_{,22}\right) + 2\psi_{2,13} - 2\psi_{1,23} &= 0, \end{aligned} \tag{1.26}$$

with κ^2 defined in (1.24).

The solutions of (1.21), decaying away from the surface as $x_3 \to \infty$ are sought for in the form

$$\phi = C_1\, e^{i\hat{k}(x_1\,\cos\alpha + x_2\,\sin\alpha - ct) - \hat{k}\,\alpha_s\,x_3},$$

and

$$\Psi = (C_2, C_3, C_4)\; e^{i\hat{k}(x_1\,\cos\alpha + x_2\,\sin\alpha - ct) - \hat{k}\,\beta_s\,x_3}, \tag{1.27}$$

where $C_1, ..., C_4$ are arbitrary constants, c and $\hat{k}$ denote the the phase speed and wave number, respectively, with the attenuation orders

$$\alpha_s = \sqrt{1 - \frac{c^2}{c_1^2}} \qquad \text{and} \qquad \beta_s = \sqrt{1 - \frac{c^2}{c_2^2}}. \tag{1.28}$$

On satisfying the boundary conditions (1.26) together with the constraint (1.18), we obtain the following homogeneous algebraic system

$$\begin{pmatrix} 2i\,\alpha_s \cos\alpha & -\sin\alpha\cos\alpha & \cos^2\alpha + \beta_s^2 & i\beta_s \sin\alpha \\ -2i\,\alpha_s \sin\alpha & \sin^2\alpha + \beta_s^2 & -\sin\alpha\cos\alpha & i\beta_s \cos\alpha \\ 1 + \beta_s^2 & 2i\beta_s \sin\alpha & -2i\beta_s \cos\alpha & 0 \\ 0 & i\cos\alpha & i\sin\alpha & \beta_s \end{pmatrix} \begin{pmatrix} C_1 \\ C_2 \\ C_3 \\ C_4 \end{pmatrix} = \begin{pmatrix} 0 \\ 0 \\ 0 \\ 0 \end{pmatrix}. \tag{1.29}$$

This system possesses non-trivial solutions provided the associated determinant vanishes, leading to the well-known secular equation (Rayleigh equation)

$$\left(1 + \beta_s^2\right)^2 - 4\,\alpha_s\,\beta_s = 0. \tag{1.30}$$

The speed of the Rayleigh wave $c = c_R$ is a root of equation (1.30). Often, this equation is represented as

$$R\,(s) = (2 - s)^2 - 4\sqrt{1 - s}\,\sqrt{1 - \kappa^{-2}\,s} = 0, \tag{1.31}$$

where

$$s = \frac{c^2}{c_2^2}, \qquad \text{and} \qquad \kappa = \frac{c_1}{c_2} < 1. \tag{1.32}$$

The existence of a unique solution of (1.31) on the interval $0 < c_R < c_2$ was presented by Sobolev et al. [1937], see also Babich and Kiselev [2018]. It is also known from Rayleigh [1885] that the equation (1.31) may be transformed to a cubic equation

$$s^3 - 8\,(s-1)\,\left(s - 2\left(1 - \kappa^{-2}\right)\right) = 0. \tag{1.33}$$

The approximate solution of (1.33) was first obtained by Bergmann and Henry [1938], and then improved by many researchers, see e.g. Vinh and Malischewsky [2007], Vinh and Ogden [2004], and also Pichugin [2008], suggesting

$$\frac{c_R}{c_2} \approx \frac{256}{293} + \nu\left(\frac{60}{307} - \nu\left(\frac{4}{125} + \nu\left(\frac{5}{84} + \frac{4}{237}\,\nu\right)\right)\right). \tag{1.34}$$

The relation between the body and Rayleigh wave speeds are illustrated in Fig. 1.3 below,

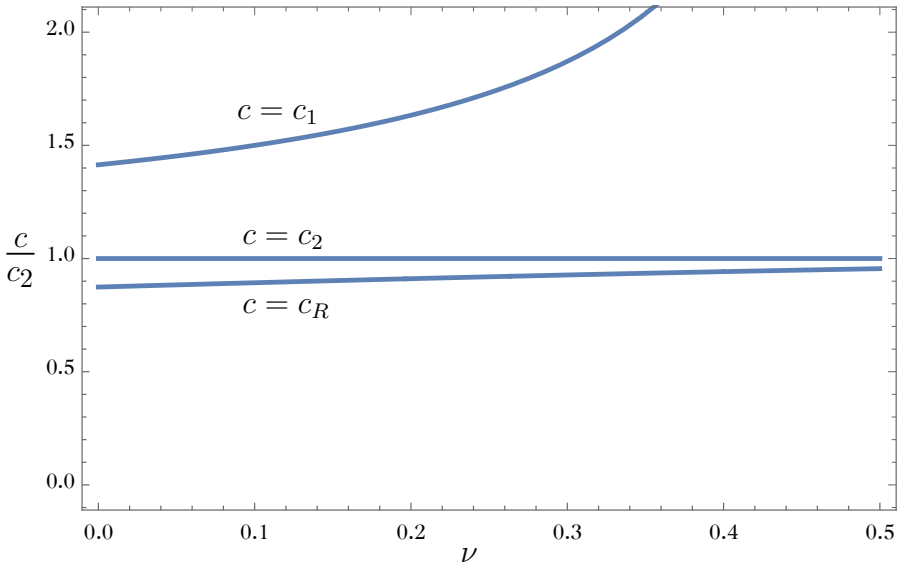

Figure 1.3: Scaled Rayleigh and body waves speed vs. the Poisson's ratio ν.

1.4.2 Surface waves of arbitrary profile

In the previous subsection, we sought for the solution in the form of a travelling harmonic wave of sinusoidal shape. Now, let us generalise it to general time-dependence, relying on the work of Chadwick [1976b], see also the earlier contributions of Friedlander [1948] and Sobolev et al. [1937]. Here we restrict our concern to the plane strain problem (1.9). The solutions of the wave equations (1.23) may be then written as

$$\phi = \phi\left(\theta, x_3\right), \qquad \psi = \psi\left(\theta, x_3\right), \qquad \text{and} \qquad \theta = x_1 - c\,t. \tag{1.35}$$

Thus, the equations of motion (1.23) reduce to

$$\phi_{,33} + \alpha_s^2\,\phi_{,11} = 0 \qquad \text{and} \qquad \psi_{,33} + \beta_s^2\,\psi_{,11} = 0, \tag{1.36}$$

with α_s and β_s defined in (1.28). Hence, the elastic potentials may be found as the plane harmonic functions

$$\phi = \phi\left(\theta, \alpha_s\, x_3\right) \qquad \text{and} \qquad \psi = \psi\left(\theta, \beta_s\, x_3\right). \tag{1.37}$$

The boundary conditions (1.25) take the form

$$2\phi_{,13} + \psi_{,11} - \psi_{,33} = 0, \qquad \text{and} \qquad \left(\kappa^2 - 2\right)\phi_{,11} + \kappa^2\phi_{,33} + 2\psi_{,13} = 0. \tag{1.38}$$

Since the potentials (1.35) are plane harmonic functions, they must satisfy the Cauchy-Riemann identities, which may be written for the function $Z = Z(x_1, \gamma\, x_3)$ as

$$Z_{,1} = \frac{1}{\gamma}\, \bar{Z}_{,3}, \qquad Z_{,3} = -\gamma\, \bar{Z}_{,1} \qquad \text{and} \qquad \bar{\bar{Z}} = -Z, \tag{1.39}$$

with the bar denoting a harmonic conjugate.

On substituting (1.37) into (1.38), we get

$$\begin{aligned} 2\alpha_s\, \phi_{,11} + \left(1 + \beta_s^2\right) \bar{\psi}_{,11} &= 0, \\ \left(1 + \beta_s^2\right) \phi_{,11} + 2\beta_s\, \bar{\psi}_{,11} &= 0. \end{aligned} \tag{1.40}$$

The solvability of this system leads to the well-known Rayleigh equation (1.30). Thus, the elastic potentials are

$$\phi = \phi\left(\theta, \alpha_R\, x_3\right) \qquad \text{and} \qquad \psi = \psi\left(\theta, \beta_R\, x_3\right), \tag{1.41}$$

where

$$\alpha_R = \sqrt{1 - \frac{c_R^2}{c_1^2}} \qquad \text{and} \qquad \beta_R = \sqrt{1 - \frac{c_R^2}{c_2^2}}, \tag{1.42}$$

with c_R as before denoting the Rayleigh wave speed.

The differential relations between the potentials on the boundary $x_3 = 0$ follow from (1.38) as

$$\psi_{,1} = -\frac{\vartheta}{\alpha_R}\, \phi_{,3} \qquad \text{and} \qquad \psi_{,3} = \beta_R\, \vartheta\, \phi_{,1}, \tag{1.43}$$

where

$$\vartheta = \frac{2\alpha_R}{1 + \beta_R^2} = \frac{1 + \beta_R^2}{2\beta_R}. \tag{1.44}$$

Moreover, utilising the properties of harmonic functions, the relation between each harmonic potentials ϕ and ψ over the entire half-plane may be determined as (for more details, see Chadwick [1976b]),

$$\begin{aligned} \psi\left(\theta_R, \beta_R\, x_3\right) &= \vartheta\, \mathcal{H}\left(\phi\right)\left(\theta_R, \beta_R\, x_3\right), \\ \phi\left(\theta_R, \alpha_R\, x_3\right) &= -\vartheta^{-1}\, \mathcal{H}\left(\psi\right)\left(\theta_R, \alpha_R\, x_3\right), \end{aligned} \tag{1.45}$$

where ϑ defined in (1.44), $\theta_R = x_1 - c_R\, t$, and $\mathcal{H}$ denotes the Hilbert transform, see, e.g Erdelyi et al. [1954], defined as

$$\mathcal{H}\left(f\right)\left(\check{x}\right) = \frac{1}{\pi}\ \text{p.v.} \int_{-\infty}^{\infty} \frac{f\left(\check{y}\right)}{\check{x} - \check{y}}\ d\check{y}, \tag{1.46}$$

thus the elastic potentials are harmonic conjugates.

The expressions (1.45) allow representing the displacements (1.22) in terms of a single plane harmonic function, say ϕ, yielding

$$\begin{aligned} u_1\left(x_1, x_3, t\right) &= \phi_{,1}\left(\theta_R, \alpha_R\, x_3\right) - \vartheta\, \beta_R\, \phi_{,1}\left(\theta_R, \beta_R\, x_3\right), \\ u_3\left(x_1, x_3, t\right) &= \phi_{,3}\left(\theta_R, \alpha_R\, x_3\right) - \frac{\vartheta}{\alpha_R}\, \phi_{,3}\left(\theta_R, \beta_R\, x_3\right). \end{aligned} \tag{1.47}$$

This representation has recently been generalised to 3D (see Kiselev and Parker [2010] for more details), giving

$$\begin{aligned} u_1 &= a\left[\beta_R\, \Phi_{,1}\left(x_1, x_2, \beta_R\, x_3, t\right) - \frac{1}{\vartheta}\, \Phi_{,1}\left(x_1, x_2, \alpha_R\, x_3, t\right)\right], \\ u_2 &= a\left[\beta_R\, \Phi_{,2}\left(x_1, x_2, \beta_R\, x_3, t\right) - \frac{1}{\vartheta}\, \Phi_{,2}\left(x_1, x_2, \alpha_R\, x_3, t\right)\right], \\ \text{and} \qquad u_3 &= a\left[\frac{1}{\beta_R}\, \Phi_{,3}\left(x_1, x_2, \beta_R\, x_3, t\right) - \frac{1}{\vartheta}\, \Phi_{,3}\left(x_1, x_2, \alpha_R\, x_3, t\right)\right], \end{aligned} \tag{1.48}$$

where a is an arbitrary constant and $\Phi(x_1, x_2, x_3, t)$ is an arbitrary harmonic function, satisfying the 3D Laplace equation

$$\nabla^2 \Phi(x_1, x_2, x_3, t) = \Phi_{,11} + \Phi_{,22} + \Phi_{,33} = 0, \ x_3 > 0, \tag{1.49}$$

with $\Phi \to 0$ as $x_3 \to \infty$.

1.4.3 Explicit hyperbolic-elliptic model for surface wave field induced by prescribed stresses

Consider now plane strain problem (1.23), for a homogeneous elastic half-space $x_3 \geq 0$, subject to boundary conditions on the surface $x_3 = 0$

$$\sigma_{13} = -Q \qquad \text{and} \qquad \sigma_{33} = -P, \tag{1.50}$$

where $P = P(x_1, t)$ and $Q = Q(x_1, t)$ are a prescribed vertical and tangential load, respectively.

Following Kaplunov and Prikazchikov [2017], a slow time perturbation of eigensolutions presented in the previous subsection 1.4.2 may be constructed. The resulting asymptotic formulation for the Rayleigh wave field is given by an elliptic equation

$$\phi_{,33} + \alpha_R^2 \phi_{,11} = 0, \tag{1.51}$$

with the boundary condition at $x_3 = 0$ in the form of a hyperbolic equation

$$\Box_R \phi = -\frac{\beta_R}{2\mu B_I} \left[\vartheta P + \mathcal{H}(Q)\right], \tag{1.52}$$

where

$$\Box_R = \partial_{11} - c_R^{-2}\,\partial_{tt}, \tag{1.53}$$

is d'Alembert operator, $\mathcal{H}(Q)$ denotes the Hilbert transform (see (1.46)), and

$$B_{_I} = \left(1-\beta_R^2\right)\frac{\alpha_R}{\beta_R} + \left(1-\alpha_R^2\right)\frac{\beta_R}{\alpha_R} + \beta_R^4 - 1, \tag{1.54}$$

with the quantities α_R and β_R defined in (1.42).

Once the longitudinal potential ϕ is obtained from the scalar formulation (1.51), (1.52), the transverse potential ψ may be determined from (1.43).

1.5 Surface waves on a coated elastic half-space

This section focuses on surface waves on an isotropic elastic half-space coated by a thin isotropic coating, with the plane strain assumption (1.9) adopted.

1.5.1 Dispersion relation for a coated half-space

Consider a thin coating of constant thickness h occupying the region $-h \leq x_3 \leq 0$, perfectly joint with an elastic half-space, employing the domain $-\infty < x_1, x_2 < \infty$ and $0 \leq x_3 \leq \infty$, see Fig. 1.4.

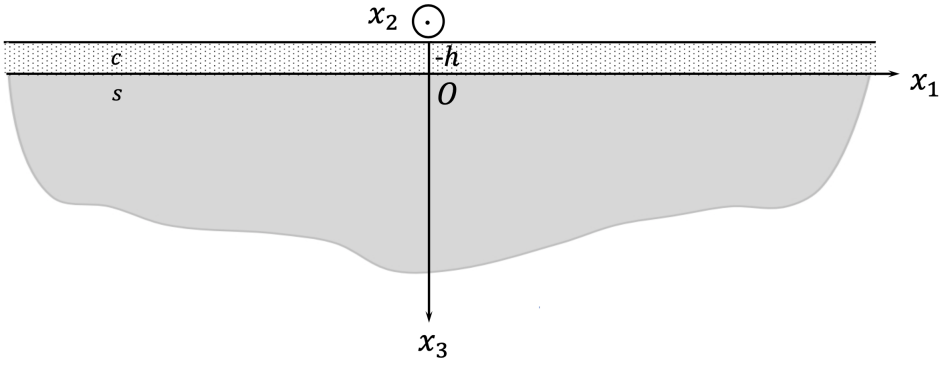

Figure 1.4: A coated elastic half-space.

Throughout this section and the following Chapter 2, the appropriate material parameters of the coating and the substrate are summarised in Table 1.1.

Parameters	**Coating (c)**	**Substrate (s)**
Young's moduli	E_0	E
Poisson's ratio	ν_0	ν
Density	ρ_0	ρ
Lamé moduli	$\lambda_0,\ \mu_0$	$\lambda,\ \mu$
Longitudinal speed	c_{10}	c_1
Transverse speed	c_{20}	c_2

Table 1.1: The parameters of coating and substrate.

The equations of motion are taken as (1.15). The traction-free boundary conditions on the upper face of the coating ($x_3 = -h$) are

$$\sigma_{r3}^{(c)} = 0, \qquad r = 1, 3, \tag{1.55}$$

with continuity conditions on the interface $x_3 = 0$, given as

$$u_r^{(c)} = u_r^{(s)}, \qquad \sigma_{r3}^{(c)} = \sigma_{r3}^{(s)}, \tag{1.56}$$

where the indices (c) and (s) indicate coating and substrate, respectively.

The displacements can be decomposed from (1.22) as

$$u_1^{(q)} = \phi_{,1}^{(q)} - \psi_{,3}^{(q)}, \qquad u_3^{(q)} = \phi_{,3}^{(q)} + \psi_{,1}^{(q)}, \qquad q = c, s, \tag{1.57}$$

leading to the wave equations of motion (1.23).

Now, we seek for solution of the form

$$\phi^{(q)} = f_q\,(x_3)\; e^{i\theta\hat{k}}, \qquad \psi^{(q)} = g_q\,(x_3)\; e^{i\theta\hat{k}}, \qquad \theta = x_1 - c\,t. \tag{1.58}$$

On substituting the latter into (1.23), we arrive at

$$\begin{gathered} f_q\,(x_3) = B_{1q}\, e^{\alpha_q \hat{k} x_3} + B_{2q}\, e^{-\alpha_q \hat{k} x_3}, \\ g_q\,(x_3) = B_{3q}\, e^{\beta_q \hat{k} x_3} + B_{4q}\, e^{-\beta_q \hat{k} x_3}, \end{gathered} \tag{1.59}$$

where B_{1q}, B_{2q}, B_{3q} and B_{4q} $(q = c, s)$ are arbitrary constants with

$$\alpha_c = \sqrt{1 - \frac{c^2}{c_{10}^2}}, \qquad \beta_c = \sqrt{1 - \frac{c^2}{c_{20}^2}}, \tag{1.60}$$

and α_s, β_s are defined in (1.28).

Inserting the solutions (1.59) into (1.58) and taking into consideration the decay conditions at $x_3 \to \infty$, we get

$$\begin{gathered} \phi^{(c)} = \left(B_{1c}\, e^{\alpha_c \hat{k} x_3} + B_{2c}\, e^{-\alpha_c \hat{k} x_3}\right) e^{i\theta\hat{k}}, \\ \psi^{(c)} = \left(B_{3c}\, e^{\beta_c \hat{k} x_3} + B_{4c}\, e^{-\beta_c \hat{k} x_3}\right) e^{i\theta\hat{k}}, \end{gathered} \tag{1.61}$$

and

$$\phi^{(s)} = B_{2s}\, e^{-\alpha_s \hat{k} x_3} e^{i\theta\hat{k}}, \qquad \text{and} \qquad \psi^{(s)} = B_{4s}\, e^{-\beta_s \hat{k} x_3} e^{i\theta\hat{k}}. \tag{1.62}$$

On substituting (1.58) into (1.57), we can write down the displacements as

$$u_1^{(c)} = \hat{k}\left[i\left(B_{1c}\,e^{\hat{k}x_3\alpha_c} + B_{2c}\,e^{-\hat{k}\,x_3\alpha_c}\right) - \beta_c\left(B_{3c}\,e^{\hat{k}x_3\beta_c} - B_{4c}\,e^{-\hat{k}x_3\beta_c}\right)\right]e^{i\theta\hat{k}},$$

$$u_3^{(c)} = \hat{k}\left[\alpha_c\left(B_{1c}\,e^{\hat{k}x_3\alpha_c} - B_{2c}\,e^{-\hat{k}x_3\alpha_c}\right) + i\left(B_{3c}\,e^{\hat{k}x_3\beta_c} + B_{4c}\,e^{-\hat{k}\,x_3\beta_c}\right)\right]e^{i\theta\hat{k}}, \tag{1.63}$$

and

$$u_1^{(s)} = \hat{k}\left(i\,B_{2s}\,e^{-\hat{k}x_3\alpha_s} + \beta_s\,B_{4s}\,e^{-\hat{k}x_3\beta_s}\right)e^{i\theta\hat{k}},$$

$$u_3^{(s)} = \hat{k}\left(i\,B_{4s}\,e^{-\hat{k}x_3\beta_s} - \alpha_s\,B_{2s}\,e^{-\hat{k}x_3\alpha_s}\right)e^{i\theta\hat{k}}. \tag{1.64}$$

For the relevant stresses, we get

$$\sigma_{33}^{(c)} = \gamma_\mu\left[\gamma_c^2\left(B_{1c}e^{\hat{k}x_3\alpha_c} + B_{2c}e^{-\hat{k}x_3\alpha_c}\right) + i\beta_c\left(B_{3c}e^{\hat{k}x_3\beta_c} - B_{4c}e^{-\hat{k}x_3\beta_c}\right)\right]e^{i\theta\hat{k}},$$

$$\sigma_{13}^{(c)} = \gamma_\mu\left[i\alpha_c\left(B_{1c}e^{\hat{k}x_3\alpha_c} - B_{2c}e^{-\hat{k}x_3\alpha_c}\right) - \gamma_c^2\left(B_{3c}e^{\hat{k}x_3\beta_c} + B_{4c}e^{-\hat{k}x_3\beta_c}\right)\right]e^{i\theta\hat{k}}, \tag{1.65}$$

and

$$\sigma_{33}^{(s)} = \gamma_\mu\left[\gamma_s^2\,B_{2s}\,e^{-\hat{k}\,x_3\alpha_s} - i\beta_s\,B_{4s}\,e^{-\hat{k}x_3\beta_s}\right]e^{i\theta\hat{k}},$$

$$\sigma_{13}^{(s)} = -\gamma_\mu\left[\gamma_s^2\,B_{4s}\,e^{-\hat{k}\,x_3\beta_s} + i\alpha_s\,B_{2s}\,e^{-\hat{k}x_3\alpha_s}\right]e^{i\theta\hat{k}}, \tag{1.66}$$

where

$$\gamma_\mu = 2\mu\,\hat{k}^2, \qquad \gamma_q^2 = \frac{1}{2}\left(1+\beta_q^2\right), \qquad q = c, s.$$

Inserting the expressions (1.63) – (1.66) into the boundary and continuity conditions (1.55) and (1.56), we obtain a homogeneous system of order six with the non-zero components of 6×6 matrix $\boldsymbol{A}$, given in (A.1). The dispersion relation follows from the sovability of this 6×6 system, when $\det(\boldsymbol{A}) = 0$, i.e.

$$\begin{aligned}
\sinh\left(\beta_c\,\hat{k}h\right)\Big[&\sinh(\alpha_c\,\hat{k}h)\left(\hat{\mu}^2\left(\Upsilon_s-1\right)\left(\Upsilon_c^2+\gamma_c^8\right)+\left(\Upsilon_c^2+\gamma_c^4\right)\left(\Upsilon_s-\gamma_s^4\right)\right.\\
&\left.-2\,\hat{\mu}\left(\Upsilon_c^2+\gamma_c^6\right)\left(\Upsilon_s^2-\gamma_s^2\right)\right)+\cosh\left(\alpha_c\,\hat{k}h\right)\alpha_c\left(\gamma_c^2-1\right)\left(\gamma_s^2-1\right)\\
&\hat{\mu}\left(\beta_s\,\gamma_c^4-\alpha_s\,\beta_c^2\right)\Big]-\beta_c\,\cosh\left(\beta_c\,\hat{k}h\right)\Big[\left(\left(\gamma_c^2-1\right)\left(\gamma_s^2-1\right)\hat{\mu}\right.\\
\sinh\left(\alpha_c\,\hat{k}h\right)&\left(\alpha_c^2\,\beta_s-\alpha_s\,\gamma_c^4\right)\Big)+\alpha_c\,\cosh\left(\alpha_c\,\hat{k}h\right)\left(2\,\gamma_c^4\,\hat{\mu}^2\left(\Upsilon_s-1\right)\right.\\
&\left.\left(\gamma_c^4+1\right)\left(\Upsilon_s-\gamma_s^4\right)-2\left(\gamma_c^2+1\right)\gamma_c^2\,\hat{\mu}\left(\Upsilon_s-\gamma_s^2\right)\right)\Big]\\
-2\,\Upsilon_c\,\gamma_c^2\Big(&\left(\gamma_c^2+1\right)\hat{\mu}\left(\Upsilon_s-\gamma_s^2\right)+\gamma_c^2\,\hat{\mu}^2\left(1-\Upsilon_s\right)+\left(\gamma_s^4-\Upsilon_s\right)\Big)=0,
\end{aligned} \tag{1.67}$$

where

$$\hat{\mu}=\frac{\mu_0}{\mu},\qquad \Upsilon_q=\alpha_q\,\beta_q,\qquad q=c,s. \tag{1.68}$$

It can be demonstrated that at $h=0$ the equation (1.67) coincides with the equation (1.30). Numerical illustrations of the dispersion relation (1.67), showing the relation of the scaled phase velocity $v^{ph}=c\,/\,c_R$ against the dimensionless wavenumber $\hat{k}h$ with $\rho_0\,/\,\rho=1$, are presented in Fig. 1.5.

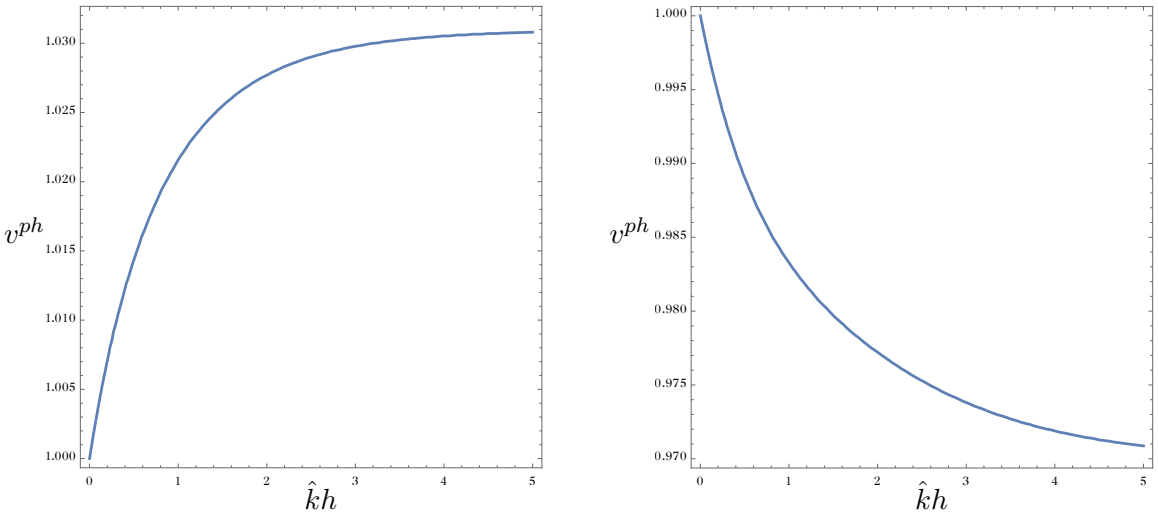

(a) $E_0 = 1$, $\nu_0 = 0.3$, $E = 0.9$ and $\nu = 0.2$. (b) $E_0 = 0.9$, $\nu_0 = 0.2$, $E = 1$ and $\nu = 0.3$.

Figure 1.5: The exact dispersion relation (1.67): dependence of scaled phase velocity v^{ph} on the dimensionless wavenumber $\hat{k}h$.

Two types of typical behaviour may be observed, associated with the sign of the group velocity in the long-wave limit, with positive and negative values corresponding to the local minimum and maximum of the phase velocity at the Rayleigh wave speed, respectively, see Fig. 1.5 (a) and (b) above.

1.5.2 Explicit model for surface elastic waves in a coated isotropic half-space

Consider the imposed boundary conditions at the surface $x_3 = -h$ of the coating are taken in the form of prescribed surface loading (1.50), with continuity of displacement at the interface $x_3 = 0$ assumed as

$$u_r^{(c)} = v_r^{(s)}, \tag{1.69}$$

where $v_r^{(s)} = v_r(x_1, t), r = 1, 3$ are displacements on the surface of the substrate.

1.5.2.1 Effective boundary conditions

First, we derive the effective boundary conditions at the interface $x_3 = 0$, modelling the effect of the thin coating, using the method of direct asymptotic integration of the equations in elasticity, see e.g. Goldenveizer et al. [1993]. Here we present a slightly modified procedure compared to Dai et al. [2010], operating in terms of displacements. Let us now specify a small parameter ϵ as

$$\epsilon = \frac{h}{L} \ll 1, \tag{1.70}$$

associated with the long-wave limit, where L is a typical wave length, and also introduce the scaling

$$\xi_0 = \frac{x_1}{L}, \qquad \eta = \frac{x_3}{\epsilon\, L}, \qquad \tau_0 = \frac{c_{20}}{L}\, t, \tag{1.71}$$

along with the dimensionless quantities

$$u_r^* = \frac{u_r^{(c)}}{L}, \quad v_r^* = \frac{v_r^{(s)}}{L}, \quad \sigma_{r3}^* = \frac{\sigma_{r3}^{(s)}}{\epsilon\, \mu_0}, \quad p^* = \frac{P}{\epsilon\, \mu_0}, \quad q^* = \frac{Q}{\epsilon\, \mu_0}, \quad r = 1, 3. \tag{1.72}$$

Throughout this thesis, we will assume that all quantities with the asterisk have the same asymptotic order. The asymptotic series for the dimensionless displacements may now be written in terms of the small parameter ϵ as

$$\begin{pmatrix} u_r^* \\ \\ \sigma_{r3}^* \end{pmatrix} = \begin{pmatrix} u_r^{(0)} \\ \\ \sigma_{r3}^{(0)} \end{pmatrix} + \epsilon \begin{pmatrix} u_r^{(1)} \\ \\ \sigma_{r3}^{(1)} \end{pmatrix} + \epsilon^2 \begin{pmatrix} u_r^{(2)} \\ \\ \sigma_{r3}^{(2)} \end{pmatrix} + \ldots, \quad r = 1, 3. \tag{1.73}$$

The equations of motion (1.15) can be represented in terms of the new variables as

$$\begin{aligned} u^*_{1,\eta\eta} + \epsilon\left(\kappa_0^2 - 1\right) u^*_{3,\xi_0\eta} + \epsilon^2\left(\kappa_0^2\, u^*_{1,\xi_0\xi_0} - u^*_{1,\tau_0\tau_0}\right) = 0, \\ \kappa_0^2\, u^*_{3,\eta\eta} + \epsilon\left(\kappa_0^2 - 1\right) u^*_{1,\xi_0\eta} + \epsilon^2\left(u^*_{3,\xi_0\xi_0} - u^*_{3,\tau_0\tau_0}\right) = 0, \end{aligned} \tag{1.74}$$

together with the boundary conditions (1.50) and (1.69), given by

$$\begin{aligned} u^*_{1,\eta} + \epsilon\, u^*_{3,\xi_0} &= -\epsilon^2\, q^* \qquad \text{at} \qquad \eta = -1, \\ \kappa_0^2\, u^*_{3,\eta} + \epsilon\left(\kappa_0^2 - 2\right) u^*_{1,\xi_0} &= -\epsilon^2\, p^* \qquad \text{at} \qquad \eta = -1, \\ u^*_r &= v^*_r \qquad \text{at} \qquad \eta = 0, \end{aligned} \tag{1.75}$$

where $\kappa_0 = c_{10}/c_{20}$.

Using (1.7) and (1.70) – (1.73), the stresses σ_{13} and σ_{33} imply

$$\begin{aligned} \epsilon^2\, \sigma^*_{13}\left(\xi_0, \eta, \tau_0\right) &= u^{(0)}_{1,\eta} + \epsilon\left(u^{(1)}_{1,\eta} + u^{(0)}_{3,\xi_0}\right) + \epsilon^2\left(u^{(2)}_{1,\eta} + u^{(1)}_{3,\xi_0}\right) + O\left(\epsilon^3\right), \\ \epsilon^2\, \sigma^*_{33}\left(\xi_0, \eta, \tau_0\right) &= \kappa_0^2\, u^{(0)}_{3,\eta} + \epsilon\left(\kappa_0^2\, u^{(1)}_{3,\eta} + \left(\kappa_0^2 - 2\right) u^{(0)}_{1,\xi_0}\right) \\ &\quad + \epsilon^2\left(\kappa_0^2\, u^{(2)}_{3,\eta} + \left(\kappa_0^2 - 2\right) u^{(1)}_{1,\xi_0}\right) + O\left(\epsilon^3\right). \end{aligned} \tag{1.76}$$

At leading order $O(1)$, we have from (1.74) that

$$u^{(0)}_{r,\eta\eta} = 0, \qquad r = 1, 3, \tag{1.77}$$

subject to

$$\begin{aligned} u^{(0)}_{r,\eta} &= 0 \qquad \text{at} \qquad \eta = -1, \\ u^{(0)}_r &= v^*_r \qquad \text{at} \qquad \eta = 0. \end{aligned} \tag{1.78}$$

Hence, we deduce

$$u_r^{(0)} = v_r^*, \quad r = 1, 3. \tag{1.79}$$

At next order $O(\epsilon)$ the problem is formulated as

$$\begin{aligned} u_{1,\eta\eta}^{(1)} + \left(\kappa_0^2 - 1\right) u_{3,\xi_0\eta}^{(0)} &= 0, \\ \kappa_0^2\, u_{3,\eta\eta}^{(1)} + \left(\kappa_0^2 - 1\right) u_{1,\xi_0\eta}^{(0)} &= 0, \end{aligned} \tag{1.80}$$

subject to the boundary conditions

$$\begin{aligned} u_{1,\eta}^{(1)} + u_{3,\xi_0}^{(0)} &= 0 \qquad \text{at} \qquad \eta = -1, \\ \kappa_0^2\, u_{3,\eta}^{(1)} + \left(\kappa_0^2 - 2\right) u_{1,\xi_0}^{(0)} &= 0 \qquad \text{at} \qquad \eta = -1, \\ u_r^{(1)} &= 0 \qquad \text{at} \qquad \eta = 0. \end{aligned} \tag{1.81}$$

Inserting (1.79) into $(1.80)_1$, and making use of the boundary conditions $(1.81)_1$ and $(1.81)_3$, we get

$$u_1^{(1)} = -\eta\, v_{3,\xi_0}^*. \tag{1.82}$$

Another displacement $u_3^{(1)}$ is obtained from the equations $(1.80)_2$ and $(1.81)_3$ as

$$u_3^{(1)} = -\eta \left(1 - 2\kappa_0^{-2}\right) v_{1,\xi_0}^*. \tag{1.83}$$

At next order $O(\epsilon^2)$, we have

$$\begin{aligned} u_{1,\eta\eta}^{(2)} + \left(\kappa_0^2 - 1\right) u_{3,\xi_0\eta}^{(1)} + \kappa_0^2\, u_{1,\xi_0\xi_0}^{(0)} - u_{1,\tau_0\tau_0}^{(0)} &= 0, \\ \kappa_0^2\, u_{3,\eta\eta}^{(2)} + \left(\kappa_0^2 - 1\right) u_{1,\xi_0\eta}^{(1)} + u_{3,\xi_0\xi_0}^{(0)} - u_{3,\tau_0\tau_0}^{(0)} &= 0, \end{aligned} \tag{1.84}$$

with the boundary conditions

$$\begin{aligned} u^{(2)}_{1,\eta} + u^{(1)}_{3,\xi_0} &= -q^* \qquad \text{at} \qquad \eta = -1, \\ \kappa_0^2\, u^{(2)}_{3,\eta} + \left(\kappa_0^2 - 2\right) u^{(1)}_{1,\xi_0} &= -p^* \qquad \text{at} \qquad \eta = -1, \\ u^{(2)}_r &= 0 \qquad \text{at} \qquad \eta = 0. \end{aligned} \tag{1.85}$$

The solutions of (1.84) satisfying (1.85) are found as

$$u^{(2)}_1 = \eta \left[\left(\left(-3 + 2\kappa_0^{-2}\right) \frac{\eta}{2} - 4\left(1 - \kappa_0^{-2}\right) \right) v^*_{1,\xi_0\xi_0} + \left(1 + \frac{\eta}{2}\right) v^*_{1,\tau_0\tau_0} - q^* \right], \tag{1.86}$$

$$u^{(2)}_3 = \eta \left[\left(1 - 2\kappa_0^{-2}\right) \frac{\eta}{2}\, v^*_{3,\xi_0\xi_0} + \kappa_0^{-2} \left(\left(1 + \frac{\eta}{2}\right) v^*_{3,\tau_0\tau_0} - p^* \right) \right].$$

The stresses (1.76) become

$$\begin{aligned} \sigma^{(0)}_{13} &= (\eta + 1) \left(v^*_{1,\tau_0\tau_0} - 4\left(1 - \kappa_0^{-2}\right) v^*_{1,\xi_0\xi_0} \right) - q^* + O(\epsilon^2), \\ \sigma^{(0)}_{33} &= (\eta + 1)\; v^*_{3,\tau_0\tau_0} - p^* + O(\epsilon^2). \end{aligned} \tag{1.87}$$

The leading order stresses are then rewritten in terms of the original dimensional variables as

$$\begin{aligned} \sigma^{(c)}_{13} &= (x_3 + h) \left[\rho_0\, v^{(s)}_{1,tt} - 4\mu_0 \left(1 - \kappa_0^{-2}\right) v^{(s)}_{1,11} \right] - Q, \\ \sigma^{(c)}_{33} &= (x_3 + h)\; \rho_0\, v^{(s)}_{3,tt} - P. \end{aligned} \tag{1.88}$$

The continuity of stresses and displacements at the interface $x_3 = 0$ facilely results in the following effective boundary conditions on the interface

$$\begin{aligned} \sigma^{(s)}_{13}\,(x_1, 0, t) &= h\rho_0 \left[v^{(s)}_{1,tt} - 4c_{20}^2 \left(1 - \kappa_0^{-2}\right) v^{(s)}_{1,11} \right] - Q, \\ \sigma^{(s)}_{33}\,(x_1, 0, t) &= h\rho_0\, v^{(s)}_{3,tt} - P. \end{aligned} \tag{1.89}$$

These conditions were first obtained in Tiersten [1969] for a free surface, using *adhoc* approach, see also (Dai et al. [2010], cf. (3.17)). We also note that refined conditions were recently discussed in Kaplunov et al. [2019b].

1.5.2.2 Asymptotic model for surface wave field

Let us implement the derived effective boundary conditions (1.89) in order to obtain an asymptotic formulation of the Rayleigh wave field.

The Helmholtz decomposition (1.22) leads to uncoupled wave equations (1.23) along with boundary conditions (1.89) becoming at $x_3 = 0$ (note that the index (s) associated with the substrate is dropped from now on for the sake of notational convenience)

$$2\phi_{,13} + \psi_{,11} - \psi_{,33} = h\,\hat{\mu}\left[c_{20}^{-2}\left(\phi_{,1tt} - \psi_{,3tt}\right) - 4\left(1 - \kappa_0^{-2}\right)\left(\phi_{,111} - \psi_{,113}\right)\right] - \frac{Q}{\mu},$$

$$\left(\kappa^2 - 2\right)\phi_{,11} + \kappa^2\,\phi_{,33} + 2\psi_{,13} = h\,\hat{\mu}\,c_{20}^{-2}\,\left(\phi_{,3tt} + \psi_{,1tt}\right) - \frac{P}{\mu}. \tag{1.90}$$

Let us establish the slow-time perturbation scheme, introducing the following dimensionless variables

$$\xi = \frac{\theta_R}{L}, \qquad \gamma = \frac{x_3}{L}, \qquad \tau = \frac{\epsilon\, c_R}{L}\, t, \tag{1.91}$$

where $\theta_R = x_1 - c_R\, t$ and τ is slow time. We note that here the parameter ϵ may be interpreted physically as a small deviation of the phase velocity of studied waves from the Rayleigh wave speed.

Equations (1.23) can be re-cast in terms of the new variables as

$$\begin{aligned}\phi_{,\gamma\gamma}+\alpha_R^2\,\phi_{,\xi\xi}+2\epsilon\left(1-\alpha_R^2\right)\phi_{,\xi\tau}-\epsilon^2\left(1-\alpha_R^2\right)\phi_{,\tau\tau}=0,\\ \psi_{,\gamma\gamma}+\beta_R^2\,\psi_{,\xi\xi}+2\epsilon\left(1-\beta_R^2\right)\psi_{,\xi\tau}-\epsilon^2\left(1-\beta_R^2\right)\psi_{,\tau\tau}=0,\end{aligned} \tag{1.92}$$

with the quantities α_R^2 and β_R^2 defined in (1.42). The boundary conditions (1.90) become

$$\begin{aligned}2\phi_{,\xi\gamma}+\psi_{,\xi\xi}-\psi_{,\gamma\gamma}=\hat{\mu}\left\{\epsilon\left(\frac{c_R^2}{c_{20}^2}-4\left(1-\kappa_0^{-2}\right)\right)\left(\phi_{,\xi\xi\xi}-\psi_{,\xi\xi\gamma}\right)\right.\\ \left.+\frac{c_R^2}{c_{20}^2}\left[2\,\epsilon^2\left(\psi_{,\xi\gamma\tau}-\phi_{,\xi\xi\tau}\right)+\epsilon^3\left(\phi_{,\xi\tau\tau}-\psi_{,\gamma\tau\tau}\right)\right]\right\}-\frac{L^2\,Q}{\mu},\end{aligned} \tag{1.93}$$

$$\begin{aligned}\left(\kappa^2-2\right)\phi_{,\xi\xi}+\kappa^2\phi_{,\gamma\gamma}+2\psi_{,\xi\gamma}=\hat{\mu}\frac{c_R^2}{c_{20}^2}\left\{\epsilon\left(\phi_{,\xi\xi\gamma}+\psi_{,\xi\xi\xi}\right)-2\epsilon^2\left(\phi_{,\xi\gamma\tau}+\psi_{,\xi\xi\tau}\right)\right.\\ \left.+\epsilon^3\left(\phi_{,\gamma\tau\tau}+\psi_{,\xi\tau\tau}\right)\right\}-\frac{L^2\,P}{\mu}\qquad\text{at}\qquad\gamma=0.\end{aligned}$$

Let us now expand the potentials ϕ and ψ as asymptotic series (cf. Kaplunov et al. [2006b])

$$\begin{aligned}\phi=\frac{1}{\epsilon}\left(\phi^{(0)}\left(\xi,\gamma,\tau\right)+\epsilon\,\phi^{(1)}\left(\xi,\gamma,\tau\right)+\epsilon^2\,\phi^{(2)}\left(\xi,\gamma,\tau\right)+...\right),\\ \psi=\frac{1}{\epsilon}\left(\psi^{(0)}\left(\xi,\gamma,\tau\right)+\epsilon\,\psi^{(1)}\left(\xi,\gamma,\tau\right)+\epsilon^2\,\psi^{(2)}\left(\xi,\gamma,\tau\right)+...\right).\end{aligned} \tag{1.94}$$

Note from the above expansion (1.94) that (1.93) becomes homogeneous at leading order.

Leading order: $O(1/\epsilon)$

Introducing (1.94) into (1.92) yields

$$\phi^{(0)}_{,\gamma\gamma} + \alpha_R^2\,\phi^{(0)}_{,\xi\xi} = 0, \qquad \text{and} \qquad \psi^{(0)}_{,\gamma\gamma} + \beta_R^2\,\psi^{(0)}_{,\xi\xi} = 0, \tag{1.95}$$

Hence, the solutions for the potentials are given by arbitrary plane harmonic functions of the first two arguments $\phi^{(0)} = \phi^{(0)}(\xi, \alpha_R\,\gamma, \tau)$ and $\psi^{(0)} = \psi^{(0)}(\xi, \beta_R\,\gamma, \tau)$.

On inserting expansions (1.94) into the boundary conditions (1.93), we get

$$\begin{aligned} 2\phi^{(0)}_{,\xi\gamma} + \psi^{(0)}_{,\xi\xi} - \psi^{(0)}_{,\gamma\gamma} &= 0, \\ \left(\kappa^2 - 2\right)\phi^{(0)}_{,\xi\xi} + \kappa^2\phi^{(0)}_{,\gamma\gamma} + 2\psi^{(0)}_{,\xi\gamma} &= 0. \end{aligned} \tag{1.96}$$

Now, employing the Cauchy-Riemann identities (1.39), equations (1.96) are then transformed as

$$\begin{aligned} 2\alpha_R\,\phi^{(0)}_{,\xi\xi} + \left(1 + \beta_R^2\right)\bar{\psi}^{(0)}_{,\xi\xi} &= 0, \\ \left(1 + \beta_R^2\right)\phi^{(0)}_{,\xi\xi} + 2\beta_R\,\bar{\psi}^{(0)}_{,\xi\xi} &= 0. \end{aligned} \tag{1.97}$$

The classical Rayleigh wave equation (1.30) then follows as a solvability condition of (1.97), along with the relation

$$\bar{\psi}^{(0)} = -\vartheta\,\phi^{(0)} \qquad \text{at} \qquad \gamma = 0, \tag{1.98}$$

where ϑ is defined in (1.44).

Next order: $O(1)$

The equations (1.92) become

$$\phi^{(1)}_{,\gamma\gamma} + \alpha_R^2\,\phi^{(1)}_{,\xi\xi} = -2\left(1-\alpha_R^2\right)\phi^{(0)}_{,\xi\tau}, \qquad \psi^{(1)}_{,\gamma\gamma} + \beta_R^2\,\psi^{(1)}_{,\xi\xi} = -2\left(1-\beta_R^2\right)\psi^{(0)}_{,\xi\tau}. \tag{1.99}$$

Corrector terms $\phi^{(1)}$ and $\psi^{(1)}$ may be represented by

$$\phi^{(1)} = \phi^{(1,0)} + \gamma\,\phi^{(1,1)}, \qquad \text{and} \qquad \psi^{(1)} = \psi^{(1,0)} + \gamma\,\psi^{(1,1)}, \tag{1.100}$$

where $\phi^{(1,0)} = \phi^{(1,0)}\left(\xi, \alpha_R\,\gamma, \tau\right)$ and $\psi^{(1,0)} = \psi^{(1,0)}\left(\xi, \beta_R\,\gamma, \tau\right)$ are arbitrary plane harmonic functions in the first two arguments. For the functions $\phi^{(1,1)}$ and $\psi^{(1,1)}$, we obtain

$$\phi^{(1,1)} = -\frac{\left(1-\alpha_R^2\right)}{\alpha_R}\,\bar{\phi}^{(0)}_{,\tau}, \qquad \psi^{(1,1)} = -\frac{\left(1-\beta_R^2\right)}{\beta_R}\,\bar{\psi}^{(0)}_{,\tau}, \tag{1.101}$$

with the bar as before denoting a harmonic conjugate, for more detail see Kaplunov et al. [2006b].

The boundary conditions (1.93) at $\gamma = 0$ give

$$2\phi^{(1)}_{,\xi\gamma} + \psi^{(1)}_{,\xi\xi} - \psi^{(1)}_{,\gamma\gamma} - \hat{\mu}\left(\frac{c_R^2}{c_{20}^2} - 4\left(1-\kappa_0^{-2}\right)\right)\left(\phi^{(0)}_{,\xi\xi\xi} - \psi^{(0)}_{,\xi\xi\gamma}\right) = -\frac{L^2\,\mathcal{H}\left(Q\right)}{\mu},$$

$$\left(\kappa^2-2\right)\phi^{(1)}_{,\xi\xi} + \kappa^2\phi^{(1)}_{,\gamma\gamma} + 2\psi^{(1)}_{,\xi\gamma} - \hat{\mu}\,\frac{c_R^2}{c_{20}^2}\left(\phi^{(0)}_{,\xi\xi\gamma} + \psi^{(0)}_{,\xi\xi\xi}\right) = -\frac{L^2\,P}{\mu}, \tag{1.102}$$

where $\hat{\mu}$ defined in (1.68) and $\mathcal{H}$ denoting the Hilbert transform (1.46).

Using (1.98)-(1.101) along with (1.39), from sovability of (1.102), we arrive at

$$\frac{1}{2B_{_I}}\left[4\alpha_R\,\beta_R-(1+\beta_R^2)^2\right]\phi^{(1,0)}_{,\xi\xi}+2\,\phi^{(0)}_{,\xi\tau}-b_{_I}\,\bar{\phi}^{(0)}_{,\xi\xi\xi} \\ =-\frac{L^2}{2\mu B_{_I}}\left[\left(1+\beta_R^2\right)P+2\beta_R\,\mathcal{H}\left(Q\right)\right], \tag{1.103}$$

where $B_{_I}$ is defined in (1.54) and

$$b_{_I}=\frac{\hat{\mu}}{2B_{_I}}\left(1-\beta_R^2\right)\left[\frac{c_R^2}{c_{20}^2}\left(\alpha_R+\beta_R\right)-4\beta_R\left(1-\kappa_0^{-2}\right)\right]. \tag{1.104}$$

In view of (1.30), the first term in (1.103) vanishes, therefore we get

$$2\,\phi^{(0)}_{,\xi\tau}+\frac{b_{_I}}{\alpha_R}\,\phi^{(0)}_{,\xi\xi\gamma}=-\frac{L^2\,\beta_R}{\mu B_{_I}}\left[\vartheta P+\mathcal{H}\left(Q\right)\right]\quad\text{at}\quad\gamma=0. \tag{1.105}$$

Using the leading order approximation

$$\phi\approx\frac{1}{\epsilon}\,\phi^{(0)},\qquad\psi\approx\frac{1}{\epsilon}\,\psi^{(0)}, \tag{1.106}$$

and operator identities

$$2\epsilon\,\frac{\partial}{\partial\xi\partial\tau}=L^2\,\Box_R+O(\epsilon^2),\qquad\frac{\partial^3}{\partial\xi^2\partial\gamma}=L^3\,\frac{\partial^2}{\partial x_1^2\partial x_3}, \tag{1.107}$$

equation (1.105) on the interface $x_3=0$ can be rewritten in terms of the original dimensional variables (x_1,x_3,t) as

$$\Box_R\,\phi+\frac{b_{_I}\,h}{\alpha_R}\,\phi_{,113}=-\frac{\beta_R}{\mu B_{_I}}\left[\vartheta P+\mathcal{H}\left(Q\right)\right]. \tag{1.108}$$

The elliptic equations for the potentials ϕ and ψ follow from (1.95)

$$\phi_{,33} + \alpha_R^2 \, \phi_{,11} = 0, \qquad \text{and} \qquad \psi_{,33} + \beta_R^2 \, \psi_{,11} = 0. \tag{1.109}$$

Note that the potentials ϕ and ψ are related by (1.98), which in view of (1.107) transforms to (1.43).

The derived model for the Rayleigh wave field contains the 2D elliptic equations (1.109), governing the decay over the interior ($x_3 \geq 0$) along with the boundary conditions (1.108) and (1.43). Observe that in case of no coating ($h = 0$), the formulation is identical to the hyperbolic-elliptic formulation presented in Subsection 1.4.3, see (1.52).

Now, equation (1.108) on the interface $x_3 = 0$ may be expressed in the form of a pseudo-differential equation on the surface by presenting the derivative $\phi_{,3}$ in terms of the potential at the surface $\phi(x_1, 0, t)$. Indeed, the solution of equation $(1.109)_1$, can be written in symbolic form as

$$\phi(x_1, x_3, t) = \exp\left(-\alpha_R \sqrt{-\partial_{11}} \; x_3\right) \phi(x_1, 0, t), \tag{1.110}$$

where $\sqrt{-\partial_{11}} = \sqrt{-\partial^2/\partial x_1^2}$ is understood as a pseudo-differential operator.

Then at $x_3 = 0$, we have

$$\phi_{,3} = -\alpha_R \sqrt{-\partial_{11}} \, \phi. \tag{1.111}$$

Inserting (1.111) into (1.108), we get

$$\Box_R \, \phi - b_I h \sqrt{-\partial_{11}} \, \phi_{,11} = -\frac{\beta_R}{\mu B_I} \left[\vartheta P + \mathcal{H}\left(Q\right)\right]. \tag{1.112}$$

Note that in the case of $Q = 0$, (1.112) coincides with the result obtained in Dai et al. [2010] (cf. equation (5.4) in cited paper). As also noted in Dai et al. [2010], an alternative representation involving the Hilbert transform can also be constructed. Indeed,

$$\sqrt{-\partial_{11}}\ \phi = -\frac{1}{\alpha_R}\,\phi_{,3} = \bar{\phi}_{,1} = \mathcal{H}\left(\phi_{,1}\right), \tag{1.113}$$

at $x_3 = 0$. Therefore, we arrive at the following equation on the interface $x_3 = 0$

$$\Box_R\,\phi - b_I h\,\mathcal{H}\left(\phi_{,111}\right) = -\frac{\beta_R}{\mu B_I}\left[\vartheta P + \mathcal{H}\left(Q\right)\right]. \tag{1.114}$$

The derived equation (1.112) leads to the approximation of the exact dispersion relation (1.67) within the long-wave region, e.g., see Shuvalov and Every [2008], giving

$$v^{ph} = \frac{c}{c_R} = 1 - \frac{b_I}{2}\mid \hat{k}h \mid + ..., \tag{1.115}$$

which demonstrates that the Rayleigh wave speed c_R is associated with a local minimum ($b < 0$) or maximum ($b > 0$) of the phase speed.

Let us now illustrate the approximate relation (1.115) by comparison with the exact dispersion relation (1.67). The blue solid and dashed lines correspond to (1.67) and (1.115), respectively.

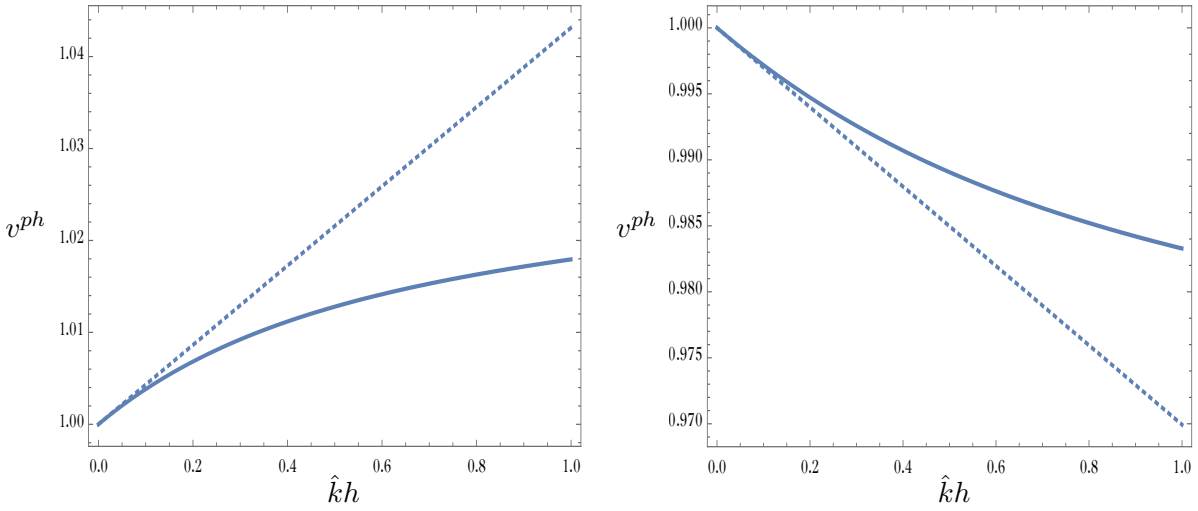

(a) $E_0 = 1$, $\nu_0 = 0.3$, $E = 0.9$ and $\nu = 0.2$. (b) $E_0 = 0.9$, $\nu_0 = 0.2$, $E = 1$ and $\nu = 0.3$.

Figure 1.6: (1.67) vs. (1.115) with $\rho_0 \,/\, \rho = 1$: dependence of v^{ph} on $\hat{k}h$.

It is seen that (1.115) provides a linear approximation in the long-wave limit.

Finally, we note that (1.114) and (1.47) can be combined, implying equations for interfacial displacements in the form

$$\Box_R \, u_1 - hb_{_I} \sqrt{-\partial_{11}} \; u_{1,11} = -\frac{\beta_R \, (1 - \beta_R^2)}{2\mu B_{_I}} \left[\vartheta \, P_{,1} + \mathcal{H} \, (Q_{,1}) \right], \tag{1.116}$$

and

$$\Box_R \, u_3 - hb_{_I} \sqrt{-\partial_{11}} \; u_{3,11} = -\frac{\alpha_R \, (1 - \beta_R^2)}{2\mu B_{_I}} \left[\mathcal{H} \, (P_{,1}) - \vartheta^{-1} \, Q_{,1} \right]. \tag{1.117}$$

Chapter 2

Explicit model for surface wave on a coated orthotropic half-space

This chapter is concerned with elastic surface wave propagating in an orthotropic elastic half-space coated by a thin orthotropic layer subject to vertical and tangential loads. The coating is modelled by means of "effective boundary conditions", derived in Section 2.2. An explicit model for the Rayleigh wave is then obtained in Section 2.3, generalising results in Dai et al. [2010], Şahin [2020], Nobili and Prikazchikov [2018], taking into account the anisotropy of the media. The model contains an elliptic equation governing the behaviour within the half-space, expressed in terms of an auxiliary plane harmonic function, along with a pseudo-differential equation on the interface between the coating and the half-space.

2.1 Problem statement

Consider a linearly elastic orthotropic half-space coated by a thin orthotropic layer, subject to boundary conditions at the surface $x_3 = -h$ of the coating, taken as (1.50), with continuity of the displacements at the interface assumed as (1.69). The constitutive relations of an orthotropic solid are given by (1.4). We also denote the material parameters of the coating ($-h \leq x_3 \leq 0$) by c^0_{11}, c^0_{33}, c^0_{13} and c^0_{55}, while for the substrate ($x_3 \geq 0$) these are supposed as c_{11}, c_{33}, c_{13} and c_{55}. Throughout this chapter we restrict the consideration to the plane strain formulation (1.9).

2.2 Effective boundary conditions

Following the same procedure as in Subsection 1.5.2, we derive the effective boundary conditions, modelling the effect of the coating at the interface $x_3 = 0$.

We operate in terms of a small parameter ϵ as defined in (1.70) along with the scaled variables (1.71) and (1.72) with

$$\hat{\tau}_0 = \frac{c_0}{L}\, t, \tag{2.1}$$

where c_0 is the wave speed, defined by

$$c_0 = \sqrt{\frac{c^0_{55}}{\rho_0}}.$$

The appropriate dimensionless scaling is given as

$$\begin{aligned} \hat{q}^* &= \frac{1}{\epsilon\, c^0_{55}}\, Q, & \hat{p}^* &= \frac{1}{\epsilon\, c^0_{55}}\, P, \\ \hat{\sigma}^*_{11} &= \frac{1}{c^0_{55}}\, \sigma_{11}, \qquad \text{and} & \hat{\sigma}^*_{r3} &= \frac{1}{\epsilon\, c^0_{55}}\, \sigma_{r3}, \qquad r = 1, 3. \end{aligned} \tag{2.2}$$

The equations of motion (1.11) – (1.13) and the constitutive relations linking the orthotropic elastic solids (1.4) are rewritten in terms of new variables as

$$\begin{aligned} &\hat{\sigma}^*_{11,\xi_0} + \hat{\sigma}^*_{31,\eta} = u^*_{i,\hat{\tau}_0\hat{\tau}_0}, \\ &\hat{\sigma}^*_{33,\eta} + \epsilon\,\hat{\sigma}^*_{31,\xi_0} = u^*_{3,\hat{\tau}_0\hat{\tau}_0}, \end{aligned} \tag{2.3}$$

and

$$\begin{aligned} \epsilon\,\hat{\sigma}^*_{11} &= \frac{1}{c^0_{55}}\left(c^0_{13}\,u^*_{3,\eta} + \epsilon\,c^0_{11}\,u^*_{1,\xi_0}\right), \\ \epsilon^2\,\hat{\sigma}^*_{33} &= \frac{1}{c^0_{55}}\left(c^0_{33}\,u^*_{3,\eta} + \epsilon\,c^0_{13}\,u^*_{1,\xi_0}\right), \\ \epsilon^2\,\hat{\sigma}^*_{31} &= u^*_{1,\eta} + \epsilon\,u^*_{3,\xi_0}. \end{aligned} \tag{2.4}$$

The associated boundary conditions (1.50) and (1.69) become

$$\begin{aligned} \hat{\sigma}^*_{13} = -\hat{q}^*, \qquad \hat{\sigma}^*_{33} = -\hat{p}^* \qquad &\text{at} \qquad \eta = -1, \\ \text{and} \qquad u^*_r = v^*_r \qquad &\text{at} \qquad \eta = 0. \end{aligned} \tag{2.5}$$

We now expand the displacements and stresses as asymptotic series in terms of the small parameter ϵ

$$\begin{pmatrix} u^*_r \\ \hat{\sigma}^*_{11} \\ \hat{\sigma}^*_{r3} \end{pmatrix} = \begin{pmatrix} u^{(0)}_r \\ \hat{\sigma}^{(0)}_{11} \\ \hat{\sigma}^{(0)}_{r3} \end{pmatrix} + \epsilon \begin{pmatrix} u^{(1)}_r \\ \hat{\sigma}^{(1)}_{11} \\ \hat{\sigma}^{(1)}_{r3} \end{pmatrix} + \ldots. \tag{2.6}$$

At leading order, we have from (2.3) and (2.4)

$$\begin{aligned} &\hat{\sigma}^{(0)}_{11,\xi_0} + \hat{\sigma}^{(0)}_{31,\eta} = u_{1,\hat{\tau}_0\hat{\tau}_0}, \\ &\hat{\sigma}^{(0)}_{33,\eta} = u^{(0)}_{3,\hat{\tau}_0\hat{\tau}_0}, \\ &u^*_{r,\eta} = 0, \end{aligned} \tag{2.7}$$

and the boundary conditions (2.5) take the form

$$\begin{aligned} &\hat{\sigma}_{13}^{(0)} = -\hat{q}^*, \qquad \sigma_{33}^{(0)} = -\hat{p}^* \qquad \text{at} \qquad \eta = -1, \\ &\text{and} \qquad u_r^{(0)} = v_r^* \qquad \text{at} \qquad \eta = 0. \end{aligned} \tag{2.8}$$

The leading order displacements satisfying $(2.7)_3$ and $(2.8)_2$ are found as

$$u_r^{(0)} = v_r^*, \tag{2.9}$$

hence, from $(2.7)_2$, $(2.8)_1$ and (2.9)

$$\hat{\sigma}_{33}^{(0)} = (\eta + 1)\ v_{3,\hat{\tau}_0\hat{\tau}_0}^* - \hat{p}^*. \tag{2.10}$$

At next order, equation $(2.4)_2$ and the boundary condition $(2.5)_2$ imply

$$u_3^{(1)} = \frac{c_{13}^0}{c_{33}^0}\, u_{1,\xi_0}^{(0)}, \tag{2.11}$$

and

$$u_r^{(1)} = 0 \qquad \text{at} \qquad \eta = 0. \tag{2.12}$$

From (2.11), satisfying the boundary condition (2.12), we infer

$$u_3^{(1)} = -\eta\, \frac{c_{13}^0}{c_{33}^0}\, v_{1,\xi_0}^*. \tag{2.13}$$

Next, substituting (2.9) and (2.13) into $(2.4)_1$, we deduce

$$\hat{\sigma}_{11}^{(0)} = \frac{\delta_{11}}{c_{55}^0}\, v_{1,\xi_0}^*, \tag{2.14}$$

where

$$\delta_{11} = c^0_{11} - \frac{\left(c^0_{13}\right)^2}{c^0_{33}}.$$

Finally, we obtain the shear stress from $(2.7)_1$, $(2.8)_1$, (2.9) and (2.14)

$$\hat{\sigma}^{(0)}_{31} = \frac{(1+\eta)}{c^0_{55}}\left(c^0_{55}\, v^*_{1,\hat{\tau}_0\hat{\tau}_0} - \delta_{11}\, v^*_{1,\xi_0\xi_0}\right) - \hat{q}^*. \tag{2.15}$$

In the original variables, the effective boundary conditions relating substrate stresses and displacements at the interface $x_3 = 0$ follow from (2.10) and (2.15) as

$$\begin{aligned} \sigma_{31} &= h\left(\rho_0\, u_{1,tt} - \delta_{11}\, u_{1,11}\right) - Q, \\ \sigma_{33} &= \rho_0\, h\, u_{3,tt} - P. \end{aligned} \tag{2.16}$$

Note that in absence of loading ($P = Q = 0$) conditions (2.16) may be verified to coincide with those obtained previously by Vinh and Linh [2012], (cf. Eqs. (10) - (12)). Previously derived conditions for an isotropic layer (1.89) follow from (2.16) if (1.5) holds.

Also, the obtained effective boundary conditions of (2.16) can be generalised to 3D setup, taking the form

$$\begin{aligned} \sigma_{31} &= h\left(\rho_0\, u_{1,tt} - c^0_{66}\, u_{1,22} - \delta_{11}\, u_{1,11} - \left(c^0_{66} + \delta_{12}\right) u_{2,12}\right) - Q_1, \\ \sigma_{32} &= h\left(\rho_0\, u_{2,tt} - c^0_{66}\, u_{2,11} - \delta_{22}\, u_{2,22} - \left(c^0_{66} + \delta_{12}\right) u_{1,12}\right) - Q_2, \\ \sigma_{33} &= \rho_0\, h\, u_{3,tt} - P, \end{aligned} \tag{2.17}$$

where

$$\delta_{ii} = c^0_{ii} - \frac{\left(c^0_{i3}\right)^2}{c^0_{33}} \qquad \text{and} \qquad \delta_{12} = c^0_{12} - \frac{c^0_{13}\, c^0_{23}}{c^0_{33}}, \quad i = 1, 2,$$

and Q_1 and Q_2 denote the components of prescribed in-plane surface load in the x_1, x_2 directions, respectively.

2.3 Asymptotic model for surface wave

Now, having the effective boundary conditions (2.16), we can derive a pseudo-differential equation on the interface $x_3 = 0$. The problem formulation for the substrate $x_3 \geq 0$ involves equations of motion (1.14) with (1.9)

$$\begin{aligned} c_{11}\, u_{1,11} + (c_{13} + c_{55})\, u_{3,13} + c_{55}\, u_{1,33} &= \rho\, u_{1,tt}, \\ c_{33}\, u_{3,33} + (c_{13} + c_{55})\, u_{1,13} + c_{55}\, u_{3,11} &= \rho\, u_{3,tt}, \end{aligned} \tag{2.18}$$

subject to

$$\begin{aligned} c_{55}\,(u_{1,3} + u_{3,1}) &= h\,(\rho_0\, u_{1,tt} - \delta_{11}\, u_{1,11}) - Q, \\ \text{and} \qquad\qquad & \\ c_{13}\, u_{1,11} + c_{33}\, u_{3,3} &= \rho_0\, h\, u_{3,tt} - P. \end{aligned} \tag{2.19}$$

Once again, we introduce the slow-time perturbation procedure, relying on the scaled variables in (1.91) together with the ansatz in the form of travelling wave

$$u_r = U_r\,(\xi, \gamma, \tau)\,, \quad r = 1, 3. \tag{2.20}$$

Thus, the perturbed equations of (2.18) are rewritten

$$\begin{aligned} \left(c_{11} - \rho\, c_R^2\right) U_{1,\xi\xi} + c_{55}\, U_{1,\gamma\gamma} + D\, U_{3,\xi\gamma} &= \rho\, c_R^2 \left(\epsilon^2\, U_{1,\tau\tau} - 2\epsilon\, U_{1,\xi\tau}\right), \\ c_{33}\, U_{3,\gamma\gamma} + D\, U_{1,\xi\gamma} + \left(c_{55} - \rho\, c_R^2\right) U_{3,\xi\xi} &= \rho\, c_R^2 \left(\epsilon^2 U_{3,\tau\tau} - 2\epsilon c_R\, U_{3,\xi\tau}\right), \end{aligned} \tag{2.21}$$

where $D = c_{13} + c_{55}$.

Equation (2.21) may be transformed to a single fourth-order PDE for U_1 as

$$\begin{aligned} &A_0\,U_{1,\xi\xi\xi\xi} + A_1\,U_{1,\xi\xi\gamma\gamma} + A_2\,U_{1,\gamma\gamma\gamma\gamma} + \epsilon\,(B_1\,U_{1,\xi\xi\xi\tau} + B_2\,U_{1,\xi\gamma\gamma\tau}) \\ &\qquad -\epsilon^2\,(D_1\,U_{1,\xi\xi\tau\tau} + D_2\,U_{1,\gamma\gamma\tau\tau}) - \epsilon^3\,E_1\,U_{1,\xi\tau\tau\tau} + \epsilon^4\,E_2\,U_{1,\tau\tau\tau\tau} = 0, \end{aligned} \tag{2.22}$$

where the coefficients specify as

$$A_0 = (c_{11} - \rho\,c_R^2)\,(c_{55} - \rho\,c_R^2)\,,$$

$$A_1 = c_{11}\,c_{33} + c_{55}^2 - D^2 - (c_{33} + c_{55})\,\rho\,c_R^2,$$

$$A_2 = c_{33}\,c_{55},$$

$$B_1 = 2\rho\,c_R^2\,(c_{11} + c_{55} - 2\rho\,c_R^2)\,,$$

$$B_2 = 2\rho\,c_R^2\,(c_{33} + c_{55})\,,$$

$$D_1 = \rho\,c_R^2\,(c_{11} + c_{55} - 6\,\rho c_R^2)\,,$$

$$D_2 = \rho\,c_R^2\,(c_{33} + c_{55})\,,$$

$$E_1 = 4\rho^2\,c_R^4,$$

$$E_2 = \rho^2\,c_R^4.$$

The conditions (2.19) at $\gamma = 0$ are then reformulated as

$$\begin{aligned} &U_{1,\gamma} + U_{3,\xi} = \frac{c_{55}^0}{c_{55}}\left[\epsilon\left(\frac{c_R^2}{c_0^2} - \frac{\delta_{11}}{c_{55}^0}\right)U_{1,\xi\xi} + \frac{c_R^2}{c_0^2}\left(\epsilon^3\,U_{1,\tau\tau} - 2\epsilon^2\,U_{1,\xi\tau}\right)\right] - \frac{L\,Q}{c_{55}}, \\ &c_{13}\,U_{1,\xi} + c_{33}\,U_{3,\gamma} = \frac{c_{55}^0\,c_R^2}{c_0^2}\left[\epsilon\,U_{3,\xi\xi} - 2\epsilon^2\,U_{3,\xi\tau} + \epsilon^3 U_{3,\tau\tau}\right] - L\,P, \end{aligned} \tag{2.23}$$

where

$$c_0 = \sqrt{\frac{c_{55}^0}{\rho_0}}.$$

Let us now expand the displacements U_r as asymptotic series

$$U_r = \frac{1}{\epsilon}\, U_r^{(0)}\,(\xi,\gamma,\tau) + U_r^{(1)}\,(\xi,\gamma,\tau) + ..., \quad r = 1,3. \tag{2.24}$$

2.3.1 Leading order

At leading order, equation $(2.21)_1$ becomes

$$\left(c_{11} - \rho\, c_R^2\right) U_{1,\xi\xi}^{(0)} + c_{55}\, U_{1,\gamma\gamma}^{(0)} + \beta\, U_{3,\xi\gamma}^{(0)} = 0, \tag{2.25}$$

while equation (2.22) gives

$$A_0\, U_{1,\xi\xi\xi\xi}^{(0)} + A_1\, U_{1,\xi\xi\gamma\gamma}^{(0)} + A_2\, U_{1,\gamma\gamma\gamma\gamma}^{(0)} = 0. \tag{2.26}$$

It may be shown that the equation (2.26) is elliptic, expressed in operator form as

$$\Delta_1\, \Delta_2\, U_1^{(0)} = 0, \tag{2.27}$$

wherein

$$\Delta_i = \partial_{\xi\xi}^2 + \lambda_i^2\, \partial_{\gamma\gamma}^2, \quad i = 1,2,$$

and λ_1 and λ_2 satisfy

$$\lambda_1^2 + \lambda_2^2 = \frac{A_1}{A_2}, \qquad \lambda_1^2\ \lambda_2^2 = \frac{A_0}{A_2}. \tag{2.28}$$

Here, we restrict ourselves to the case when λ_1 and λ_2 are positive real numbers. Hence, the solution of (2.27) may be expressed in terms of a pair of plane harmonic functions

$$U_1^{(0)} = \phi^{(0)}\left(\xi, \lambda_1\,\gamma, \tau\right) + \psi^{(0)}\left(\xi, \lambda_2\,\gamma, \tau\right). \tag{2.29}$$

Inserting the solution (2.29) into equation (2.25), calling upon the Cauchy-Riemann identities (1.39), we arrive at

$$U_3^{(0)} = \beta_1\,\bar{\phi}^{(0)}\left(\xi, \lambda_1\,\gamma, \tau\right) + \beta_2\,\bar{\psi}^{(0)}\left(\xi, \lambda_2\,\gamma, \tau\right), \tag{2.30}$$

where

$$\beta_i = \frac{\rho\,c_R^2 - c_{11} + \lambda_i^2\,c_{55}}{D\,\lambda_i}, \quad i = 1, 2. \tag{2.31}$$

Plugging the solutions (2.29) and (2.30) into the boundary conditions (2.23) at leading order, we have at $\gamma = 0$

$$\begin{aligned} &\beta_1\,\bar{\phi}_{,\xi}^{(0)} + \phi_{,\gamma}^{(0)} + \beta_2\,\bar{\psi}_{,\xi}^{(0)} + \psi_{,\gamma}^{(0)} = 0, \\ &c_{13}\,\phi_{,\xi}^{(0)} + c_{33}\,\beta_1\,\bar{\phi}_{,\gamma}^{(0)} + c_{13}\,\psi_{,\xi}^{(0)} + c_{33}\,\beta_2\,\bar{\psi}_{,\xi}^{(0)} = 0. \end{aligned} \tag{2.32}$$

Applying again the Cauchy-Riemann identities (1.39), we deduce

$$\begin{aligned} &\left(\beta_1 - \lambda_1\right)\bar{\phi}_{,\xi}^{(0)} + \left(\beta_2 - \lambda_2\right)\bar{\psi}_{,\xi}^{(0)} = 0, \\ &\left(c_{13} + c_{33}\,\beta_1\,\lambda_1\right)\phi_{,\xi}^{(0)} + \left(c_{13} + c_{33}\,\beta_2\,\lambda_2\right)\psi_{,\xi}^{(0)} = 0 \quad \text{at} \quad \gamma = 0. \end{aligned} \tag{2.33}$$

On taking harmonic conjugate of equation $(2.33)_1$, the classical surface wave equation follows as a solvability condition, given

$$\text{Det}\begin{bmatrix} \beta_1 - \lambda_1 & \beta_2 - \lambda_2 \\ c_{13} + c_{33}\,\beta_1\,\lambda_1 & c_{13} + c_{33}\,\beta_2\,\lambda_2 \end{bmatrix} = 0, \tag{2.34}$$

or, equivalently

$$\hat{\vartheta} = \frac{\beta_1 - \lambda_1}{\beta_2 - \lambda_2} = \frac{c_{13} + c_{33}\,\beta_1\,\lambda_1}{c_{13} + c_{33}\,\beta_2\,\lambda_2}. \tag{2.35}$$

Now, it is possible to relate the elastic potentials to each other as

$$\psi^{(0)} = -\hat{\vartheta}\ \phi^{(0)} \qquad \text{at} \qquad \gamma = 0. \tag{2.36}$$

Accordingly, the displacements U_1 and U_2 can be expressed in terms of a single plane harmonic function on the surface $\gamma = 0$, say $\phi^{(0)}$ as

$$U_1^{(0)} = \phi^{(0)}(\xi, \lambda_1\gamma, \tau) - \hat{\vartheta}\,\phi^{(0)}(\xi, \lambda_2\gamma, \tau). \tag{2.37}$$

and

$$U_3^{(0)} = \beta_1\,\bar{\phi}^{(0)}\,(\xi, \lambda_1\,\gamma, \tau) - \hat{\vartheta}\,\beta_2\ \bar{\phi}^{(0)}\,(\xi, \lambda_2\,\gamma, \tau)\,. \tag{2.38}$$

2.3.2 Next order correction

On proceeding to the next order, equations $(2.21)_1$ and (2.22) become

$$\left(c_{11} - \rho\,c_R^2\right) U_{1,\xi\xi}^{(1)} + c_{55}\,U_{1,\gamma\gamma}^{(1)} + D\,U_{3,\xi\gamma}^{(1)} = -2\rho\,c_R^2\,U_{1,\xi\tau}^{(0)}, \tag{2.39}$$

$$A_2\,\Delta_1\ \Delta_2\,U_1^{(1)} = -2\rho\,c_R^2\left[\left(c_{11} + c_{55} - 2\rho\,c_R^2\right) U_{1,\xi\xi\xi\tau}^{(0)} + \left(c_{33} + c_{55}\right) U_{1,\xi\gamma\gamma\tau}^{(0)}\right]. \tag{2.40}$$

The expression of $U_1^{(1)}$ and the derivatives $U_{3,\gamma}^{(1)}$, $U_{3,\xi}^{(1)}$ are found similar to Nobili and Prikazchikov [2018] as

$$U_1^{(1)}(\xi,\gamma,\tau) = \phi^{(1)}(\xi,\lambda_1\gamma,\tau) + \psi^{(1)}(\xi,\lambda_2\gamma,\tau) + \frac{\gamma}{2A_2(\lambda_2^2-\lambda_1^2)}\left[\frac{\Lambda_1}{\lambda_1}\bar{\phi}_{,\tau}^{(0)} - \frac{\Lambda_2}{\lambda_2}\bar{\psi}_{,\tau}^{(0)}\right], \tag{2.41}$$

$$U_{3,\gamma}^{(1)}(\xi,\gamma,\tau) = \beta_1\lambda_1\phi_{,\xi}^{(1)}(\xi,\lambda_1\gamma,\tau) + \beta_2\lambda_2\psi_{,\xi}^{(1)}(\xi,\lambda_2\gamma,\tau) - D^{-1}\left[2\rho c_R^2 + \frac{\Lambda_1}{c_{33}(\lambda_2^2-\lambda_1^2)}\right]\phi_{,\tau}^{(0)} - D^{-1}\left[2\rho c_R^2 + \frac{\Lambda_2}{c_{33}(\lambda_1^2-\lambda_2^2)}\right]\psi_{,\tau}^{(0)} + \frac{\gamma}{2A_2(\lambda_2^2-\lambda_1^2)}\left[\Lambda_1\beta_1\bar{\phi}_{,\xi\tau}^{(0)} - \Lambda_2\beta_2\bar{\psi}_{,\xi\tau}^{(0)}\right], \tag{2.42}$$

and

$$U_{3,\xi}^{(1)}(\xi,\gamma,\tau) = \beta_1\bar{\phi}_{,\xi}^{(1)} + \beta_2\bar{\psi}_{,\xi}^{(1)} - \frac{1}{\lambda_1 D}\left[2\rho c_R^2 + \frac{\Lambda_1(2c_{55}\lambda_1-\beta_1 D)}{2A_2\lambda_1(\lambda_2^2-\lambda_1^2)}\right]\bar{\phi}_{,\tau}^{(0)} - \frac{1}{\lambda_2 D}\left[2\rho c_R^2 + \frac{\Lambda_2(2c_{55}\lambda_2-\beta_2 D)}{2A_2\lambda_2(\lambda_1^2-\lambda_2^2)}\right]\bar{\psi}_{,\tau}^{(0)} + \frac{\gamma}{2A_2(\lambda_2^2-\lambda_1^2)}\left[\frac{\Lambda_2\beta_2}{\lambda_2}\psi_{,\xi\tau}^{(0)} - \frac{\Lambda_1\beta_1}{\lambda_1}\phi_{,\xi\tau}^{(0)}\right], \tag{2.43}$$

where

$$\Lambda_i = -2\rho c_R^2\left[c_{11}+c_{55}-(c_{33}+c_{55})\lambda_i^2 - 2\rho c_R^2\right].$$

The boundary conditions (2.23) lead to

$$U^{(1)}_{1,\gamma} + U^{(1)}_{3,\xi} = \frac{c^0_{55}}{c_{55}}\left(\frac{c^2_R}{c^2_0} - \frac{\delta_{11}}{c^0_{55}}\right) U^{(1)}_{1,\xi\xi} - \frac{L\,Q}{c_{55}},$$

$$c_{13}\,U^{(1)}_{1,\xi} + c_{33}\,U^{(1)}_{3,\gamma} = \frac{c^0_{55}\,c^2_R}{c^2_0}\,U^{(0)}_{3,\xi\xi} - L\,P \qquad \text{at} \qquad \gamma = 0. \tag{2.44}$$

On substituting the solutions (2.29), (2.30) and (2.41)-(2.43) into (2.44), making use of the Cauchy-Riemann identities (1.39), we get at $\gamma = 0$

$$(\beta_1 - \lambda_1)\,\bar{\phi}^{(1)}_{,\xi} + (\beta_2 - \lambda_2)\,\bar{\psi}^{(1)}_{,\xi} - (\beta_1 - \lambda_1)\left(M_{11}\,\bar{\phi}^{(0)}_{,\tau} + M_{12}\,\bar{\psi}^{(0)}_{,\tau}\right)$$

$$-\frac{c^0_{55}}{c_{55}}\left(\frac{c^2_R}{c^2_0} - \frac{\delta_{11}}{c^0_{55}}\right)\left(\phi^{(0)}_{,\xi\xi} + \psi^{(0)}_{,\xi\xi}\right) = -\frac{L\,\mathcal{H}\,(Q)}{c_{55}}, \tag{2.45}$$

and

$$(c_{13} + c_{33}\,\beta_1\,\lambda_1)\,\phi^{(1)}_{,\xi} + (c_{13} + c_{33}\,\beta_2\,\lambda_2)\,\psi^{(1)}_{,\xi} - (c_{13} + c_{33}\,\beta_1\,\lambda_1)$$

$$\left(M_{21}\,\phi^{(0)}_{,\tau} + M_{22}\,\psi^{(0)}_{,\tau}\right) - \frac{c^0_{55}\,c^2_R}{c^2_0}\left(\beta_1\,\bar{\phi}^{(0)}_{,\xi\xi} + \beta_2\,\bar{\psi}^{(0)}_{,\xi\xi}\right) = -L\,P, \tag{2.46}$$

where

$$(\beta_1 - \lambda_1)\,M_{1i} = \frac{1}{\lambda_i\,D}\left[2\rho\,c^2_R + \Lambda_j\frac{(\beta_j\,D + (D - 2c_{55})\,\lambda_i)}{2A_2\,\lambda_i\,(\lambda^2_i - \lambda^2_j)}\right],$$

and

$$(c_{13} + c_{33}\,\beta_1\,\lambda_1)\,M_{2i} = \frac{1}{D}\left[2\rho\,c_{33}\,c^2_R - \frac{\Lambda_i}{(\lambda^2_i - \lambda^2_j)}\right], \quad i \neq j = 1, 2.$$

On differentiating (2.45) and (2.46) with respect to ξ and using (2.36), after some algebraic manipulations we get

$$\left[\frac{c_{13}+c_{33}\,\beta_2\,\lambda_2}{c_{13}+c_{33}\,\beta_1\,\lambda_1}-\frac{(\beta_2-\lambda_2)}{(\beta_1-\lambda_1)}\right]\psi^{(1)}_{,\xi\xi}-\left[(M_{21}-M_{11})-\hat{\vartheta}\,(M_{22}-M_{12})\right]\phi^{(0)}_{,\xi\tau}$$

$$-\left[\frac{(\rho_0\,c_R^2-\delta_{11})\left(1-\hat{\vartheta}\right)}{c_{55}\,(\beta_1-\lambda_1)}+\frac{\rho_0\,c_R^2\left(\beta_1-\hat{\vartheta}\,\beta_2\right)}{c_{13}+c_{33}\,\beta_1\,\lambda_1}\right]\bar{\phi}^{(0)}_{,\xi\xi\xi} \tag{2.47}$$

$$=-\frac{L\,P_{,\xi}}{c_{13}+c_{33}\,\beta_1\,\lambda_1}+\frac{L\,\mathcal{H}\,(Q_{,\xi})}{c_{55}\,(\beta_1-\lambda_1)}\qquad\text{at}\qquad\gamma=0.$$

From the solvability condition (2.34), we have

$$2\,\phi^{(0)}_{,\xi\tau}+\frac{b_o}{\lambda_1}\,\phi^{(0)}_{,\xi\xi\gamma}=-\frac{L}{B_o}\left[\frac{P_{,\xi}}{c_{13}+c_{33}\,\beta_1\,\lambda_1}-\frac{\mathcal{H}\,(Q_{,\xi})}{c_{55}\,(\beta_1-\lambda_1)}\right]\quad\text{at}\quad\gamma=0, \tag{2.48}$$

where

$$B_o=-\frac{1}{2}\left[M_{21}-M_{11}-\hat{\vartheta}\,(M_{22}-M_{12})\right], \tag{2.49}$$

and

$$b_o=\frac{1}{B_o}\left[\frac{(\rho_0\,c_R^2-\delta_{11})\left(1-\hat{\vartheta}\right)}{c_{55}\,(\beta_1-\lambda_1)}+\frac{\rho_0\,c_R^2\left(\beta_1-\hat{\vartheta}\,\beta_2\right)}{c_{13}+c_{33}\,\beta_1\,\lambda_1}\right]. \tag{2.50}$$

On returning to the original variables by using the approximate operator relation (1.107) along with the auxiliary harmonic function (1.106), we arrive at the elliptic equation for the auxiliary function ϕ

$$\phi_{,11}+\lambda_1^2\,\phi_{,33}=0, \tag{2.51}$$

along with the associated boundary conditions on the interface $x_3 = 0$

$$\Box_R\,\phi + \frac{hb_o}{\lambda_1}\,\phi_{,113} = -\frac{1}{B_o}\left[\frac{P_{,1}}{c_{13}+c_{33}\,\beta_1\,\lambda_1} - \frac{\mathcal{H}\,(Q_{,1})}{c_{55}\,(\beta_1-\lambda_1)}\right]. \tag{2.52}$$

Equation (2.52) can also be written as pseudo-differential equations on the interface $x_3 = 0$, namely

$$\Box_R\,\phi - hb_o\,\sqrt{-\partial_{11}}\;\phi_{,11} = -\frac{1}{B_o}\left[\frac{P_{,1}}{c_{13}+c_{33}\,\beta_1\,\lambda_1} - \frac{\mathcal{H}\,(Q_{,1})}{c_{55}\,(\beta_1-\lambda_1)}\right]. \tag{2.53}$$

Note that in the case of a homogeneous half-space ($h = 0$), the equation (2.53) reduces to the hyperbolic equations (38) in Nobili and Prikazchikov [2018].

It is also observed that (2.53) may be expressed in terms of the surface displacements $u_r(x_1, 0, t)$ $(r = 1, 3)$, i.e

$$\Box_R\,u_1 - hb_o\,\sqrt{-\partial_{11}}\;\;u_{1,11} = \frac{\left(\hat{\vartheta}-1\right)}{B_o}\left[\frac{P_{,1}}{c_{13}+c_{33}\,\beta_1\,\lambda_1} - \frac{\mathcal{H}\,(Q_{,1})}{c_{55}\,(\beta_1-\lambda_1)}\right], \tag{2.54}$$

and

$$\Box_R\,u_3 - hb_o\,\sqrt{-\partial_{11}}\;u_{3,11} = \frac{\left(\hat{\vartheta}\,\alpha_2-\alpha_1\right)}{B_o}\left[\frac{\mathcal{H}\,(P_{,1})}{c_{13}+c_{33}\,\beta_1\,\lambda_1} + \frac{Q_{,1}}{c_{55}\,(\beta_1-\lambda_1)}\right], \tag{2.55}$$

following from (2.37) and (2.38).

2.3.3 Particular cases

Let us use the isotropic notation $\alpha_R = \lambda_2$, $\beta_R = \lambda_1$, where α_R and β_R defined in (1.42) (observing that the two factors λ_1 and λ_2 can be swapped). Then, from the

equation (2.31), we obtain $\beta_1 = -\beta_R^{-1}$, $\beta_2 = -\alpha_R$. Below the particular cases of the obtained model are summarised. For the sake of brevity we only discuss the variation of pseudo-differential equation on the interface, say (2.54).

2.3.3.1 Orthotropic coating on isotropic half-space

In this case, (2.54) reduces to

$$\Box_R\, u_1 - h b_{OI}\, \sqrt{-\partial_{11}}\, u_{1,11} = -\frac{\beta_R\,(1-\beta_R^2)}{2\mu B_I}\left[\vartheta P_{,1} + \mathcal{H}\,(Q_{,1})\right], \tag{2.56}$$

where the constants B_I defined in (1.54) and

$$b_{OI} = \frac{(1-\beta_R^2)}{2\mu B_I}\left[c_R^2\,\rho_0\,(\alpha_R+\beta_R) - \beta_R\,\delta_{11}\right]. \tag{2.57}$$

2.3.3.2 Isotropic coating on orthotropic half-space

In this case, equation (2.54) becomes

$$\Box_R\, u_1 - h b_{IO}\, \sqrt{-\partial_{11}}\, u_{1,11} = \frac{\left(\hat{\vartheta}-1\right)}{B_O}\left[\frac{P_{,1}}{c_{13}+c_{33}\,\beta_1\,\lambda_1} - \frac{\mathcal{H}\,(Q_{,1})}{c_{55}\,(\beta_1-\lambda_1)}\right], \tag{2.58}$$

where the constants B_O defined in (2.49) and

$$b_{IO} = \frac{1}{B_O}\left[\frac{\left(\rho_0\,c_R^2 - 4\mu_0\left(1-\kappa_0^{-2}\right)\right)\left(1-\hat{\vartheta}\right)}{c_{55}\,(\beta_1-\lambda_1)} + \frac{\rho_0\,c_R^2\left(\beta_1 - \hat{\vartheta}\,\beta_2\right)}{c_{13}+c_{33}\,\beta_1\,\lambda_1}\right], \tag{2.59}$$

where κ_0 defined in (1.75).

2.3.3.3 Isotropic coated half-space

Now, equation (2.54) reduces to the formulation within the 2D isotropic medium as (1.116).

Thus, the explicit asymptotic model for Rayleigh wave on the orthotropic elastic half-space coated by a thin orthotropic layer has been obtained. The model contains the elliptic equation (2.51), describing attenuation away from the surface over the interior, whereas the behaviour on the interface between the coating and the half-space is governed by a wave equation, singularly perturbed by a pseudo-differential operator, see (2.54) and (2.55). It should be noted that the form of the operator in (2.54) or (2.55) implies similar dispersion to that of the isotropic case considered in subsection 1.5.2.2, see (1.115). Finally, the asymptotic formulations for the particular cases have been presented.

The obtained hyperbolic-elliptic formulations may be implemented for a wide class of loads applied at the surface of the coating, providing the contribution of the Rayleigh wave to the overall dynamic response.

Chapter 3

Surface waves on a vertically inhomogeneous elastic layer coated half-space

This chapter is concerned with surface waves propagating on a 3D isotropic elastic half-space coated by a thin vertically inhomogeneous layer, subject to the effect of prescribed vertical surface loading. First, we derive the effective boundary conditions within the long-wave limit, for modelling a thin inhomogeneous coating. Then we specify the effective boundary conditions for homogeneous multi-layered coatings. A singularly perturbed hyperbolic equation on the interface is presented in Section 3.2, extending the previous considerations in Subsection 1.5.2 and Chapter 2. An interesting special case associated with a zero group velocity in the long-wave limit is discussed in Section 3.3. The effect of the perturbative pseudo-differential operator on the structure of the quasi-front emerging for a point impulse loading, is analysed

in Section 3.4. Numerical illustrations of surface wave field are presented in Section 3.5. Some results in this chapter has been presented in Mubaraki et al. [2019].

3.1 Effective boundary conditions for a thin vertically inhomogeneous elastic layer

Consider a linearly isotropic, elastic half-space over the domain $-\infty < x_1, x_2 < \infty$ and $x_3 \geq 0$, coated by a thin layer of thickness h described by $-\infty < x_1, x_2 < \infty$ and $-h \leq x_3 \leq 0$, see Fig. 3.1.

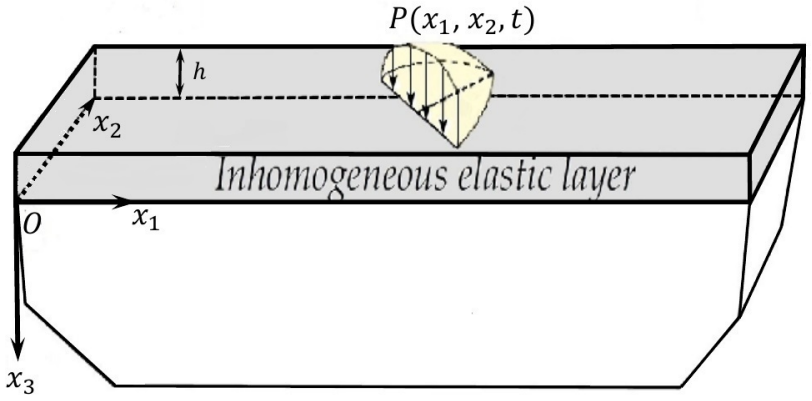

Figure 3.1: An elastic half-space coated by a vertically inhomogeneous layer.

We assume the material parameters of the coating layer a depth-dependent, i.e.,

$$\lambda_c = \lambda(x_3), \mu_c = \mu(x_3), \rho_c = \rho(x_3), c_{1c} = c_1(x_3) \text{ and } c_{2c} = c_2(x_3), \tag{3.1}$$

where

$$c_{1c} = \sqrt{\frac{\lambda_c + 2\mu_c}{\rho_c}} \qquad \text{and} \qquad c_{2c} = \sqrt{\frac{\mu_c}{\rho_c}}.$$

The boundary conditions on the surface $x_3 = -h$ are formulated as

$$\sigma_{i3}^{(c)} = 0, \qquad \text{and} \qquad \sigma_{33}^{(c)} = -P, \qquad i = 1, 2, \tag{3.2}$$

where $P = P(x_1, x_2, t)$ is a prescribed vertical surface load.

The continuity conditions at the interface $x_3 = 0$ are taken in the form

$$u_k^{(c)} = v_k^{(s)}, \qquad (k = 1, 2, 3), \tag{3.3}$$

where $v_k^{(s)} = v_k(x_1, x_2, t)$ are displacements on substrate.

As before, prior to the modelling of surface waves propagation, the entire effect of the thin inhomogeneous elastic coating is replaced by means of effective boundary conditions. To begin, we choose a small parameter ϵ associated with the long-wave regime as in (1.70), along with the scaled variables

$$\xi_i = \frac{x_i}{L}, \qquad \eta = \frac{x_3}{h}, \qquad \tau_0 = \frac{t\, c_{20}}{L}, \tag{3.4}$$

and also we introduce the dimensionless quantities

$$u_k^* = \frac{u_k}{L}, \quad v_k^* = \frac{v_k}{L}, \quad \sigma_{ij}^* = \frac{\sigma_{ij}}{\mu_0}, \quad \sigma_{k3}^* = \frac{\sigma_{k3}}{\epsilon\,\mu_0}, \quad p^* = \frac{P}{\epsilon\,\mu_0}, \tag{3.5}$$

where $c_{20} = c_2(0)$, $\mu_0 = \mu(0)$, $\rho_0 = \rho(0)$, $i \neq j = 1, 2$, $k = 1, 2, 3$.

Then, the equations of motion (1.11) – (1.13) and the constitutive relations (1.7) can be written explicitly as

$$\begin{aligned} &\sigma_{ii,\xi_i}^* + \sigma_{ij,\xi_j}^* + \sigma_{i3,\eta}^* = \rho_*\, u_{i,\tau_0\tau_0}^*, \\ &\sigma_{33,\eta}^* + \epsilon\left(\sigma_{3i,\xi_i}^* + \sigma_{3j,\xi_j}^*\right) = \rho_*\, u_{3,\tau_0\tau_0}^*, \end{aligned} \tag{3.6}$$

and

$$\begin{aligned}
&\sigma^*_{ij} = \kappa_2^2 \left(u^*_{i,\xi_j} + u^*_{j,\xi_i} \right), \qquad \epsilon^2\, \sigma^*_{i3} = \kappa_2^2 \left(u^*_{i,\eta} + \epsilon\, u^*_{3,\xi_i} \right), \\
&\epsilon\, \sigma^*_{ii} = \left(\kappa_1^2 - 2\kappa_2^2 \right) u^*_{3,\eta} + \epsilon \left(\kappa_1^2\, u^*_{i,\xi_i} + \left(\kappa_1^2 - 2\kappa_2^2 \right) u^*_{j,\xi_j} \right), \\
&\epsilon^2\, \sigma^*_{33} = \kappa_1^2\, u^*_{3,\eta} + \epsilon \left(\kappa_1^2 - 2\kappa_2^2 \right) \left(u^*_{i,\xi_i} + u^*_{j,\xi_j} \right),
\end{aligned} \tag{3.7}$$

where $\rho_* (z) = \rho_c / \rho_0$, $\kappa_1^2 (z) = (\lambda_c + 2\mu_c) / \mu_0$, and $\kappa_2^2 (z) = \mu_c / \mu_0$.

On substituting the expression of $u^*_{3,\eta}$ from $(3.7)_4$ into $(3.7)_2$, we deduce

$$\sigma^*_{ii} = 4\kappa_2^2 \left(1 - \kappa_c^{-2} \right) u^*_{i,\xi_i} + \left(1 - 2\kappa_c^{-2} \right) \left(2\kappa_2^2\, u^*_{j,\xi_j} + \epsilon\, \sigma^*_{33} \right). \tag{3.8}$$

where $\kappa_c^2 (z) = \kappa_1^2 / \kappa_2^2$. The boundary conditions (3.2) and (3.3) become

$$\begin{aligned}
&\sigma^*_{i3} = 0, \qquad \sigma^*_{33} = -p^* \qquad \text{at} \qquad \eta = -1, \\
&\text{and} \qquad u^*_k = v^*_k \qquad \text{at} \qquad \eta = 0.
\end{aligned} \tag{3.9}$$

Now, we expand the displacements and stresses as asymptotic series, i.e.,

$$\begin{pmatrix} u^*_k \\ \sigma^*_{ii} \\ \sigma^*_{ij} \\ \sigma^*_{k3} \end{pmatrix} = \begin{pmatrix} u^{(0)}_k \\ \sigma^{(0)}_{ii} \\ \sigma^{(0)}_{ij} \\ \sigma^{(0)}_{k3} \end{pmatrix} + \epsilon \begin{pmatrix} u^{(1)}_k \\ \sigma^{(1)}_{ii} \\ \sigma^{(1)}_{ij} \\ \sigma^{(1)}_{k3} \end{pmatrix} + \ldots, \tag{3.10}$$

then, at leading order, we infer

$$\begin{aligned}
&\sigma^{(0)}_{ii,\xi_i} + \sigma^{(0)}_{ij,\xi_j} + \sigma^{(0)}_{i3,\eta} = \rho_*\, u^{(0)}_{i,\tau_0\tau_0}, \\
&\sigma^{(0)}_{33,\eta} = \rho_*\, u^{(0)}_{3,\tau_0\tau_0}, \qquad \sigma^{(0)}_{ij} = \kappa_2^2 \left(u^{(0)}_{i,\xi_j} + u^{(0)}_{j,\xi_i} \right), \\
&\sigma^{(0)}_{ii} = 4\kappa_2^2 \left(1 - \kappa_c^{-2} \right) u^{(0)}_{i,\xi_i} + 2\kappa_2^2 \left(1 - 2\kappa_c^{-2} \right) u^{(0)}_{j,\xi_j}, \\
&u^{(0)}_{k,\eta} = 0,
\end{aligned} \tag{3.11}$$

subject to the boundary conditions

$$\begin{aligned} &\sigma_{i3}^{(0)} = 0, \qquad \sigma_{33}^{(0)} = -p^* \qquad \text{at} \qquad \eta = -1, \\ &\text{and} \qquad\quad u_k^{(0)} = v_k^*, \qquad \text{at} \qquad \eta = 0. \end{aligned} \tag{3.12}$$

Equations $(3.11)_5$ and $(3.12)_2$ imply

$$u_k^{(0)} = v_k^*, \qquad k = 1, 2, 3. \tag{3.13}$$

Then, equation $(3.11)_2$ with the boundary condition $(3.12)_1$ give

$$\sigma_{33}^{(0)} = v_{3,\tau_0\tau_0}^* \int_{-1}^{\eta} \rho_* (z)\, dz - p^*. \tag{3.14}$$

In addition, equations $(3.11)_1$, $(3.11)_4$, $(3.12)_1$ and (3.13) yield

$$\begin{aligned} \sigma_{i3}^{(0)} = &\left(\int_{-1}^{\eta} \rho_* (z)\, dz \right) v_{i,\tau_0\tau_0}^* - 4 \left(\int_{-1}^{\eta} \kappa_2^2 (z) \left(1 - \kappa_c^{-2} (z)\right) dz \right) v_{i,\xi_i\xi_i}^* \\ &- \left(\int_{-1}^{\eta} \kappa_2^2 (z)\, dz \right) v_{i,\xi_j\xi_j}^* - \left(\int_{-1}^{\eta} \kappa_2^2 (z) \left(3 - 4\kappa_c^{-2} (z)\right) dz \right) v_{j,\xi_i\xi_j}^*. \end{aligned} \tag{3.15}$$

Finally, at the interface $x_3 = 0$, the effective boundary conditions may now be obtained, which then formulated in terms of the original variables as

$$\begin{aligned} \sigma_{i3} &= h \left(\tilde{\rho}\, u_{i,tt} - \tilde{\delta}\, u_{i,ii} - \tilde{\mu}\, u_{i,jj} - \left(\tilde{\delta} - \tilde{\mu}\right) u_{j,ij} \right), \\ \sigma_{33} &= h\, \tilde{\rho}\, u_{3,tt} - P, \end{aligned} \tag{3.16}$$

where $\delta = 4\mu_c \left(1 - \kappa_c^{-2}\right)$ and a tilde upper a quantity indicates its mean value over the thickness of the coating layer

$$\tilde{g} = \frac{1}{h} \int_{-h}^{0} g (x_3)\, dx_3. \tag{3.17}$$

Observe that in the case of a homogeneous isotropic layer, the obtained result of effective boundary conditions (3.16) are reduced to the well-known ones first established in Tiersten [1969], see also Dai et al. [2010].

3.1.1 Particular case: multi-layered coating

Let us consider a particular case of an inhomogeneous coating, namely a N-layered laminate on an elastic half-space, with perfect bounding assumed on the interfaces, see Fig. 3.2.

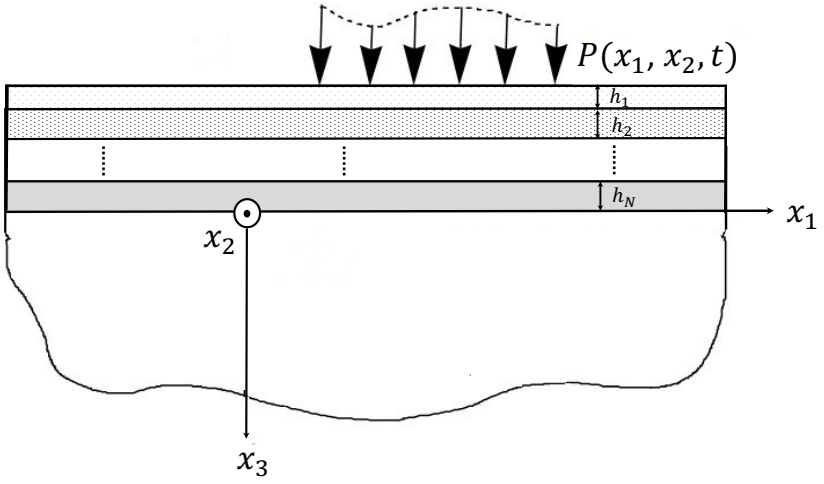

Figure 3.2: An elastic half-space coated by N-layered homogeneous coatings.

We denote the appropriate homogeneous material parameters of N-layered coatings by $\rho_{\hat{q}}, \lambda_{\hat{q}}, \mu_{\hat{q}}, c_{\hat{q}1}, c_{\hat{q}2}$, $\hat{q} = 1, 2, ...N$. Then, the effective boundary conditions (3.16) are reduced in the case of N-layered homogeneous coating to

$$\sigma_{i3} = \sum_{\hat{q}=1}^{N} \left[h_{\hat{q}}\, \rho_{\hat{q}}\, u_{i,tt} - \left(h_{\hat{q}}\, \mu_{\hat{q}}\, u_{i,jj} + 4 h_{\hat{q}}\, \mu_{\hat{q}} \left(1 - \kappa_{\hat{q}}^{-2}\right) u_{i,ii} \right.\right.$$
$$\left.\left. + h_{\hat{q}}\, \mu_{\hat{q}} \left(3 - 4\kappa_{\hat{q}}^{-2}\right) u_{j,ij} \right) \right], \qquad (3.18)$$
$$\sigma_{33} = \sum_{\hat{q}=1}^{N} h_{\hat{q}}\, \rho_{\hat{q}}\, u_{3,tt} - P \qquad \text{at} \qquad x_3 = 0, \qquad (i \neq j = 1, 2),$$

where

$$c_{\hat{q}1} = \sqrt{\frac{\lambda_{\hat{q}} + 2\mu_{\hat{q}}}{\rho_{\hat{q}}}}, \qquad c_{\hat{q}2} = \sqrt{\frac{\mu_{\hat{q}}}{\rho_{\hat{q}}}}, \qquad \kappa_{\hat{q}} = \frac{c_{\hat{q}1}}{c_{\hat{q}2}}, \qquad \text{and} \qquad \hat{q} = 1, 2, ..., N.$$

Note that for a single layer coating the derived boundary conditions (3.18) reduce to the the previous result (1.89).

3.2 Asymptotic model for surface waves

The hyperbolic-elliptic model for the surface wave field may now be constructed by using the effective boundary conditions (3.16), generalising the previous results of Dai et al. [2010] to the case of a coating with vertically inhomogeneous material properties. We start from the conventional Navier equations of motion (1.15), associated with the following boundary value problem for a homogeneous isotropic substrate at $x_3 = 0$

$$\begin{aligned}
&\mu\,(u_{1,3} + u_{3,1}) = h\left(\tilde{\rho}\,u_{1,tt} - \tilde{\delta}\,u_{1,11} - \tilde{\mu}\,u_{1,22} - \left(\tilde{\delta} - \tilde{\mu}\right)\,u_{2,11}\right),\\
&\mu\,(u_{2,3} + u_{3,2}) = h\left(\tilde{\rho}\,u_{2,tt} - \tilde{\delta}\,u_{2,22} - \tilde{\mu}\,u_{2,11} - \left(\tilde{\delta} - \tilde{\mu}\right)\,u_{1,12}\right),\\
&\lambda\,(u_{1,1} + u_{2,2}) + (\lambda + 2\mu)\,u_{3,3} = h\,\tilde{\rho}\,u_{3,tt} - P.
\end{aligned} \tag{3.19}$$

Then, the Radon integral transform is applied (see Georgiadis and Lykotrafitis [2001] for more details)

$$g^{(\beta)}\,(x, \beta, x_3, t) = \int_{-\infty}^{\infty} g\,(x\,\cos\beta - y\,\sin\beta, x\,\sin\beta + y\,\cos\beta, x_3, t)\,dy, \tag{3.20}$$

with

$$x = x_1\,\cos\beta + x_2\,\sin\beta, \qquad y = x_2\,\cos\beta - x_1\,\sin\beta,$$

where β is the angle varying on the interval $[0, 2\pi]$.

In what follows the Radon transform of a quantity is denoted by the superscript (β). Let us now introduce transformed displacements within the Cartesian frame (x, y), taking the following forms

$$u_x^{(\beta)} = u_1^{(\beta)} \cos\beta + u_2^{(\beta)} \sin\beta, \qquad u_y^{(\beta)} = u_2^{(\beta)} \cos\beta - u_1^{(\beta)} \sin\beta. \tag{3.21}$$

Next, we impose the assumption

$$u_y^{(\beta)} = 0, \tag{3.22}$$

corresponding to the fact that anti-plane motion would not contribute to the excitation of surface waves. Henceforth, the Radon integral transform allows to reduce the original 3D problem to the 2D problem in elasticity. The Navier equations of motion (1.15) are then rewritten in terms of the transformed displacements (3.21), which correspond to the plane problem, that is

$$\begin{aligned} (\lambda + 2\mu)\, u_{x,xx}^{(\beta)} + (\lambda + \mu)\, u_{3,x3}^{(\beta)} + \mu\, u_{x,33}^{(\beta)} &= \rho\, u_{x,tt}^{(\beta)}, \\ (\lambda + 2\mu)\, u_{3,33}^{(\beta)} + (\lambda + \mu)\, u_{x,x3}^{(\beta)} + \mu\, u_{3,xx}^{(\beta)} &= \rho\, u_{3,tt}^{(\beta)}. \end{aligned} \tag{3.23}$$

The associated transformed boundary conditions (3.19) at $x_3 = 0$ may be written as

$$\begin{aligned} \mu \left(u_{x,3}^{(\beta)} + u_{3,x}^{(\beta)} \right) &= h \left(\tilde{\rho}\, u_{x,tt}^{(\beta)} - \tilde{\delta}\, u_{x,xx}^{(\beta)} \right), \\ \mu \left(\kappa^2\, u_{3,3}^{(\beta)} + \left(\kappa^2 - 2 \right) u_{x,x}^{(\beta)} \right) &= h\, \tilde{\rho}\, u_{3,tt}^{(\beta)} - P^{(\beta)}, \end{aligned} \tag{3.24}$$

where κ is defined in (1.32).

Then, the Helmholtz decomposition (1.16) is introduced for transformed displacements

$$u_x^{(\beta)} = \phi_{,x}^{(\beta)} - \psi_{,3}^{(\beta)}, \qquad u_3^{(\beta)} = \phi_{,3}^{(\beta)} + \psi_{,x}^{(\beta)}, \tag{3.25}$$

leading to uncoupled transformed wave equations

$$\phi_{,xx}^{(\beta)} + \phi_{,33}^{(\beta)} - \frac{1}{c_1^2}\,\phi_{,tt}^{(\beta)} = 0, \qquad \psi_{,xx}^{(\beta)} + \psi_{,33}^{(\beta)} - \frac{1}{c_2^2}\,\psi_{,tt}^{(\beta)} = 0, \tag{3.26}$$

along with the boundary conditions at $x_3 = 0$, given as

$$\begin{aligned} 2\phi_{,x3}^{(\beta)} + \psi_{,xx}^{(\beta)} - \psi_{,33}^{(\beta)} &= \frac{h}{\mu}\left[\tilde{\rho}\left(\phi_{,xtt}^{(\beta)} - \psi_{,3tt}^{(\beta)}\right) - \tilde{\delta}\left(\phi_{,xxx}^{(\beta)} - \psi_{,xx3}^{(\beta)}\right)\right], \\ \left(\kappa^2 - 2\right)\phi_{,xx}^{(\beta)} + \kappa^2\,\phi_{,33}^{(\beta)} + 2\psi_{,x3}^{(\beta)} &= \frac{h}{\mu}\,\tilde{\rho}\left(\phi_{,3tt}^{(\beta)} + \psi_{,\chi tt}^{(\beta)}\right) - \frac{P^{(\beta)}}{\mu}. \end{aligned} \tag{3.27}$$

Following Dai et al. [2010], Kaplunov and Prikazchikov [2017], a slow-time perturbation scheme is established as

$$\chi = \frac{x - c_R\,t}{L}, \qquad \gamma = \frac{x_3}{L}, \qquad \tau = \frac{\epsilon\,c_R}{L}\,t, \tag{3.28}$$

then equations (3.26) are rewritten in terms of the new variables as

$$\begin{aligned} \phi_{,\gamma\gamma}^{(\beta)} + \alpha_R^2\,\phi_{,\chi\chi}^{(\beta)} + 2\epsilon\left(1 - \alpha_R^2\right)\phi_{,\chi\tau}^{(\beta)} - \epsilon^2\left(1 - \alpha_R^2\right)\phi_{,\tau\tau}^{(\beta)} = 0, \\ \psi_{,\gamma\gamma}^{(\beta)} + \beta_R^2\,\psi_{,\chi\chi}^{(\beta)} + 2\epsilon\left(1 - \beta_R^2\right)\psi_{,\chi\tau}^{(\beta)} - \epsilon^2\left(1 - \beta_R^2\right)\psi_{,\tau\tau}^{(\beta)} = 0, \end{aligned} \tag{3.29}$$

subject to the boundary conditions at $\gamma = 0$, restated as

$$\begin{aligned} 2\phi_{,\chi\gamma}^{(\beta)} + \psi_{,\chi\chi}^{(\beta)} - \psi_{,\gamma\gamma}^{(\beta)} = \frac{1}{\mu}\Big\{\epsilon\left(c_R^2\,\tilde{\rho} - \tilde{\delta}\right)\left(\phi_{,\chi\chi\chi}^{(\beta)} - \psi_{,\chi\chi\gamma}^{(\beta)}\right) \\ + c_R^2\,\tilde{\rho}\left[2\,\epsilon^2\left(\psi_{,\chi\gamma\tau}^{(\beta)} - \phi_{,\chi\chi\tau}^{(\beta)}\right) + \epsilon^3\left(\phi_{,\chi\tau\tau}^{(\beta)} - \psi_{,\gamma\tau\tau}^{(\beta)}\right)\right]\Big\}, \end{aligned} \tag{3.30}$$

and

$$\begin{aligned}\left(\kappa^2-2\right)\phi^{(\beta)}_{,\chi\chi}+\kappa^2\,\phi^{(\beta)}_{,\gamma\gamma}+2\psi^{(\beta)}_{,\chi\gamma}=\frac{\tilde{\rho}}{\mu}\left\{\epsilon\,c_R^2\left(\phi^{(\beta)}_{,\chi\chi\gamma}+\psi^{(\beta)}_{,\chi\chi\chi}\right)\right.\\ \left.+c_R^2\left[\epsilon^3\left(\phi^{(\beta)}_{,\gamma\tau\tau}+\psi^{(\beta)}_{,\chi\tau\tau}\right)-2\epsilon^2\left(\phi^{(\beta)}_{,\chi\gamma\tau}+\psi^{(\beta)}_{,\chi\chi\tau}\right)\right]\right\}-\frac{P^{(\beta)}}{\mu},\end{aligned} \tag{3.31}$$

with α_R and β_R defined in (1.42).

Let us now expand the potentials $\phi^{(\beta)}$ and $\psi^{(\beta)}$ as asymptotic series

$$\begin{aligned}\phi^{(\beta)}&=\frac{1}{\epsilon}\left(\phi^{(0)}\left(\chi,\gamma,\tau\right)+\epsilon\,\phi^{(1)}\left(\chi,\gamma,\tau\right)+\epsilon^2\,\phi^{(2)}\left(\chi,\gamma,\tau\right)+...\right),\\ \psi^{(\beta)}&=\frac{1}{\epsilon}\left(\psi^{(0)}\left(\chi,\gamma,\tau\right)+\epsilon\,\psi^{(1)}\left(\chi,\gamma,\tau\right)+\epsilon^2\,\psi^{(2)}\left(\chi,\gamma,\tau\right)+...\right).\end{aligned} \tag{3.32}$$

At leading order, the boundary conditions (3.30) and (3.31) with (3.32) give

$$\begin{aligned}2\phi^{(0)}_{,\chi\gamma}+\psi^{(0)}_{,\chi\chi}-\psi^{(0)}_{,\gamma\gamma}=0,\\ \left(\kappa^2-2\right)\phi^{(0)}_{,\chi\chi}+\kappa^2\phi^{(0)}_{,\gamma\gamma}+2\psi^{(0)}_{,\chi\gamma}=0.\end{aligned} \tag{3.33}$$

In view of (1.39), we have

$$\begin{aligned}2\alpha_R\,\phi^{(0)}_{,\chi\chi}+\left(1+\beta_R^2\right)\bar{\psi}^{(0)}_{,\chi\chi}=0,\\ \left(1+\beta_R^2\right)\phi^{(0)}_{,\chi\chi}+2\beta_R\,\bar{\psi}^{(0)}_{,\chi\chi}=0,\end{aligned} \tag{3.34}$$

which leads to the Rayleigh equation (1.30) along with the relation between the elastic potentials $\phi^{(0)}$ and $\psi^{(0)}$ on the surface $\gamma=0$ as in (1.98).

For analysis of correction terms, we get the solution in terms of two arbitrary plane harmonic functions $\phi^{(1)}$ and $\psi^{(1)}$, which take similar expressions as in (1.100). Putting

these into the boundary conditions (3.30) and (3.31), we have

$$2\phi^{(1,0)}_{,\chi\gamma} + \psi^{(1,0)}_{,\chi\chi} - \psi^{(1,0)}_{,\gamma\gamma} + 2\phi^{(1,1)}_{,\chi} - 2\psi^{(1,1)}_{,\gamma} + \\ -\frac{1}{\mu}\left(c_R^2\,\tilde{\rho} - \tilde{\delta}\right)\left(\phi^{(0)}_{,\chi\chi\chi} - \psi^{(0)}_{,\chi\chi\gamma}\right) = 0,$$

$$\left(\kappa^2 - 2\right)\phi^{(1,0)}_{,\chi\chi} + \kappa^2\,\phi^{(1,0)}_{,\gamma\gamma} + 2\psi^{(1,0)}_{,\chi\gamma} + 2\kappa^2\phi^{(1,1)}_{,\gamma} + 2\psi^{(1,1)}_{,\chi} \\ -\frac{c_R^2\,\tilde{\rho}}{\mu}\left(\phi^{(0)}_{,\chi\chi\gamma} + \psi^{(0)}_{,\chi\chi\chi}\right) = -\frac{L^2\,P^{(\beta)}}{\mu} \qquad \text{at} \qquad \gamma = 0. \tag{3.35}$$

Using (1.39), from sovability of latter, we arrive at

$$2\,\phi^{(0)}_{,\chi\tau} + \frac{b_c}{\alpha_R}\,\phi^{(0)}_{,\chi\chi\gamma} = -\frac{L^2\,(1+\beta_R^2)}{2\mu B_{_I}} P^{(\beta)} \quad \text{at} \quad \gamma = 0, \tag{3.36}$$

where $B_{_I}$ is a material constant known for the uncoated half-space, defined in (1.54), and the constant b_c inheriting properties for both of the coating and substrate is given by

$$b_c = \frac{(1-\beta_R^2)}{2\mu B_{_I}}\left[c_R^2\,\tilde{\rho}\,(\alpha_R + \beta_R) - \tilde{\delta}\,\beta_R\right]. \tag{3.37}$$

As before, on applying the leading order approximation (1.106), with operator identities (1.107), the equation (3.36) can now be rewritten in terms of the original dimensional variables (x, x_3, t) as

$$\phi^{(\beta)}_{,xx} - \frac{1}{c_R^2}\,\phi_{,tt} + \frac{b_c\,h}{\alpha_R}\,\phi^{(\beta)}_{,xx3} = -\frac{(1+\beta_R^2)}{2\mu B_{_I}}\,P^{(\beta)} \quad \text{at} \quad x_3 = 0. \tag{3.38}$$

The elliptic equations for the potentials $\phi^{(\beta)}$ and $\psi^{(\beta)}$ are obtained from equations (3.29) as

$$\phi^{(\beta)}_{,33} + \alpha_R^2\, \phi^{(\beta)}_{,xx} = 0, \qquad \text{and} \qquad \psi^{(\beta)}_{,33} + \beta_R^2\, \psi^{(\beta)}_{,xx} = 0. \tag{3.39}$$

Finally, we note a relation between the potentials at the surface

$$\begin{aligned} \psi^{(\beta)}_{,x}\,(x,0,t) &= -\frac{2}{1+\beta_R^2}\,\phi^{(\beta)}_{,3}\,(x,0,t)\,, \\ \psi^{(\beta)}_{,3}\,(x,0,t) &= \frac{1+\beta_R^2}{2}\,\phi^{(\beta)}_{,x}\,(x,0,t)\,, \end{aligned} \tag{3.40}$$

following from (3.33).

Now, introducing a pair of functions $\psi_1^{(\beta)}$ and $\psi_2^{(\beta)}$ such that

$$\psi_1^{(\beta)} = \psi^{(\beta)} \cos\beta \qquad \text{and} \qquad \psi_2^{(\beta)} = \psi^{(\beta)} \sin\beta, \tag{3.41}$$

and applying inverse Radon transform to (3.38) – (3.40), we obtain the pseudo-static elliptic equations

$$\phi_{,33} + \alpha_R^2\, \Delta\, \phi = 0, \qquad \text{and} \qquad \psi_{i,33} + \beta_R^2\, \Delta\, \psi_i = 0, \tag{3.42}$$

governing the decay over the interior ($x_3 \geq 0$), where Δ denotes the 2D Laplacian in the coordinates (x_1, x_2). The associated boundary conditions become

$$\Delta\, \phi - \frac{1}{c_R^2}\, \phi_{,tt} + \frac{b_c\, h}{\alpha_R}\, \Delta\, \phi_{,3} = -\frac{(1+\beta_R^2)}{2\mu B_{_I}}\, P \quad \text{at} \quad x_3 = 0, \tag{3.43}$$

along with

$$\phi_{,i}\left(x_1, x_2, 0, t\right) = \frac{2}{1+\beta_R^2}\,\psi_{i,3}\left(x_1, x_2, 0, t\right), \quad (i = 1, 2), \tag{3.44}$$

and

$$\phi_{,3}\left(x_1, x_2, 0, t\right) = -\frac{1+\beta_R^2}{2}\,\left(\psi_{1,1} + \psi_{2,2}\right)\left(x_1, x_2, 0, t\right). \tag{3.45}$$

Consequently, the solution of equation $(3.42)_1$ can be represented by (see Dai et al. [2010])

$$\phi(x_1, x_2, x_3, t) = \exp\left(-\alpha_R\sqrt{-\Delta}\;x_3\right)\phi(x_1, x_2, 0, t), \tag{3.46}$$

where $\sqrt{-\Delta}$ is understood as a pseudo-differential operator.

Then at $x_3 = 0$, we have

$$\phi_{,3} = -\alpha_R\sqrt{-\Delta}\;\phi. \tag{3.47}$$

Inserting (3.47) into (3.43), we get

$$\Delta\,\phi - \frac{1}{c_R^2}\phi_{,tt} - b_c\,h\sqrt{-\Delta}\,\Delta\,\phi = -\frac{(1+\beta_R^2)}{2\mu B_{_I}}\,P. \tag{3.48}$$

3.3 Possibility of zero group velocity in the long-wave limit

Let us study whether zero group velocity in the long-wave limit is possible, i.e. consider $b_c = 0$. In this case the pseudo-differential term in (3.48) vanishes, with the

hyperbolic equation on the interface being identical to that if load P was applied on the surface of a substrate in absence of the coating layer.

From (3.37) it follows that $b_c = 0$ implies

$$\tilde{\delta} = \frac{\tilde{\rho}\, c_R^2}{\beta_R}\,(\alpha_R + \beta_R)\,. \tag{3.49}$$

In the case of an N-layered homogeneous coating, the constant b_0 is defined according to (3.37), with

$$\tilde{\rho} = \frac{h_1\,\rho_1 + ... + h_N\,\rho_N}{h_1 + ... + h_N} \qquad \text{and} \qquad \tilde{\delta} = 4\left(\frac{h_1\,\mu_1\left(1-\kappa_1^{-2}\right) + ... + h_N\,\mu_N\left(1-\kappa_N^{-2}\right)}{h_1 + ... + h_N}\right),$$

therefore, we deduce

$$b_0 = 0 \iff \sum_{\hat{q}=1}^{N} \frac{h_{\hat{q}}\,E_{\hat{q}}}{1-\nu_{\hat{q}}^2} = \frac{c_R^2}{\beta_R}\,(\alpha_R + \beta_R) \sum_{\hat{q}=1}^{N} h_{\hat{q}}\,\rho_{\hat{q}}, \tag{3.50}$$

where $E_{\hat{q}}$, $\nu_{\hat{q}}$ and $\rho_{\hat{q}}$ $(\hat{q} = 1, 2, ..., N)$ are Young's moduli, Poisson's ratio and density of the $\hat{q}$-layer.

In case of a single homogeneous coating layer (3.50) reduces to

$$b_{_I} = 0 \Longleftrightarrow E_0 = \frac{\rho_0\,(1-\nu_0^2)\,c_R^2}{\beta_R}\,(\alpha_R + \beta_R)\,. \tag{3.51}$$

It is worth noting that this relation involving material parameters of both coating and substrate is independent of thickness. Let us now assume $d = \nu_0\,/\,\nu$ and $\rho_0\,/\,\rho = 1$, then we can illustrate the dependence of $E_0\,/\,E$ on the Poisson's ratio ν when the condition (3.51) is satisfied, see Fig. 3.3.

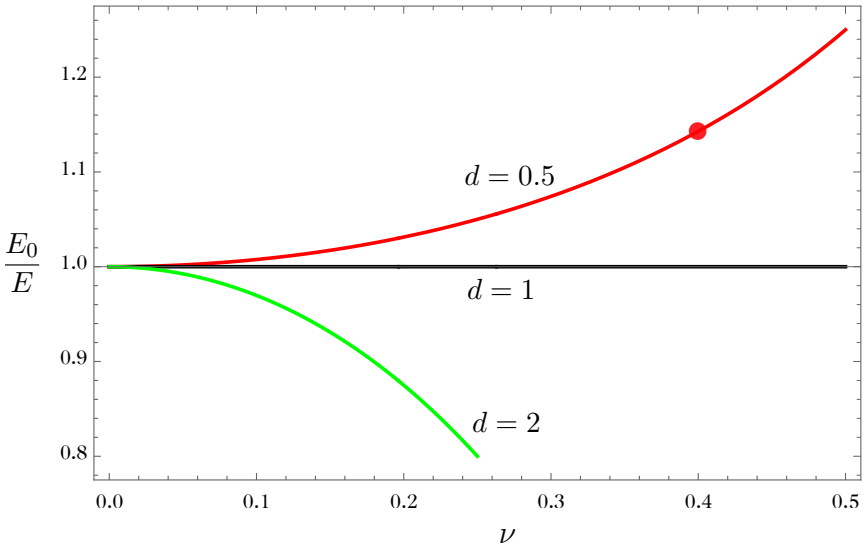

Figure 3.3: The relation of $E_0 \,/\, E$ vs Poisson's ratio ν, for which (3.51) holds.

It is seen from the above figure that, for example at $\nu_0 = 0.2$ and $\nu = 0.4$, the ratio of the Young moduli corresponding to the zero group velocity in the long wave limit is approximately $E_0 \,/\, E \approx 1.1428572$. As a result, the constant $b_{_I}$ is equal to zero. On using these material properties of the layer and substrate, the numerical comparison between the exact solution (1.67) shown by a solid blue line, against the two-term approximation (1.115), depicted by the dashed black line, is shown in Fig. 3.4.

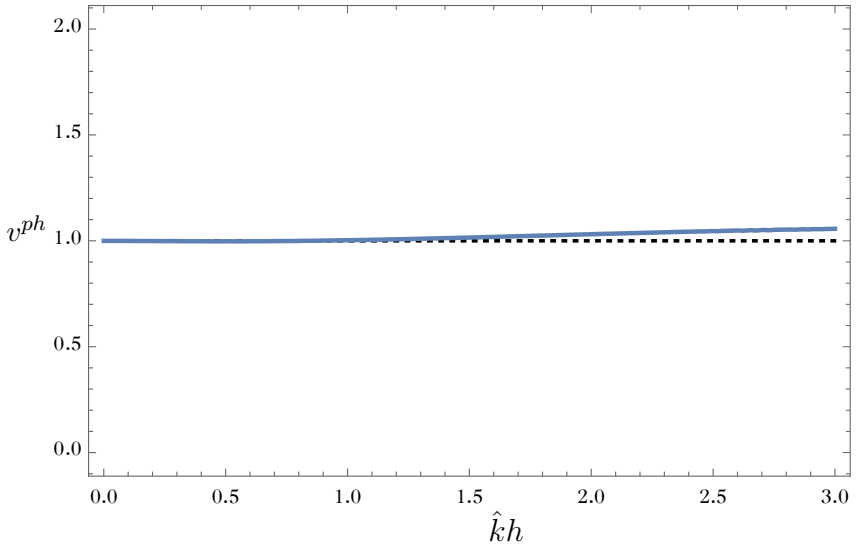

Figure 3.4: The relation between v^{ph} vs. $\hat{k}h$ when the layer is vanished.

3.4 Illustrative example: impact loading

Let us illustrate the developed formulation by considering a plane-strain problem for a concentrated impact vertical force

$$P = P_0\,\delta(x_1)\,\delta(t), \tag{3.52}$$

acting on the surface of a vertically inhomogeneous coating. Introducing the scaling

$$\xi_0 = \frac{x_1}{L}, \qquad \tau_{_R} = \frac{c_R}{L}\,t, \qquad h_c = \frac{h \mid b_c \mid}{L} \ll 1,$$

with

$$\varphi = -\frac{4\,\mu B_{_I}}{c_R\,(1+\beta_R^2)\,P_0}\,\phi_{|_{x_3=0}},$$

from (3.48) we have

$$\varphi_{,\xi_0\xi_0} - \varphi_{,\tau_{_R}\tau_{_R}} - h_c\,\mathrm{sign}\,(b_c)\,\sqrt{-\partial_{\xi_0\xi_0}}\;\varphi_{,\xi_0\xi_0} = -\delta(\xi_0)\,\delta(\tau_{_R}). \tag{3.53}$$

The latter equation may be solved by applying the matched asymptotic procedure, see Dai et al. [2010], resulting in

$$\varphi = \frac{1}{2}\left[1 - \mathrm{sign}\,(b_c)\left(\frac{1}{2} + \mathrm{sign}\,(X)\,(C(X)+S(X)) - C^2(X) - S^2(X)\right)\right], \tag{3.54}$$

where $X = (\xi_0 - \tau_{_R})\,\mathrm{sign}\,(b_c)\,/\,\sqrt{2h_c\,\tau_{_R}}$, $C(X)$ and $S(X)$ are Fresnel integrals

$$C(z) = \int_0^z \cos\left(\frac{\pi}{2}\,t^2\right)dt \quad \text{and} \quad S(z) = \int_0^z \sin\left(\frac{\pi}{2}\,t^2\right)dt,$$

see Abramowitz and Stegun [1965].

We observe that (1.22),(1.47) and (1.98) can be combined, obtaining equation for interfacial displacement u_1 in terms of potentials, say ϕ. Then, the scaled longitudinal displacement profile U_1 at the interface may be computed as

$$U_1 = -\frac{8\,\mu B_{_I}}{c_R\,(1-\beta_R^4)\,P_0}\,u_1. \tag{3.55}$$

3.5 Numerical results

The solutions (3.54) and (3.55) are displayed numerically in Figs 3.5 – 3.8, showing the dependence of φ and U_1 on ξ_0, with $\tau_{_R} = 1$. As can be seen from the below graphs, there are possibilities of receding and advancing quasi-fronts, as noticed previously in Dai et al. [2010], associated with the local minimum or maximum of the phase velocity at the Rayleigh wave speed in the long-wave limit. In fact, the velocity of oscillations also differ depending on the material parameters of the inhomogeneous coating and the substrate. The properties of materials employed in calculations are summarised below in Table 3.1.

N	Materials	$\rho_{_N}$, kg/m^3	$E_{_N}$, GPa	$\nu_{_N}$
1	Rubber	930	0.1	0.49
2	Teflon	2200	0.5	0.46
3	Polyethylene	960	0.8	0.45
4	Polycarbonate	1200	2.4	0.37
5	Nylon	1130	2.95	0.39
6	Polystyrene	1040	3.1	0.35

Table 3.1: The material parameters.

3.5.1 Inhomogeneous layer

Let us first consider an inhomogeneous coating layer with continuous variation of properties with depth, with Young's modulus E, the Poisson's ratio ν, and the density ρ depending on the vertical coordinate x_3 by exponential law (see e.g. Kulchytsky-Zhyhailo and Bajkowski [2015])

$$Y(x_3) = Y_0\, e^{\iota x_3}, \quad \iota = \frac{1}{h} \ln\left(\frac{Y_s}{Y_0}\right), \tag{3.56}$$

where $Y \in \{E, \nu, \rho\}$, and subscript c or s are associated with coating or substrate respectively, with $h = 0.3$. The solutions (3.54) and (3.55) are shown in the following Figs 3.5 – 3.8.

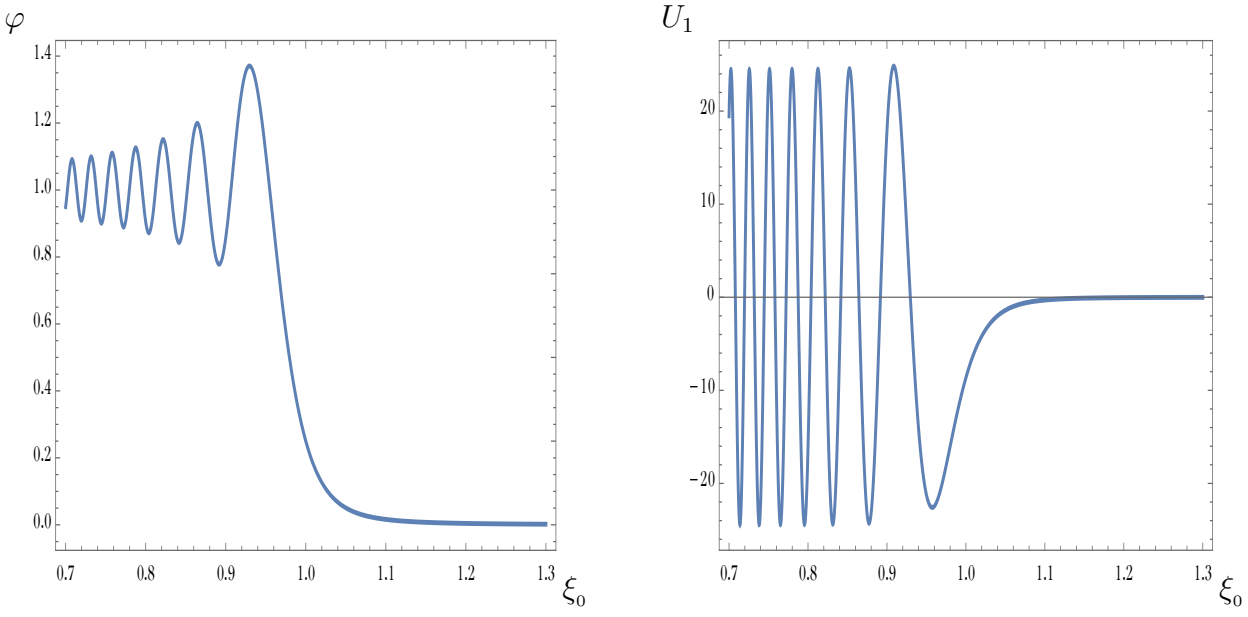

Figure 3.5: Rubber top hardening to teflon substrate.

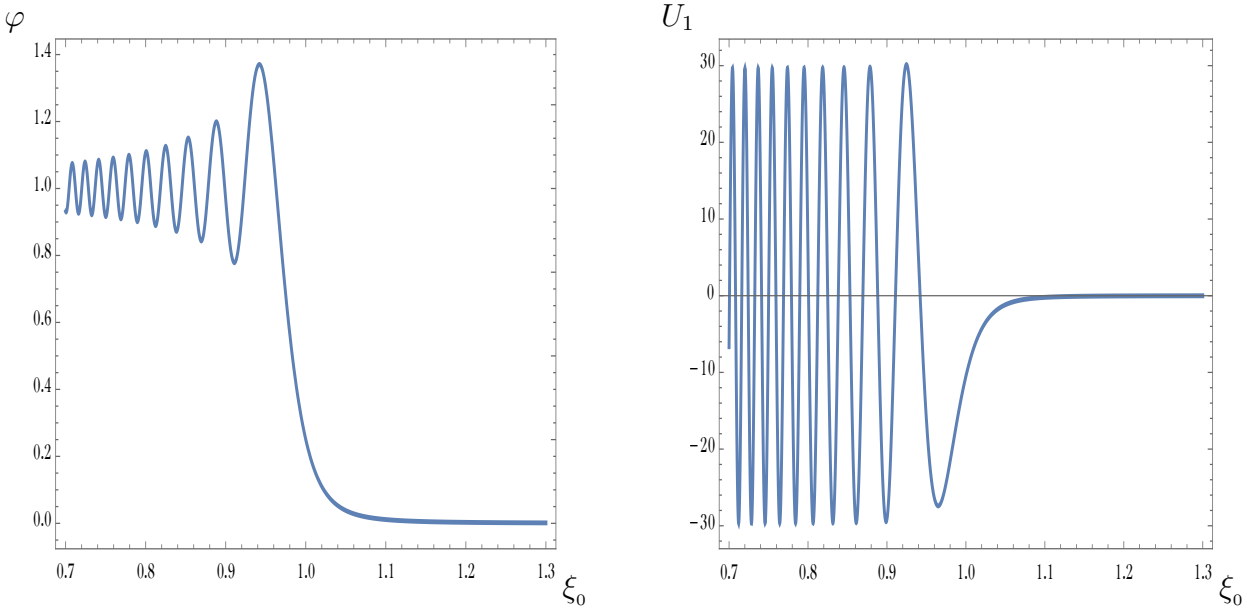

Figure 3.6: Rubber top hardening to polystyrene substrate.

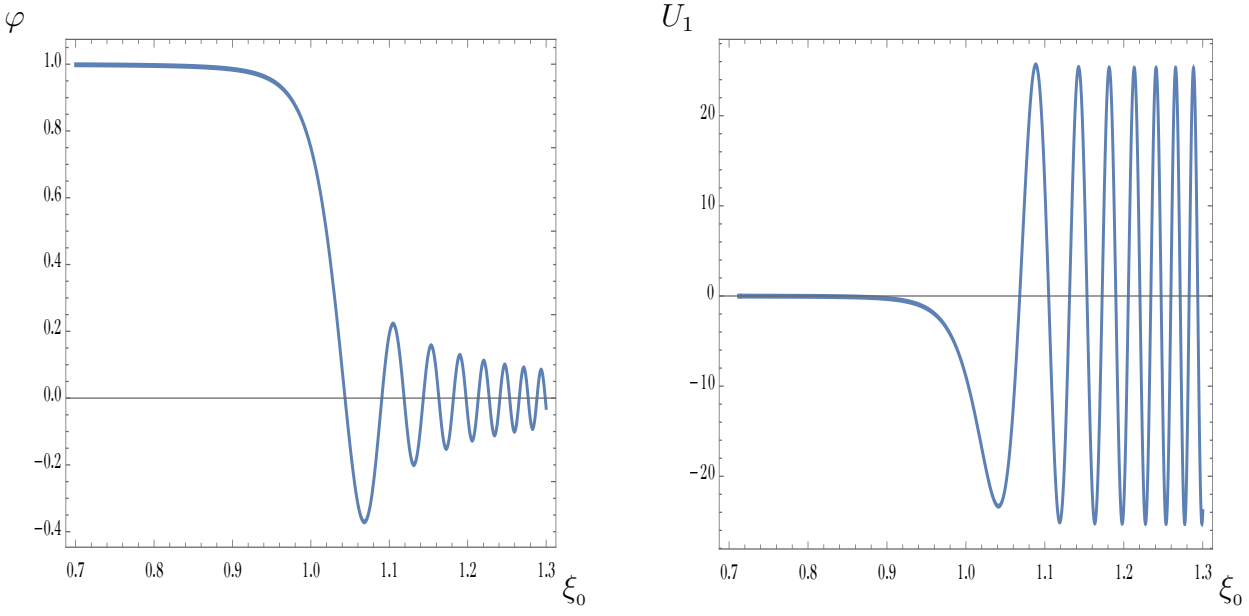

Figure 3.7: Polystyrene top softening to rubber substrate.

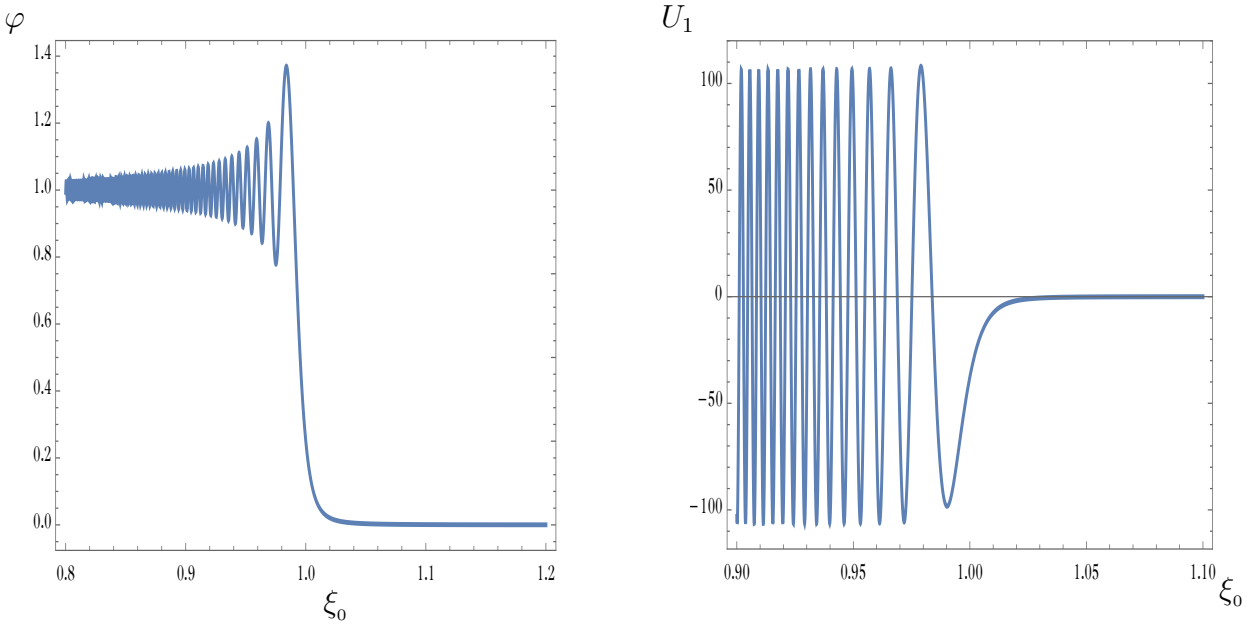

Figure 3.8: Nylon layer hardening slightly to polystyrene substrate.

The above Figs 3.5 - 3.8 are showing that depending on various stiffness of the layers we observe faster or slower oscillations and decay of the solution (3.54). We note in the case of surface properties of stiff polystyrene softening towards the rubber substrate gives the local maximum of the phase velocity at the Rayleigh wave speed ($b_c > 0$), with oscillations of the advancing front, being relatively slow, see Fig 3.7. On the other hand, cases of the soft teflon or the stiff polystyrene substrate covered by the layer with soft rubber or the stiff nylon properties on the upper surface correspond to $b_c < 0$, resulting in the oscillations of the receding front being relatively or rapidly fast, see Figs 3.5, 3.6 and 3.8. We also note that when the constant $b_c = 0$ (or in absent of the coating), the plot of (3.54) becomes

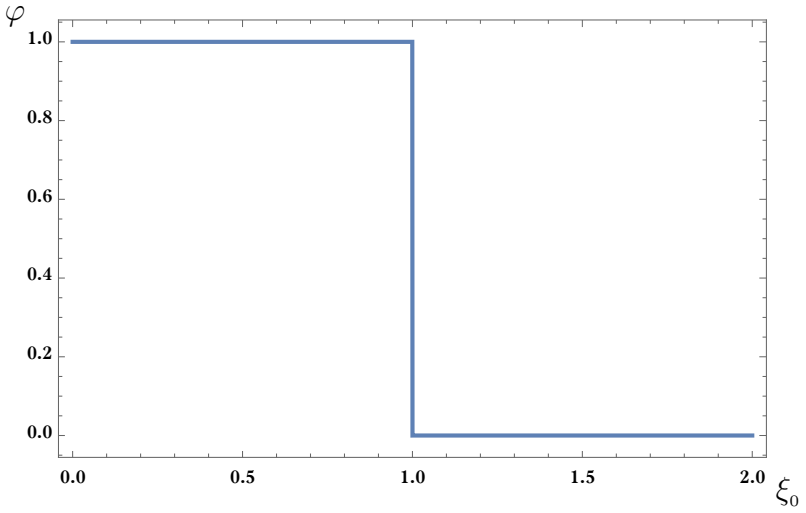

Figure 3.9: Discontinuity when $b_c = 0$.

3.5.2 Homogeneous multi-layers

Let us consider $N = 2$ as an illustrative example of homogeneous N-layered coating, with the thicknesses taken as $h_1 = 0.1$ and $h_2 = 0.2$.

For analysis of the dynamic response induced by the loading (3.52) on the homogeneous two-layered laminate, coating the elastic half-space, the relative thickness h_c becomes $h_c = (h_1 + h_2) \mid b_0 \mid /L$. Numerical results of scaled potential (3.54) and dimensionless displacement (3.55) are illustrated in the following Figs 3.10 – 3.17.

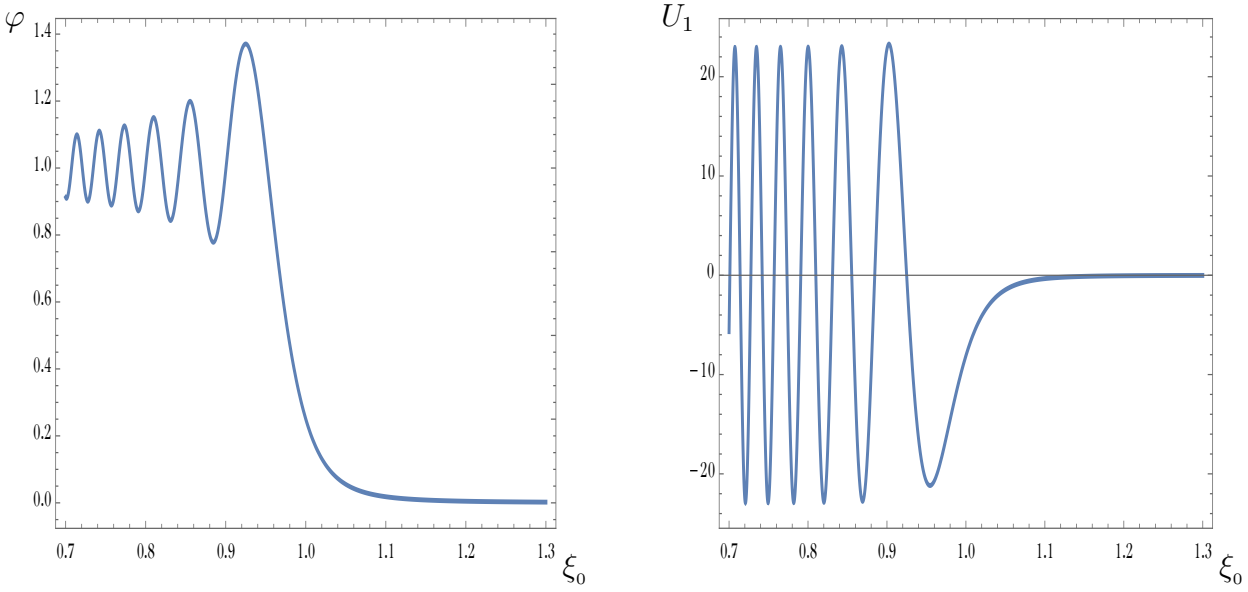

Figure 3.10: Rubber-teflon two layered laminate coating the polyethylene.

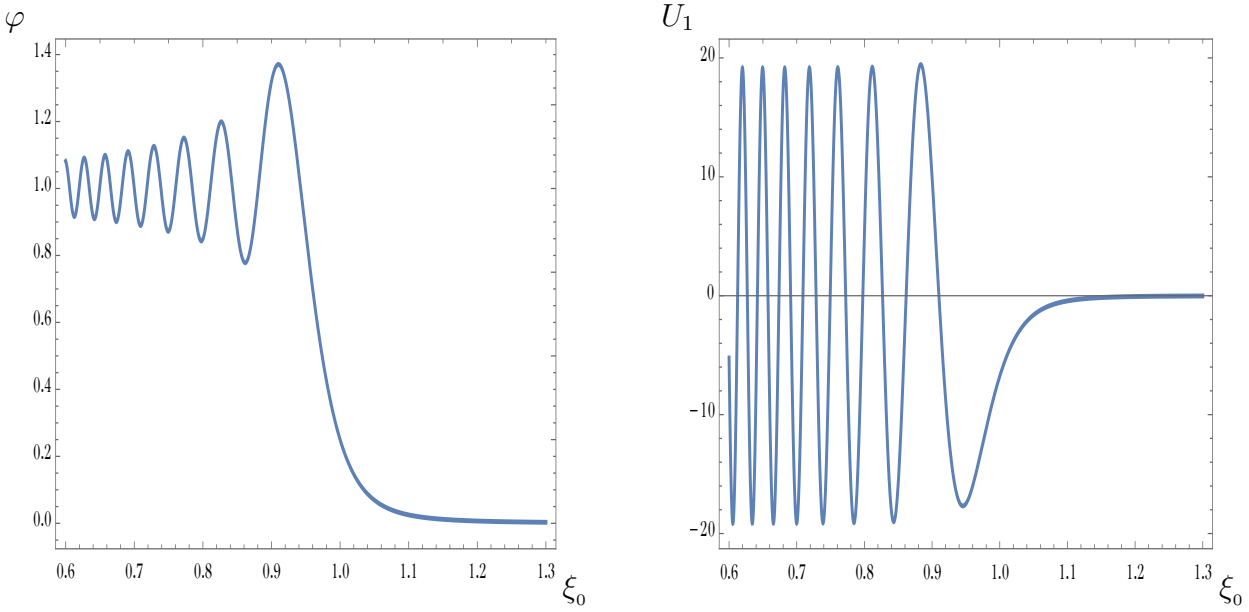

Figure 3.11: Two-layered rubber-teflon coating and polystyrene substrate.

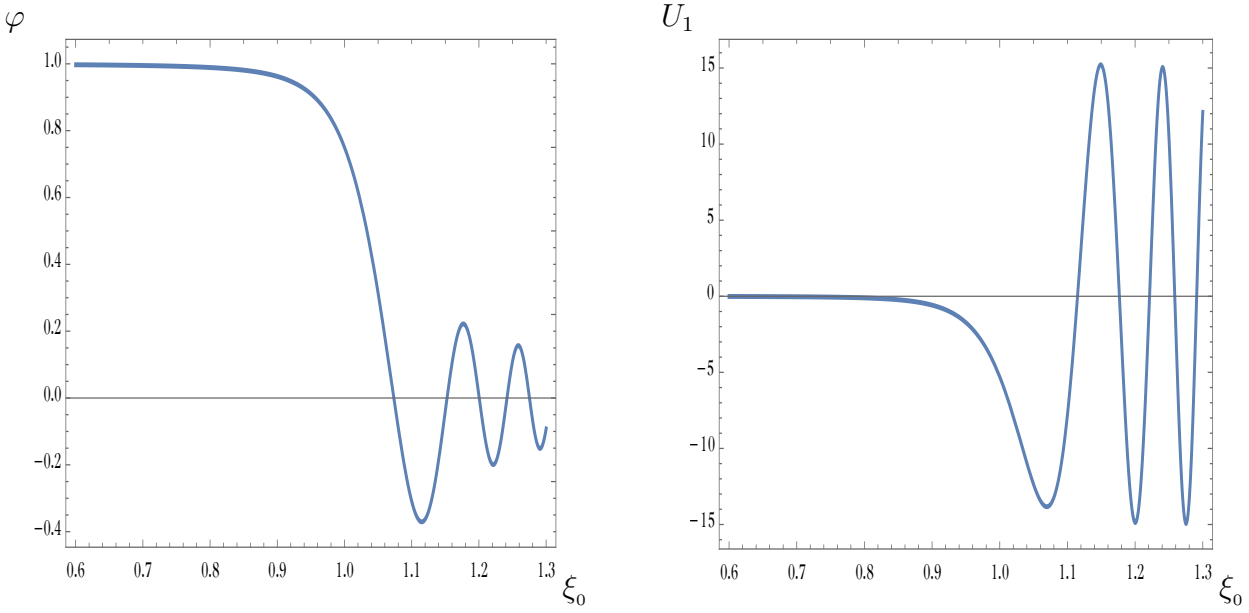

Figure 3.12: Rubber-polystyrene coating and teflon substrate.

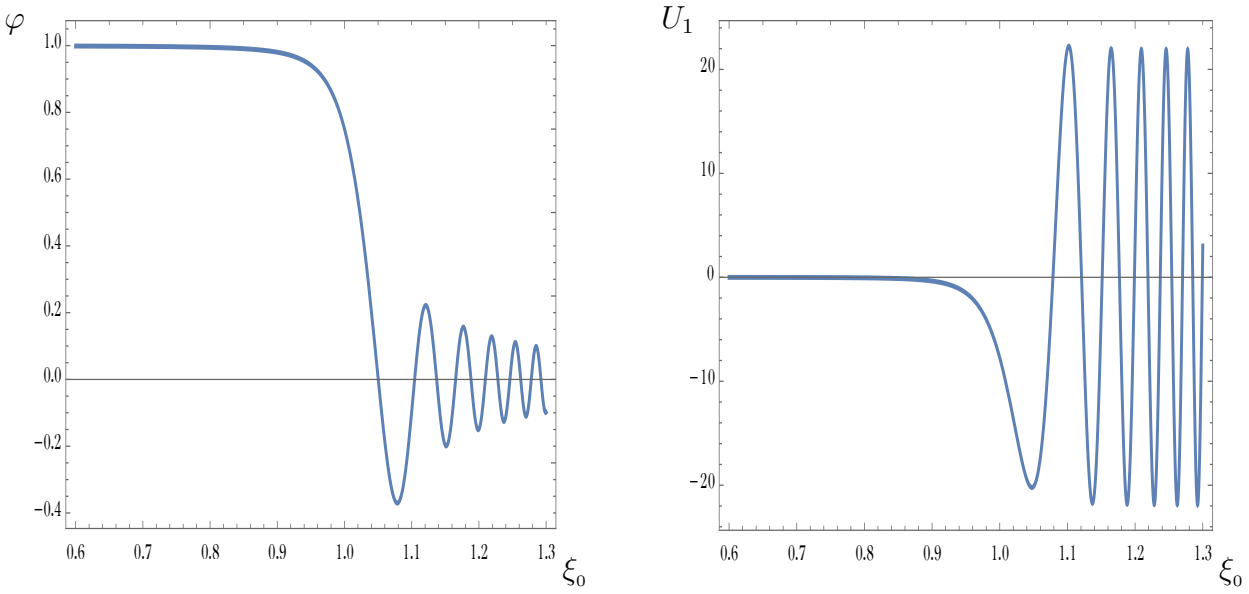

Figure 3.13: Polystyrene-rubber coating and teflon substrate.

The Figs. 3.10 and 3.11 describe the rapid oscillations of the receding front, corresponding to the soft layers of rubber and teflon in the coatings, with contrast in softness and stiffness of the polyethylene and polystyrene in the substrate, respectively. Swapping between the properties of the previous material of layers and the substrate causes the oscillations to convert to advancing front and become relatively slow, see Figs. 3.12 and 3.13.

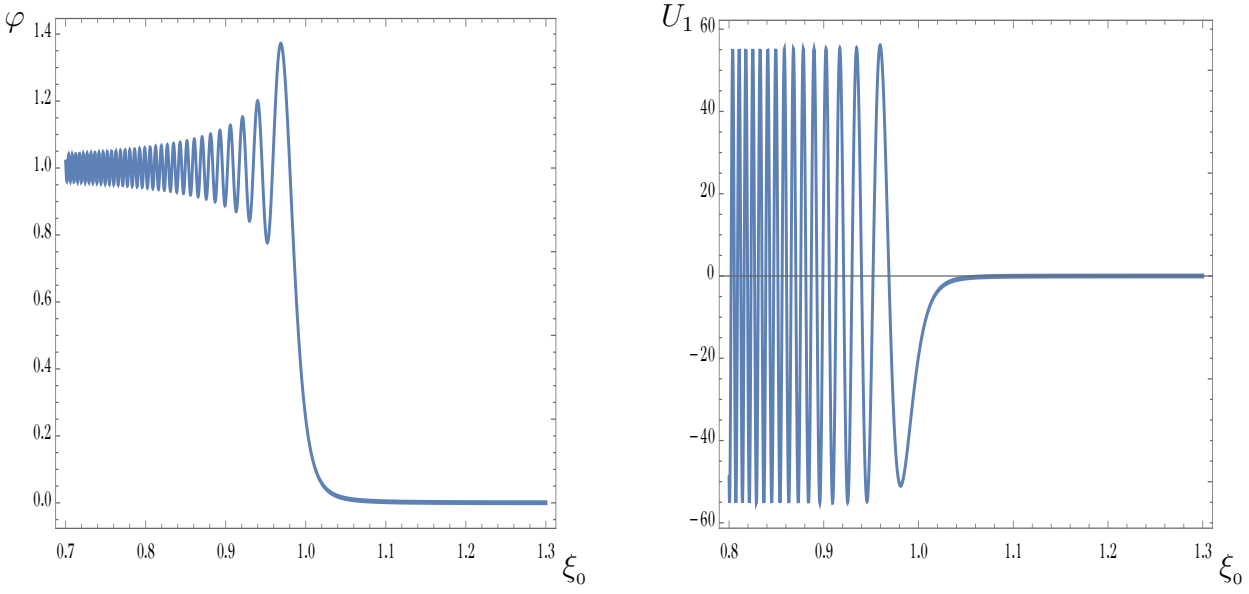

Figure 3.14: Polycarbonate-nylon coating and polystyrene substrate.

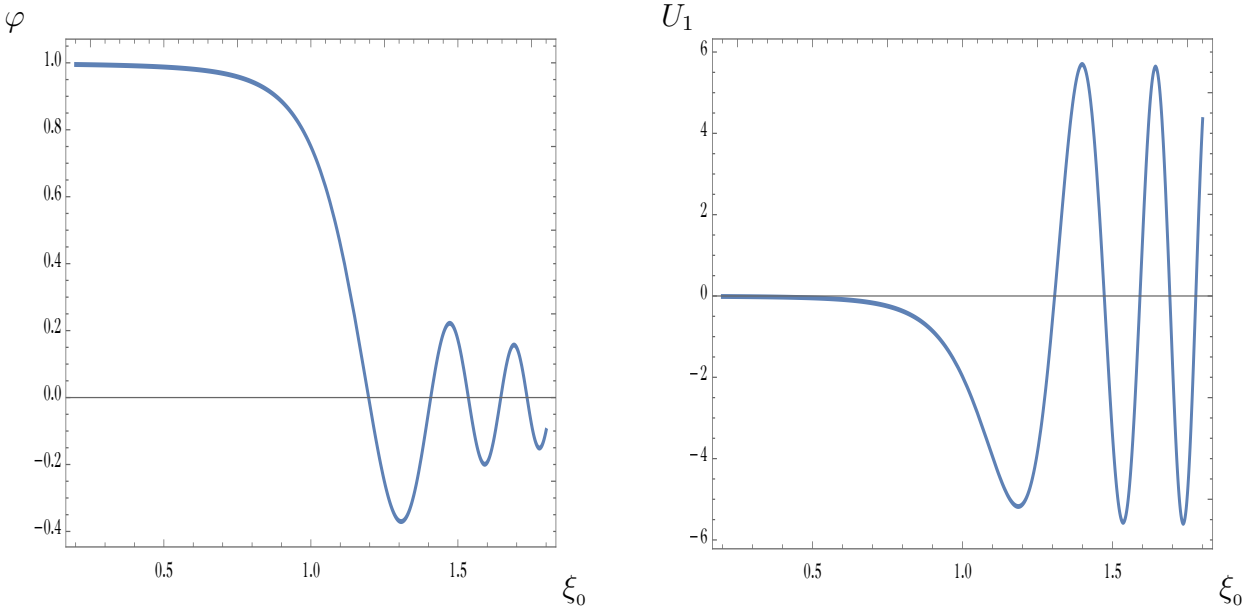

Figure 3.15: Nylon-polystyrene coating and rubber substrate.

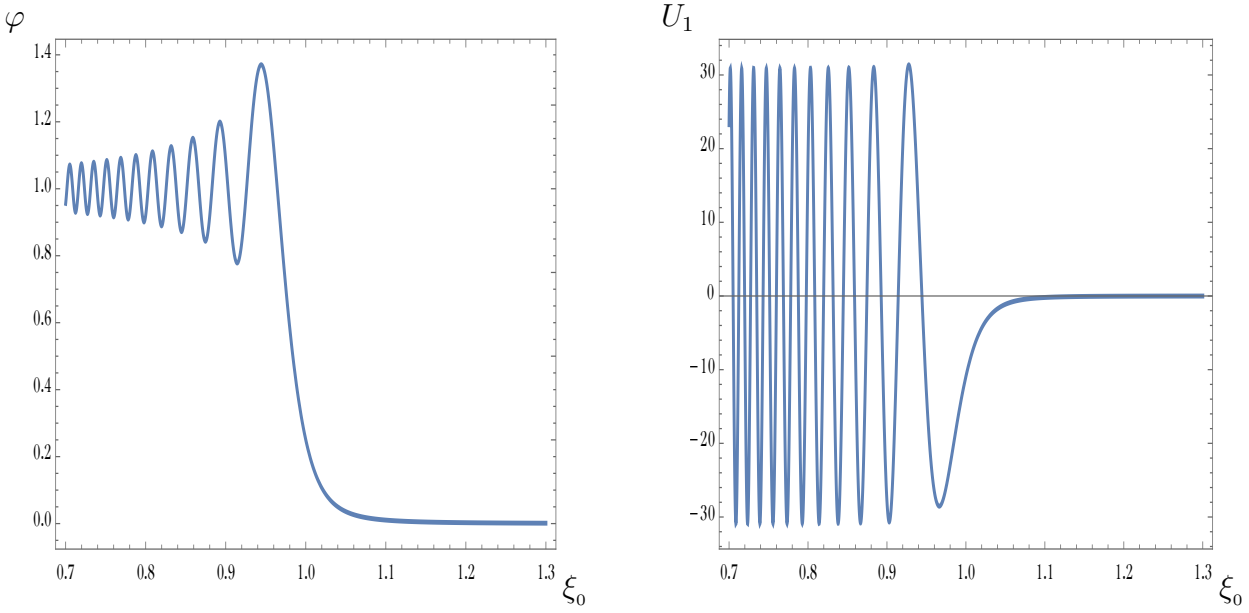

Figure 3.16: Nylon-rubber coating and polystyrene substrate.

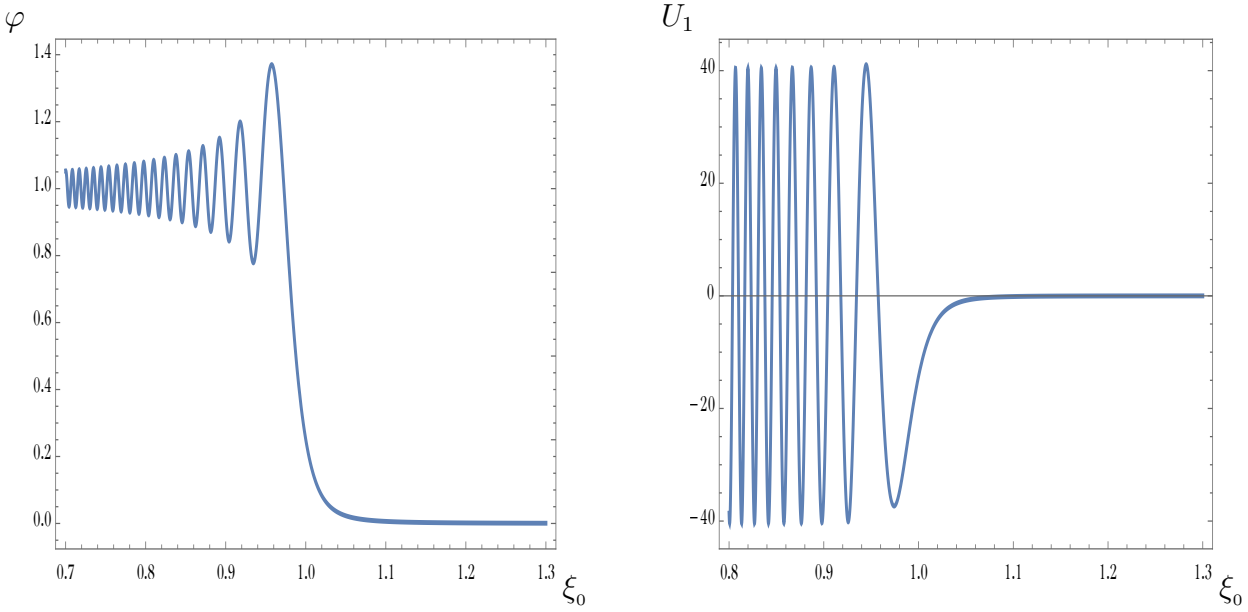

Figure 3.17: Rubber-nylon coating and polystyrene substrate.

In the case of stiff polystyrene substrate, with coating involving stiff polycarbonate and nylon layers, stiff nylon and soft rubber layers, and soft rubber with stiff nylon layers, the corresponding results are related to the local maximum of the phase velocity at the Rayleigh wave speed ($b_c > 0$), and the obtained oscillations demonstrate receding fronts, see Figs. 3.14, 3.16 and 3.17, respectively. On the other hand, if the substrate is made of soft rubber, with the coating composed of stiff nylon and polystyrene, that results in the minimum of the phase velocity ($b_c < 0$). Thus, the advancing front is gained, with oscillations being relatively slow, see Fig. 3.15.

In this chapter, propagation of surface waves on an isotropic elastic half- space coated by a thin inhomogeneous layer has been studied. The derived effective boundary conditions for modelling the thin inhomogeneous layer are derived. Then, the asymptotic formulation for the surface wave has been obtained in terms of harmonic functions

by using the perturbation technique. The resulting pseudo-differential equation is on the substrate-coating interface a singular perturbed equation. The implementation of the model allowed a straightforward analysis of the problem of a point vertical load applied to a half-space coated by a thin, vertically inhomogeneous layer, otherwise being quite challenging in the "exact" formulation.

Chapter 4

Moving load on an elastic half-space coated with a thin vertically inhomogeneous layer

The chapter is focused on applications of the previous results to the near-critical steady-state regimes of a moving point and disturbed load on a thin vertically inhomogeneous layer coated an elastic half-plane. The material properties of the thin coating, including the Lamé elastic moduli and the density, are supposed to be depth-dependent. First, in Section 4.1 the formulation following from the hyperbolic-elliptic model for the Rayleigh wave is rewritten in a moving coordinate system. The latter formulation allows considerable simplifications; in particular, it allows a natural classification to sub-Rayleigh and super-Rayleigh resonant regimes. In Sections 4.2, 4.3 and a pseudo-differential equation on the interface is studied, and the effect of poles on the real axis is analysed. Finally, some numerical examples are presented.

4.1 Formulation of the problem

Consider a concentrated load, moving steadily at a constant speed c along the surface of a coated half-space. We assume the coating layer to be vertically inhomogeneous, see Fig. 4.1.

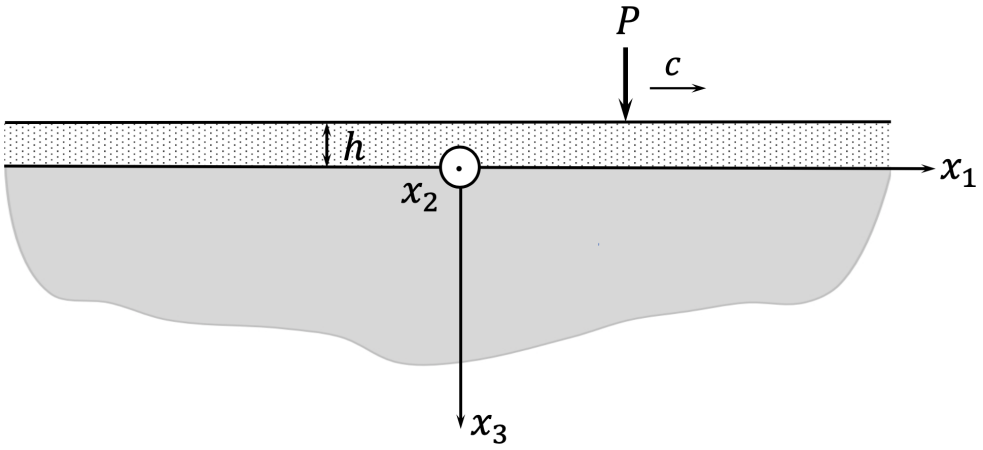

Figure 4.1: Moving point load on a coated elastic half-space.

The associated asymptotic formulation has been derived in Section 3.2, relying on the hyperbolic-elliptic formulation for the Rayleigh wave. For the present problem, the suggested model for a surface wave includes an elliptic equation for the interior $x_3 > 0$, given as in $(3.42)_1$, along with the pseudo-differential equation (3.48) on the interface, which may be reduced in plane-strain case to

$$\Box_R\,\phi - b_c\,h\,\sqrt{-\partial_{11}}\;\phi_{,11} = -\frac{(1+\beta_R^2)}{2\mu B_{_I}}\,P \qquad \text{at} \qquad x_3 = 0, \tag{4.1}$$

where the constants $B_{_I}$ and b_c are defined in (1.54) and (3.37), respectively.

The shear potential ψ is then determined from (4.1) and (1.43) at the surface $x_3 = 0$. Now, let us rewrite the boundary value problem $(1.109)_1$ and (4.1) in the moving coordinate system $(\theta, x_3) = (x_1 - c\,t,\, x_3)$, hence the steady-state limit is governed by

$$\phi_{,33} + \alpha_R^2\,\phi_{,\theta\theta} = 0, \tag{4.2}$$

subject to

$$\hat{\eta}\,\phi_{,\theta\theta} - b_c\,h\,\sqrt{-\partial_{\theta\theta}}\;(\phi_{,\theta\theta}) = -\frac{(1+\beta_R^2)}{2\mu B_{_I}}\,P \qquad \text{at} \qquad x_3 = 0, \tag{4.3}$$

where

$$\hat{\eta} = 1 - \frac{c^2}{c_R^2}.$$

and b_c has been defined in (3.37).

Let us consider the steady-state problems centring on the near-resonant regimes in which the speed of the moving load c is close to the resonant Rayleigh wave c_R in the substrate, i.e.,

$$|\,1 - \frac{c}{c_R}\,| \ll 1. \tag{4.4}$$

It worth to observe that the contribution of the Rayleigh wave to the total, dynamic response is dominant compared to that of body waves; accordingly, the explicit model for the Rayleigh wave is applicable.

4.2 Analysis on the interface with moving point load

Let us concentrate on the analysis of equation (4.3) on the interface $x_3 = 0$. Note that on putting $h = 0$ the problem formulation (4.2), (4.3) will reduce to that for an uncoated elastic half-space which is the leading order Taylor expansion of the exact solution Cole [1958], for more details see Kaplunov and Prikazchikov [2017]. In this case, the loading on the surface of the coating is assumed to take in the form

$$P = P_0\,\delta\,(\theta)\,. \tag{4.5}$$

Another observation which immediately follows from (4.3) is the presence of two small parameters, a geometric one, associated with the long-wave approximation, as well as $\hat{\eta}$ corresponding to the near-resonant vicinity.

Introducing the scaling

$$\zeta = \left|\frac{\hat{\eta}}{b_c}\right| \frac{\theta}{h},$$

along with

$$\sigma_c = -\frac{2\mu B_{_I}\, b_c\, h}{(1+\beta_R^2)\, P_0}\ \phi_{,\theta\theta},$$

we rewrite the pseudo-differential equation (4.3) on the interface as

$$\mathrm{sgn}\,(b_c\,\hat{\eta})\ \sigma_c - \sqrt{-\partial_{\zeta\zeta}}\ \sigma_c = \ \delta(\zeta). \tag{4.6}$$

On applying the Fourier integral transform, the solution of the latter is obtained as

$$\sigma_c = \frac{1}{2\pi} \int_{-\infty}^{\infty} \frac{e^{i\omega\,\zeta}\; d\omega}{\operatorname{sgn}(b_c\,\hat{\eta}) - |\omega|}. \tag{4.7}$$

It is clear that the $\operatorname{sgn}(b_c\,\hat{\eta})$ is important because this is related to possibility of having poles on the real axis in the denominator.

4.2.1 Sub-case 1: No poles on the real axis

Let us consider the first-situation $b_c\,\hat{\eta} < 0$, then the integral (4.7) leads to

$$\sigma_c = \frac{1}{2\pi} \int_{-\infty}^{\infty} \frac{e^{i\omega\,\zeta}\; d\omega}{-1 - |\omega|} = -\frac{1}{\pi} \operatorname{Re} \int_{0}^{\infty} \frac{e^{i\omega\zeta}\; d\omega}{1+\omega} = \mathcal{F}_1\left(|\zeta|\right), \tag{4.8}$$

where

$$\mathcal{F}_1(z) = \frac{1}{\pi}\left[\operatorname{si}(z)\sin z + \operatorname{Ci}(z)\cos z\right], \tag{4.9}$$

where si and Ci denote the sine and cosine integral functions, respectively, namely

$$\operatorname{si}(z) = -\int_{z}^{\infty} \frac{\sin t}{t}\, dt, \qquad \text{and} \qquad \operatorname{Ci}(z) = -\int_{z}^{\infty} \frac{\cos t}{t}\, dt,$$

see e.g. Abramowitz and Stegun [1965]. Observe that this case occurs either in the sub-Rayleigh regime ($c < c_R$) with a local minimum of the phase velocity at the Rayleigh wave speed ($b_c < 0$), or in the super-critical regime ($c > c_R$) along with a local maximum of the phase velocity ($b_c > 0$), for more details see Dai et al. [2010].

4.2.2 Sub-case 2: Poles on the real axis

The second-situation $b_c\,\hat{\eta} > 0$, (4.7) can be transformed as

$$\sigma_c = \frac{1}{2\pi}\int_{-\infty}^{\infty} \frac{e^{i\omega\,\zeta}}{1-|\omega|}\;d\omega = \frac{1}{\pi}\,\mathrm{Re}\int_{0}^{\infty} \frac{e^{i\omega\zeta}}{1-\omega}\;d\omega = -\frac{1}{\pi}\,\mathrm{Re}\int_{0}^{\infty} \frac{e^{i\omega\theta}}{\omega-\frac{\hat{\eta}}{h\,b_c}}\;d\omega. \tag{4.10}$$

The poles on the real axis of the latter integral may be treated using the limiting absorption principle, basically, introducing small viscosity in the system and tracing the associated shift of the pole either in the upper or in the lower half-space, implying the appropriate contour of integration, see e.g. Kalinchuk and Belyankova [2009], Schulenberger and Wilcox [1971], i.e.,

$$\mu_c \to \mu_c\,(I + \epsilon\,\partial_t) \equiv \mu_c\left(I - \frac{\epsilon}{c}\,\partial_\theta\right). \tag{4.11}$$

Using the properties of the Fourier transform, we obtain

$$\mu_c \to \mu_c\left(I - \frac{i\,\epsilon\,\omega}{c}\right). \tag{4.12}$$

For the quantity (3.37), we deduce

$$\mathrm{Im}\,b_c = \frac{2\mu_c\,\epsilon\,\omega}{\mu B_I\,c}\left[\left(1-\beta_R^2\right)\beta_R\,\tilde{\delta}\right] > 0, \tag{4.13}$$

where $\tilde{\delta}$ defined in (3.16).

Thus, the pole $\omega = \dfrac{\hat{\eta}}{hb_c}$ will transit to the upper or lower quarter plane in cases of $\hat{\eta} > 0$ and $\hat{\eta} < 0$, respectively. Therefore, the integral (4.7) can now be computed by using the following contours, shown in Fig. 4.2.

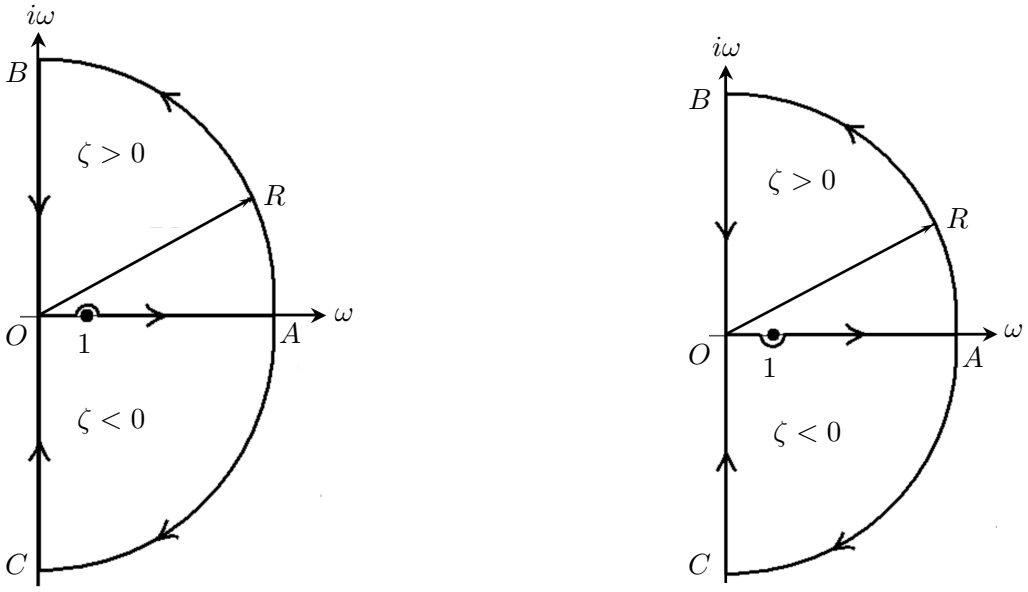

(a) $\hat{\eta} > 0$. (b) $\hat{\eta} < 0$.

Figure 4.2: Integration contours with $R \to \infty$ for (4.7).

Consider the case sub-Rayleigh ($\hat{\eta} > 0$) with $\zeta > 0$ (see Fig. 4.2 (a)), then the associated contour gives

$$\int\limits_{OABO} \frac{e^{i\omega\,\zeta}}{1-\omega}\; d\omega = \left(\int\limits_{OA} \frac{e^{i\omega\,\zeta}}{1-\omega} + \int\limits_{BO} \frac{e^{i\omega\,\zeta}}{1-\omega} \right) d\omega. \tag{4.14}$$

Here, the pole is not contained in the upper contour, thus, the integral over the contour $OABO$ is equal to zero, resulting

$$\sigma_c = \frac{1}{\pi}\,\mathrm{Re} \int\limits_0^{\infty} \frac{e^{i\omega\zeta}}{1-\omega}\; d\omega = \frac{1}{\pi}\,\mathrm{Re} \int\limits_{OB} \frac{e^{i\omega\,\zeta}}{1-\omega}\; d\omega. \tag{4.15}$$

Taking $\varpi = i\omega$, we obtain

$$\sigma_c = \frac{1}{\pi}\,\mathrm{Re} \int\limits_0^{\infty} \frac{i\,e^{-\zeta\varpi}}{1-i\,\varpi}\; d\varpi = \frac{1}{\pi} \int\limits_0^{\infty} \frac{\varpi\,e^{-\zeta\varpi}}{1+\varpi^2}\; d\varpi = \mathcal{F}_1\left(\zeta\right). \tag{4.16}$$

The case $\zeta < 0$ may be treated in similar way, however, the pole should be included into the contour. On using the residue theory, the integral (4.7) gives

$$\begin{aligned}\sigma_c = \frac{1}{\pi}\,\mathrm{Re}\int\limits_0^\infty \frac{e^{i\omega\zeta}}{1-\omega}\,d\omega = 2\,\mathrm{Im}\,\underset{\omega=1}{Res}\,\frac{e^{i\omega\zeta}}{\omega-1} - \frac{1}{\pi}\,\mathrm{Re}\int\limits_{OC}\frac{e^{i\omega\zeta}}{\omega-1}\,d\omega \\ = -2\,\sin\,\zeta + \mathcal{F}_1\left(-\zeta\right).\end{aligned} \tag{4.17}$$

Next, we consider the case of the super-Rayleigh ($\hat{\eta} < 0$) (see Fig. 4.2 (b)) with $\zeta > 0$, the pole may be incorporated, hence

$$\begin{aligned}\sigma_c = \frac{1}{\pi}\,\mathrm{Re}\int\limits_0^\infty \frac{e^{i\omega\zeta}}{1-\omega}\,d\omega = 2\,\mathrm{Im}\,\underset{\omega=1}{Res}\,\frac{e^{i\omega\zeta}}{1-\omega} - \frac{1}{\pi}\,\mathrm{Re}\int\limits_{OB}\frac{e^{i\omega\zeta}}{\omega-1}\,d\omega \\ = 2\,\sin\,\zeta + \mathcal{F}_1\left(\zeta\right),\end{aligned} \tag{4.18}$$

and also, we get at $\zeta < 0$

$$\sigma_c = \frac{1}{\pi}\,\mathrm{Re}\int\limits_0^\infty \frac{e^{i\omega\zeta}}{1-\omega}\,d\omega = \mathcal{F}_1\left(-\zeta\right). \tag{4.19}$$

From above discussion, we can deduce in the case of the sub-Rayleigh regime ($c < c_R$) with ($b_c > 0$), the formula (4.7) yields

$$\sigma_c = -2\,H\left(-\zeta\right)\,\sin\zeta + \mathcal{F}_1\left(|\zeta|\right), \tag{4.20}$$

whereas in the case of the super-Rayleigh regime ($c > c_R$) with ($b_c < 0$) the solution becomes

$$\sigma_c = 2\,H\left(\zeta\right)\sin\zeta + \mathcal{F}_1\left(|\zeta|\right), \tag{4.21}$$

with $\mathcal{F}_1$ defined in (4.9) and $H(\zeta)$ denoting the Heaviside function.

4.2.3 Numerical results

In this subsection, an illustrative example of the obtained results is presented.

Let us consider the Young's modulus E_c of the thin coating layer is depth-dependent, taking the form as in (3.56). Here, we assume mass densities $\rho_c = \rho = 1$, Poisson's ratios $\nu_c = \nu = 0.25$ and thickness of coating layer $h = 1$, as well as the sub-Rayleigh and super-Rayleigh regimes calculated for $c = 0.9\, c_R$, and $c = 1.1\, c_R$, respectively.

We consider the first situation of the hardness of the thin coating decays with depth, where the top surface is ten times stiffer than the substrate. The related graphs in Fig. 4.3 illustrate the dependence of the quantity σ_c on the scaled moving coordinate ζ. Accordingly, the constant b_c can be calculated utilising (3.37), as a result, the constant $b_c \approx -1.32$. In Fig. 4.3 (a) the sub-Rayleigh regime is depicted ($\hat{\eta} > 0$), associating with the case of no poles in (4.7), while Fig. 4.3 (b) shows the super-Rayleigh regime ($\hat{\eta} < 0$), illustrating the effect of poles in (4.7) for positive ζ, i.e. radiation of energy in front of the moving source.

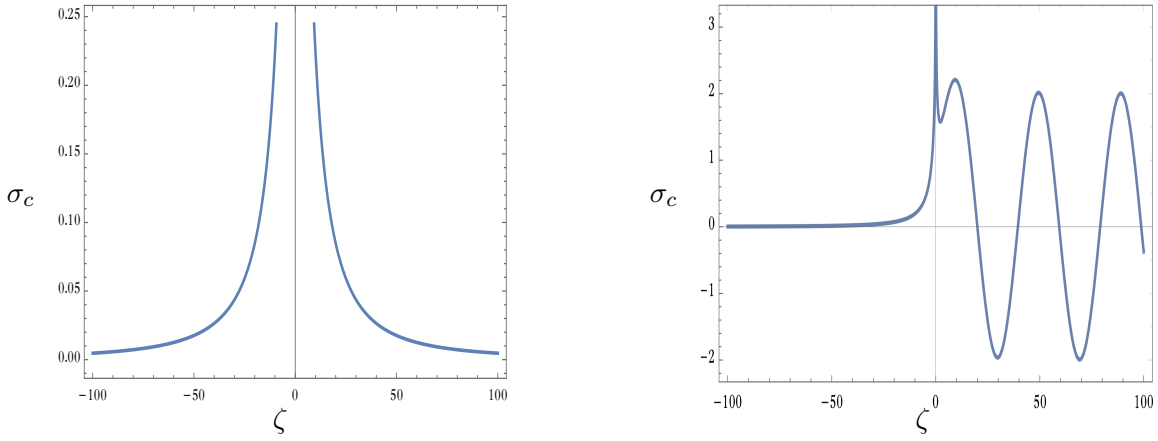

(a) $\hat{\eta} > 0$. (b) $\hat{\eta} < 0$.

Figure 4.3: Dependence of the quantity σ_c on the moving coordinate ζ for the case of softening within the layer ($E_0/E = 10$).

On the next two graphs, we present that case when the coating layer is hardening throughout the thickness, with the surface being ten times softer than the substrate. According to (3.37), the computation of the constant b_c gives $b_c \approx 0.276$. The plots in Figs. 4.4 (a) and 4.4 (b) present the variation of the quantity σ_c on the moving coordinate ζ. Now the radiation from the moving source occurs in the sub-Rayleigh regime in Fig. 4.4 (a).

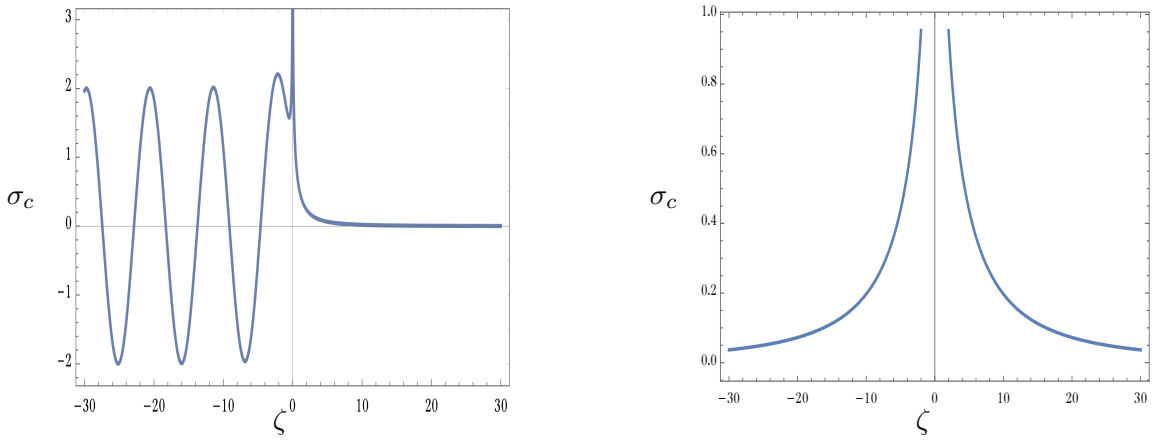

(a) $\hat{\eta} > 0$. (b) $\hat{\eta} < 0$.

Figure 4.4: Dependence of the quantity σ_c on the moving coordinate ζ for the case of hardening within the layer ($E_0/E = 0.1$).

Note that the above obtained results have been presented in Althobaiti et al. [2020].

4.3 Analysis on the interface with the distributed load

Let us consider the effect of load distribution on the surface of coating, which is moving at a constant speed c. Thus the load takes in the form

$$P = \frac{P_0\, l}{\pi\,(l^2 + \theta^2)}\,, \tag{4.22}$$

where $\theta = x_1 - c\,t$, and l is the parameter, determining the distributed load, see Fig. 4.5.

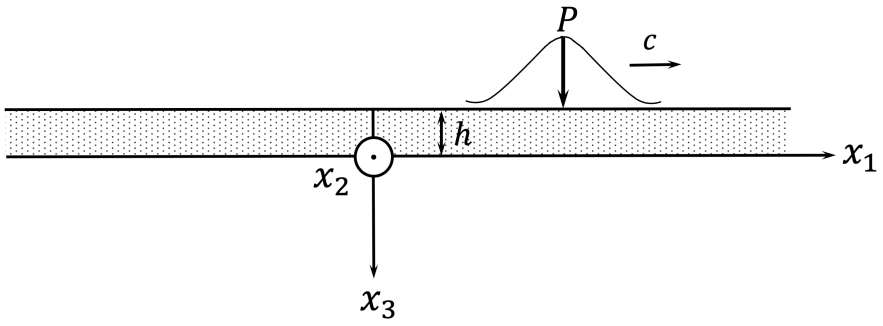

Figure 4.5: Distributed load on a coated elastic half-space.

Now, let us introduce the dimensionless coordinate

$$\Theta = \frac{\theta}{l}, \qquad \text{and} \qquad h_l = \frac{b_c\, h}{l}, \tag{4.23}$$

along with

$$\chi_l = -\frac{2\mu B_I \pi\, h_l}{(1+\beta_R^2)\, l\, P_0}\;\phi_{,\Theta\Theta}, \qquad \lambda = a_s\,\Theta, \qquad a_s = \left|\frac{\hat{\eta}}{b_c}\right|, \tag{4.24}$$

then, the equation (4.3) is taken the form

$$\operatorname{sgn}(h_l\,\hat{\eta})\;\chi_l - \sqrt{-\partial_{\lambda\lambda}}\;\chi_l = \frac{a_s}{(a_s^2+\lambda^2)}. \tag{4.25}$$

The solution of the latter equation may be obtained by applying the Fourier integral transform

$$\chi_l = \frac{1}{2}\int_{-\infty}^{\infty} \frac{e^{-a_s\,|\omega|}\;e^{i\omega\,\lambda}}{\operatorname{sgn}(h_l\,\hat{\eta}) - |\omega|}\,d\omega. \tag{4.26}$$

4.3.1 Sub-case 1: No poles acting on the real axis

Consider first the situation $h_l\,\hat{\eta} < 0$, then the integral (4.26) is readily evaluated as

$$\chi_l = \frac{1}{2}\int_{-\infty}^{\infty} \frac{e^{-a_s\,|\omega|}\;e^{i\omega\,\lambda}}{\operatorname{sgn}(h_l\,\hat{\eta}) - |\omega|}\,d\omega = -\mathrm{Re}\int_{0}^{\infty} \frac{e^{a_s\,\omega}\,e^{i\omega\,\lambda}}{1+\omega}\,d\omega = \mathcal{F}_2\left(\bar{\Omega}\right), \tag{4.27}$$

where

$$\mathcal{F}_2\left(\bar{\Omega}\right) = \mathrm{Re}\left[\mathrm{e}^{\bar{\Omega}}\;\Gamma\left(0,\bar{\Omega}\right)\right], \qquad \bar{\Omega} = a_s - i\,\lambda, \tag{4.28}$$

with $\Gamma(0,z)$ denoting the incomplete gamma function, i.e

$$\Gamma(0,z) = \int_{z}^{\infty} \frac{e^{-t}}{t}\,dt,$$

for more details, see e.g. Abramowitz and Stegun [1965].

4.3.2 Sub-case 2: Poles on the real axis

The second sub-case $h_l\,\hat{\eta} > 0$, the integral (4.26) may be treated in a similar way as in Subsection 4.2.2. As result, in the case of the sub-Rayleigh regime ($\hat{\eta} > 0$), with ($h_l > 0$) and $\lambda > 0$, the formula (4.26) yields

$$\chi_l = -2\pi\, e^{a_s}\, H(-\lambda)\, \sin(-\lambda) + 2\mathrm{Re}\left[\mathrm{e}^{-\Omega}\left(\pi i - \mathrm{Ei}\left(\Omega\right)\right)\right], \tag{4.29}$$

while in the situation of the super-critical regime ($\hat{\eta} < 0$) the solution takes the form

$$\chi_l = 2\pi\, e^{a_s}\, H(\lambda)\, \sin(\lambda) + 2\mathrm{Re}\left[\mathrm{e}^{\Omega}\left(\pi i - \mathrm{Ei}\left(-\Omega\right)\right)\right], \tag{4.30}$$

where $\Omega = a_s + i\,\lambda$ and $\mathrm{Ei}\,(z)$ is the exponential integral, defined by

$$\mathrm{Ei}\,(z) = -\int_{-z}^{\infty} \frac{e^{-t}}{t}\, dt,$$

for more details, see e.g. Abramowitz and Stegun [1965].

4.3.3 Numerical example

In this section, we follow the illustrative examples in Subsection 4.2.3, showing the the variation of the quantity χ_l on the moving coordinate λ, which computed by equation (4.26). Comparison with results for concentrated load clearly demonstrates smoothing of discontinuity at $\epsilon = 0$ for distributed load.

In Fig. 4.6 (a) the sub-Rayleigh regime ($\hat{\eta} > 0$) associates with the case of no poles in (4.26), while Fig. 4.6 (b) corresponds to the influence of poles in (4.26) for positive λ, namely the radiation from the moving source in the super-Rayleigh mode ($\hat{\eta} < 0$).

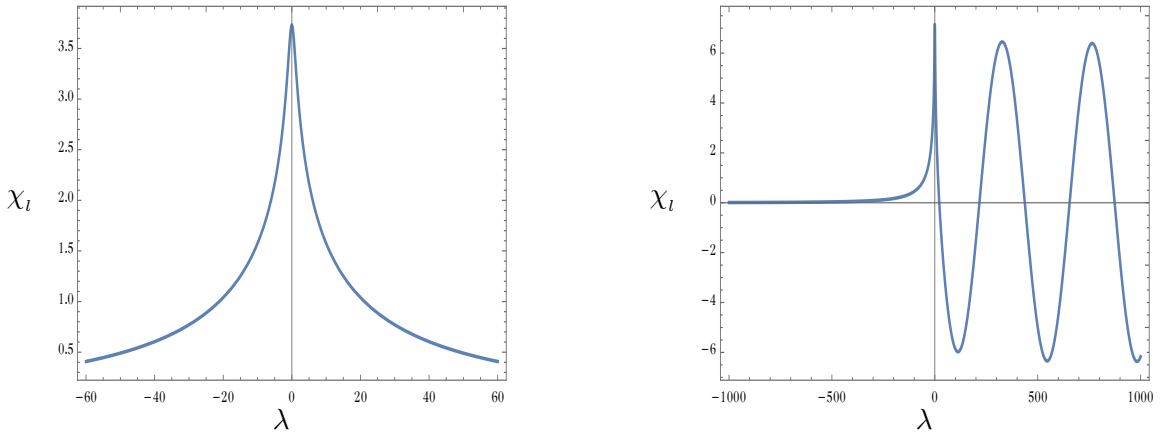

(a) $\hat{\eta} > 0$. (b) $\hat{\eta} < 0$.

Figure 4.6: Dependence of the quantity χ_l on the moving coordinate λ for the case of softening within the layer ($E_0/E = 10$).

From Figs. 4.7 (a) and (b), It can be seen that the radiation from the moving source happens in the sub-Rayleigh regime ($\hat{\eta} > 0$).

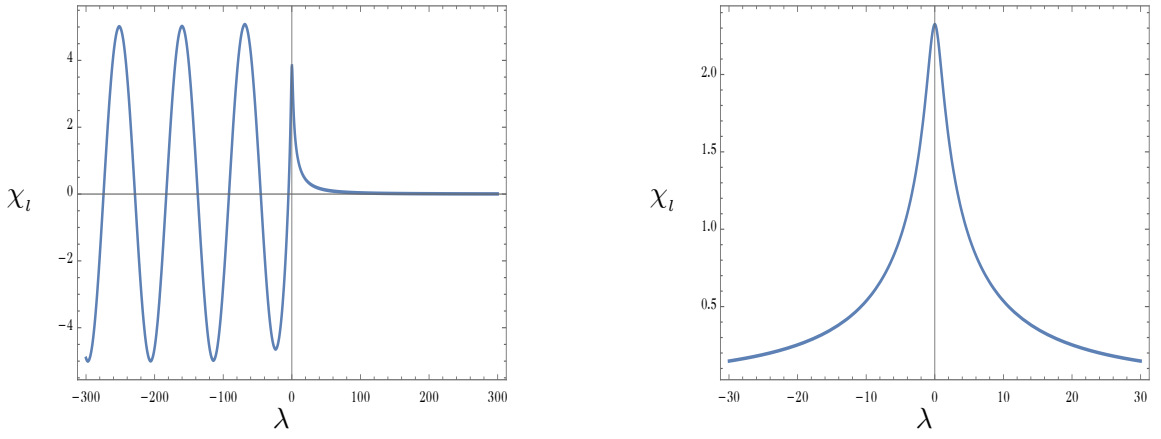

(a) $\hat{\eta} > 0$. (b) $\hat{\eta} < 0$.

Figure 4.7: Dependence of the quantity χ_l on the moving coordinate λ for the case of hardening within the layer ($E_0/E = 0.1$).

Results for the steady-state problem for moving concentrated and disturbed loads on a half-space coated by a thin vertically inhomogeneous layer have been presented. The hyperbolic-elliptic model for the Rayleigh wave field allowed an explicit near-resonant solution, as well as an obvious classification of the regimes.

Chapter 5

Explicit model of surface waves under the influence of gravity

This chapter is aimed at developing the methodology of hyperbolic-elliptic asymptotic models for surface waves with the effect of gravity.

First, the equations of motion incorporating the effect of gravity are presented in Section 5.1. Next, the exact dispersion equation for a coated half-space with gravity is obtained, and its approximation is constructed. The explicit model for surface waves on an elastic half-space is derived incorporating the effect of gravity in Section 5.3, extending to the case of a thin vertically inhomogeneous coating in Section 5.4. The effect of gravity is shown to be related to a regular pertubative term in the wave equation on the surface in the form of a pseudo-differential operator.

5.1 Governing equations

The 3D dynamic equations of motion interoperating the gravitational field are given by Biot [1965], see also Ting [2011] and Vinh and Seriani [2009]

$$\begin{aligned}
&\sigma_{11,1} + \sigma_{12,2} + \sigma_{13,3} + \rho g\, u_{3,1} = \rho\, u_{1,tt},\\
&\sigma_{21,1} + \sigma_{22,2} + \sigma_{23,3} + \rho g\, u_{3,2} = \rho\, u_{2,tt},\\
&\sigma_{31,1} + \sigma_{32,2} + \sigma_{33,3} - \rho g\,(u_{1,1} + u_{2,2}) = \rho\, u_{3,tt},
\end{aligned} \tag{5.1}$$

where g is an acceleration of gravity.

For plane-strain problem, we have

$$\begin{aligned}
&\sigma_{11,1} + \sigma_{13,3} + \rho g\, u_{3,1} = \rho\, u_{1,tt},\\
&\sigma_{31,1} + \sigma_{33,3} - \rho g\, u_{1,1} = \rho\, u_{3,tt}.
\end{aligned} \tag{5.2}$$

The equations of motion may be rewritten in terms of displacements u_r $(r = 1, 3)$ by inserting (1.7) into (5.2), yielding

$$\begin{aligned}
&(\lambda + 2\mu)\, u_{1,11} + \mu\, u_{1,33} + (\lambda + \mu)\, u_{3,13} - \rho\, u_{1,tt} = -\rho g\, u_{3,1},\\
&(\lambda + 2\mu)\, u_{3,33} + \mu\, u_{3,11} + (\lambda + \mu)\, u_{1,13} - \rho\, u_{3,tt} = \rho g\, u_{1,1}.
\end{aligned} \tag{5.3}$$

Now, we express the components of displacement by two elastic potentials (1.22), obtaining

$$\begin{aligned}
&\phi_{,11} + \phi_{,33} - \frac{1}{c_1^2}\,\phi_{,tt} = -\frac{g}{c_1^2}\,\psi_{,1},\\
&\psi_{,11} + \psi_{,33} - \frac{1}{c_2^2}\,\psi_{,tt} = \frac{g}{c_2^2}\,\phi_{,1}.
\end{aligned} \tag{5.4}$$

5.2 Dispersion equation for a coated half-space with gravity

In this section, the exact dispersion relation for surface waves on a coated elastic half-space with the influence of gravity is established.

Consider an elastic half-space, occupying the domain $-\infty < x_1, x_2 < \infty$ and $0 \leq x_3 \leq \infty$, covered by a thin coating of constant thickness h, taking the region $-h \leq x_3 \leq 0$, along with influence of gravity, see Fig. 5.1.

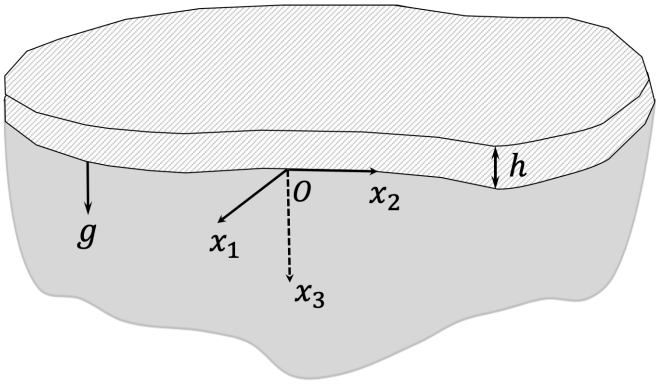

Figure 5.1: A coated elastic half-space under the gravity effect.

For the plane-strain problem, the imposed boundary conditions at $x_3 = -h$ and $x_3 = 0$ are given as in (1.55) and (1.56), respectively. The appropriate material parameters of the coating and the substrate are taken as in the Table 1.1.

On introducing the solutions (1.58) into (5.4), we arrive at

$$\begin{aligned} \frac{d^2 f_q}{dx_3^2} - \hat{k}^2 \alpha_q^2 f_q &= -i\hat{k}^2 \kappa_q^{-2} \varepsilon_q g_q, \\ \frac{d^2 g_q}{dx_3^2} - \hat{k}^2 \beta_q^2 g_q &= i\hat{k}^2 \varepsilon_q f_q, \end{aligned} \tag{5.5}$$

where α_q and β_q $(q = c, s)$ defined in (1.28) and (1.60), respectively, with

$$\varepsilon_c = \frac{g}{\hat{k}\, c_{20}^2}, \qquad \varepsilon_s = \varepsilon = \frac{g}{\hat{k}\, c_2^2}, \qquad \kappa_c = \frac{c_{10}}{c_{20}}, \qquad \kappa_s = \kappa = \frac{c_1}{c_2}. \tag{5.6}$$

From equation (5.5), we have

$$g_q = \frac{i\,\kappa_q^2}{\varepsilon_q\,\hat{k}^2}\left(\frac{d^2}{dx_3^2} - \hat{k}^2\,\alpha_q^2\right) f_q, \tag{5.7}$$

and

$$\left[\left(\frac{d^2}{dx_3^2} - \hat{k}^2\,\hat{\lambda}_{1q}^2\right)\left(\frac{d^2}{dx_3^2} - \hat{k}^2\,\hat{\lambda}_{2q}^2\right)\right] f_q = 0, \tag{5.8}$$

where

$$\hat{\lambda}_{1q}^2 + \hat{\lambda}_{2q}^2 = \alpha_q^2 + \beta_q^2, \qquad \text{and} \qquad \hat{\lambda}_{1q}^2\,\hat{\lambda}_{2q}^2 = \alpha_q^2\,\beta_q^2 - \frac{\varepsilon_q^2}{\kappa_q^2}. \tag{5.9}$$

The solution of (5.8), decaying a way from the surface $x_3 = 0$, may be expressed in the form

$$f_c = C_{1c}\, e^{\hat{k}\hat{\lambda}_{1c}\, x_3} + C_{2c}\, e^{-\hat{k}\hat{\lambda}_{1c}\, x_3} + C_{3c}\, e^{\hat{k}\hat{\lambda}_{2c}\, x_3} + C_{4c}\, e^{-\hat{k}\hat{\lambda}_{2c}\, x_3}, \tag{5.10}$$

and

$$f_s = C_{1s}\, e^{-\hat{k}\hat{\lambda}_{1s}\, x_3} + C_{2s}\, e^{-\hat{k}\hat{\lambda}_{2s}\, x_3}, \tag{5.11}$$

where C_{1c}, C_{2c}, C_{3c}, C_{4c}, C_{1s} and C_{2s} are constants.

Substituting (5.10) and (5.11) into (5.7), we deduce

$$g_c = \gamma_{1c}\left(C_{1c}\, e^{\hat{k}\hat{\lambda}_{1c}\, x_3} + C_{2c}\, e^{-\hat{k}\hat{\lambda}_{1c}\, x_3}\right) + \gamma_{2c}\left(C_{3c}\, e^{\hat{k}\hat{\lambda}_{2c}\, x_3} + C_{4c}\, e^{-\hat{k}\hat{\lambda}_{2c}\, x_3}\right), \tag{5.12}$$

and

$$g_s = \gamma_{1s}\, C_{1s}\, e^{-\hat{k}\hat{\lambda}_{1s}\, x_3} + \gamma_{2s}\, C_{2s}\, e^{-\hat{k}\hat{\lambda}_{2s}\, x_3}, \tag{5.13}$$

where

$$\gamma_{jq} = \frac{i\,\kappa_q^2}{\varepsilon_q}\left(\hat{\lambda}_{jq}^2 - \alpha_q^2\right), \; j = 1, 2. \tag{5.14}$$

Inserting the solutions (5.10) – (5.13) into the boundary conditions (1.55) and (1.56), therefore, the related dispersion relation is obtained by

$$\mathrm{Det}\,(\mathbf{T}) = 0, \tag{5.15}$$

where the matrix $\mathbf{T}$ is given in (*B*.1).

5.2.1 Particular case: uncoated half-space

In the case of no coating ($h = 0$), the dispersion equation (5.15) reduces to

$$\frac{2i\,\hat{\lambda}_{1s} + \gamma_{1s}\left(1 + \hat{\lambda}_{1s}^2\right)}{2i\,\hat{\lambda}_{2s} + \gamma_{2s}\left(1 + \hat{\lambda}_{2s}^2\right)} = \frac{i\left(1 - \hat{\lambda}_{1s}^2\right)\kappa_s^2 - 2\left(i + \gamma_{1s}\,\hat{\lambda}_{1s}\right)}{i\left(1 - \hat{\lambda}_{2s}^2\right)\kappa_s^2 - 2\left(i + \gamma_{2s}\,\hat{\lambda}_{2s}\right)}. \tag{5.16}$$

We now assume

$$\varepsilon_s = \varepsilon = \frac{g}{c_2^2\,\hat{k}} \ll 1, \tag{5.17}$$

representing the effect of gravity and defining the range of wavenumbers, allowing weak coupling between equations (5.4). Then, we obtain from (5.16)

$$K_0 + K_1\,\varepsilon + K_2\,\varepsilon^2 + O\left(\varepsilon^3\right) = 0, \tag{5.18}$$

where

$$K_0 = \left(1+\beta_s^2\right)^2 - 4\,\alpha_s\,\beta_s, \qquad K_1 = \frac{4\left(1-\alpha_s\,\beta_s\,\kappa^2\right)}{\kappa^2\left(\alpha_s+\beta_s\right)},$$
$$K_2 = \frac{1}{\kappa^2\left(\alpha_s^2-\beta_s^2\right)^2}\left[\frac{2\alpha_s}{\beta_s}\left(\alpha_s^2-6\beta_s^2\right)+\alpha_s^2\left(\beta_s^2\left(2\kappa^2-1\right)+1\right)\right.$$
$$\left.-\beta_s^4\left(\kappa^2-2\right)+3\beta_s^2-\kappa^2+3+\frac{2\beta_s^3}{\alpha_s}\right].$$

Thus, the leading order approximation reveals the classical Rayleigh equation (1.30). The exact secular relation (5.16) and its asymptotic expansion (5.18), depicted by the solid and dashed blue lines, respectively, are shown in Fig. 5.2.

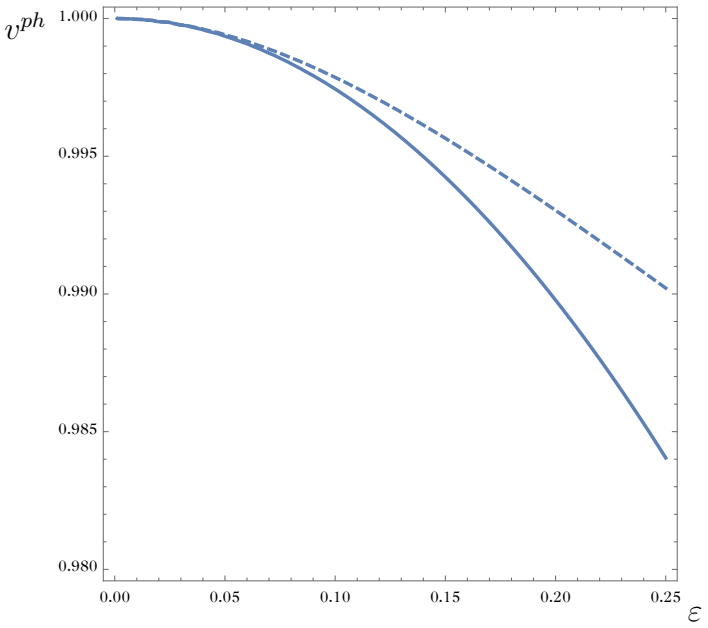

Figure 5.2: Dependence of dimensionless $v^{ph} = c/c_R$ on the small parameter ε with $E = 1$, $\rho = 1$ and $\nu = 0.25$.

5.3 Explicit model for surface waves on an elastic half-space with gravity

In this section, the hyperbolic-elliptic asymptotic models for surface waves on the elastic half-space with the influence of gravity is derived.

5.3.1 The problem formulation

Consider an elastic, isotropic, compressible half-space occupying the domain $0 < x_1, x_2 < \infty$ and $x_3 \geq 0$, subject to a prescribed surface loading, along with influence of gravity, see Fig. 5.3.

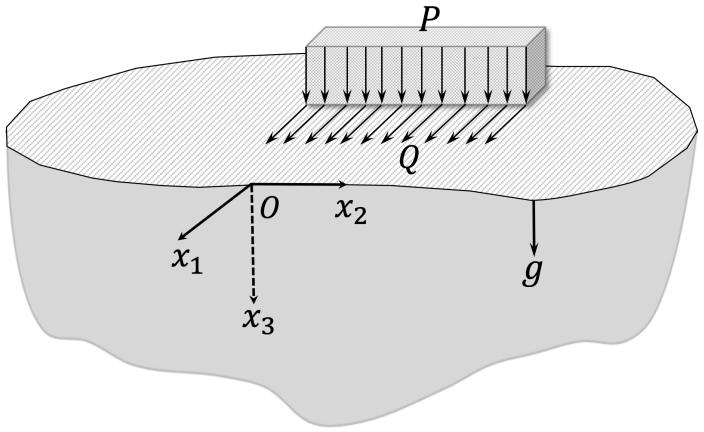

Figure 5.3: An elastic half-space under the gravity effect.

For the plane strain problem, the imposed boundary conditions at the surface $x_3 = 0$ are given as in (1.50).

5.3.2 Asymptotic formulation for surface waves

In this subsection, an asymptotic model for surface waves on an elastic half-space associated with the effect of gravity will be derived.

As before, we are operating with wave numbers satisfying

$$\varepsilon = \frac{g\,L}{c_2^2} \ll 1, \quad \left(\hat{k} = \frac{2\pi}{L}\right), \tag{5.19}$$

where L is a typical wave length.

Then, equations (5.4) and boundary conditions (1.50) are rearranged in terms of the scaling (1.91) as

$$\begin{aligned} &\phi_{,\gamma\gamma} + \alpha_R^2\,\phi_{,\xi\xi} + 2\varepsilon\left(1-\alpha_R^2\right)\phi_{,\xi\tau} - \varepsilon^2\left(1-\alpha_R^2\right)\phi_{,\tau\tau} = -\varepsilon\,\kappa^{-2}\,\psi_{,\xi}, \\ &\psi_{,\gamma\gamma} + \beta_R^2\,\psi_{,\xi\xi} + 2\varepsilon\left(1-\beta_R^2\right)\psi_{,\xi\tau} - \varepsilon^2\left(1-\beta_R^2\right)\psi_{,\tau\tau} = \varepsilon\,\phi_{,\xi}, \end{aligned} \tag{5.20}$$

subject to

$$\begin{aligned} 2\phi_{,\xi\gamma} + \psi_{,\xi\xi} - \psi_{,\gamma\gamma} &= -\frac{L^2\,Q}{\mu}, \\ \left(\kappa^2-2\right)\phi_{,\xi\xi} + \kappa^2\phi_{,\gamma\gamma} + 2\psi_{,\xi\gamma} &= -\frac{L^2\,P}{\mu} \qquad \text{at} \qquad \gamma = 0, \end{aligned} \tag{5.21}$$

where α_R and β_R defined in (1.42).

Expanding the Lamé elastic potentials ϕ and ψ as asymptotic series (1.94).

At leading order, the boundary equations (5.21) yield the solvability condition (1.30), revealing the free Rayleigh wave, along with the relation between the elastic potentials $\phi^{(0)}$ and $\psi^{(0)}$ on the surface $x_3 = 0$, given as (1.98). For analysis at next order, we introduce the two arbitrary plane harmonic functions $\phi^{(1)}$ and $\psi^{(1)}$ defined as in (1.100), deducing that

$$\begin{aligned} \bar{\phi}^{(1,1)} &= \frac{(1-\alpha_R^2)}{\alpha_R}\,\phi^{(0)}_{,\tau} + \frac{\kappa^{-2}}{(1+\beta_R^2)}\,\bar{\phi}^{(0)}, \\ \psi^{(1,1)} &= \frac{1}{2\beta_R}\left(\frac{(1-\beta_R^4)}{\beta_R}\,\phi^{(0)}_{,\tau} + \bar{\phi}^{(0)}\right), \end{aligned} \tag{5.22}$$

follows by applying the Cauchy-Riemann identities (1.39) into equations (5.20), together with the relation (1.44) and (1.98).

At next order, the boundary conditions (5.21) at $x_3 = 0$ become

$$2\phi^{(1,0)}_{,\xi\gamma} + \psi^{(1,0)}_{,\xi\xi} - \psi^{(1,0)}_{,\gamma\gamma} + 2\phi^{(1,1)}_{,\xi} - 2\psi^{(1,1)}_{,\gamma} = -\frac{L^2\,Q}{\mu},$$

$$\left(\kappa^2 - 2\right)\phi^{(1,0)}_{,\xi\xi} + \kappa^2\,\phi^{(1,0)}_{,\gamma\gamma} + 2\psi^{(1,0)}_{,\xi\gamma} + 2\kappa^2\phi^{(1,1)}_{,\gamma} + 2\psi^{(1,1)}_{,\xi} = -\frac{L^2\,P}{\mu}. \tag{5.23}$$

Employing (1.39) and (5.22), we infer at $x_3 = 0$

$$\begin{aligned} &2\alpha_R\,\phi^{(1,0)}_{,\xi\xi} + \left(1+\beta_R^2\right)\bar{\psi}^{(1,0)}_{,\xi\xi} + 2\left(\frac{1-\alpha_R^2}{\alpha_R} - \frac{2\left(1-\beta_R^2\right)\alpha_R}{1+\beta_R^2}\right)\phi^{(0)}_{,\xi\tau} \\ &\qquad +2\left(\frac{\kappa^{-2}}{1+\beta_R^2} - \frac{1}{2}\right)\bar{\phi}^{(0)}_{,\xi} = -\frac{L^2\,\mathcal{H}\left(Q\right)}{\mu}, \\ &-\left(1+\beta_R^2\right)\phi^{(1,0)}_{,\xi\xi} - 2\beta_R\,\bar{\psi}^{(1,0)}_{,\xi\xi} + 2\left(\frac{2\alpha_R}{\left(1+\beta_R^2\right)\beta_R} - 1\right)\phi^{(0)}_{,\xi\tau} \\ &\qquad +2\left(\frac{1}{2\beta_R} - \frac{\alpha_R}{\left(1+\beta_R^2\right)}\right)\bar{\phi}^{(0)}_{,\xi} = -\frac{L^2\,P}{\mu}. \end{aligned} \tag{5.24}$$

The solvability of the last system gives at $x_3 = 0$

$$\begin{aligned} &\left[4\alpha_R\,\beta_R - \left(1+\beta_R^2\right)^2\right]\phi^{(1,0)}_{,\xi\xi} + 4\left[\left(1-\alpha_R^2\right)\frac{\beta_R}{\alpha_R} + \left(1-\beta_R^2\right)\frac{\alpha_R}{\beta_R} - \left(1-\beta_R^4\right)\right]\phi^{(0)}_{,\xi\tau} \\ &\qquad +2\left[\vartheta + \kappa^{-2}\vartheta^{-1} - \left(\alpha_R + \beta_R\right)\right]\bar{\phi}^{(0)}_{,\xi} = -\frac{2L^2\beta_R}{\mu}\left[\vartheta\,P + \mathcal{H}\left(Q\right)\right]. \end{aligned} \tag{5.25}$$

The first term in (5.25) vanishes in the view of (1.30), therefore we get at $x_3 = 0$

$$2\phi^{(0)}_{,\xi\tau} + B_{_g}\,\bar{\phi}^{(0)}_{,\xi} = -\frac{L^2\beta_{_R}}{\mu B_{_I}}\,[\vartheta\,P + \mathcal{H}\,(Q)], \tag{5.26}$$

where $B_{_I}$ specified in (1.54) with

$$B_{_g} = \frac{1}{B_{_I}}\left(\vartheta + \kappa^{-2}\,\vartheta^{-1} - (\alpha_{_R} + \beta_{_R})\right). \tag{5.27}$$

On using the leading order approximation (1.106) and operator identities (1.107), the equation (5.26) may be then rewritten in terms of the original dimensional variables (x_1, x_3, t) at $x_3 = 0$ as

$$\Box_{_R}\,\phi + \frac{g}{c_2^2}\,B_{_g}\,\bar{\phi}_{,1} = -\frac{\beta_{_R}}{\mu B_{_I}}\,[\vartheta\,P + \mathcal{H}\,(Q)]\,. \tag{5.28}$$

Therefore, we obtain the elliptic equations (1.109), governing the decay over the interior ($x_3 \geq 0$), subject to boundary conditions at interface (5.28) and (1.43). Equation (5.28) can be recast in terms of the associated pseudo-differential operator at $x_3 = 0$ as

$$\Box_{_R}\,\phi + \frac{g}{c_2^2}\,B_{_g}\,\sqrt{-\partial_{11}}\,\phi = -\frac{\beta_{_R}}{\mu B_{_I}}\,[\vartheta\,P + \mathcal{H}\,(Q)]\,, \tag{5.29}$$

or rewritten through the Hilbert transform

$$\Box_{_R}\,\phi + \frac{g}{c_2^2}\,B_{_g}\,\mathcal{H}\,\phi_{,1} = -\frac{\beta_{_R}}{\mu B_{_I}}\,[\vartheta\,P + \mathcal{H}\,(Q)]\,. \tag{5.30}$$

Note that this model can be extended to the 3D problem with a vertical load. Indeed,

the Radon transform is applicable. As a result, the obtained model contains the elliptic equations (3.42), governing the decay over the interior ($x_3 \geq 0$), subject to boundary condition $x_3 = 0$

$$\Delta\,\phi - \frac{1}{c_R^2}\phi_{,tt} + \frac{g}{c_2^2}\,B_{_g}\,\sqrt{-\Delta}\,\phi = -\frac{(1+\beta_R^2)}{2\mu B_{_I}}\,P, \tag{5.31}$$

where $\sqrt{-\Delta}$ is a pseudo-differential operator.

Therefore, potentials ϕ and $\Psi = (-\psi_2, \psi_1, 0)$ are related by (3.44) and (3.45).

5.3.3 An approximate secular equation of surface waves

From (5.29) or (5.30), we can obtain the approximation of secular equation for surface waves under the effect of gravity, which is given by

$$v^{ph} = \frac{c}{c_R} = \sqrt{1 - \frac{g\,B_{_g}}{\mid \hat{k} \mid\; c_2^2} + ... \;}\,. \tag{5.32}$$

The relation between $B_{_g}$ and ν is shown in Fig. 5.4.

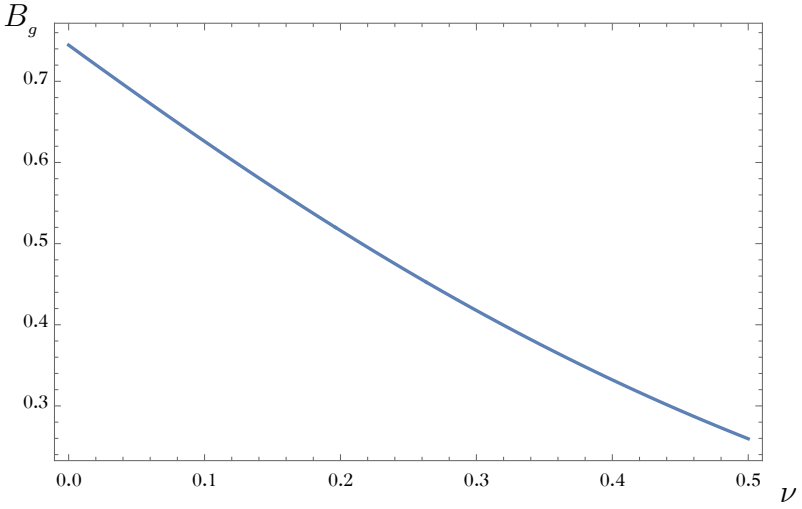

Figure 5.4: The values of $B_{_g}$ against Poisson's ratio ν.

Numerical comparison of the exact relation (5.16) and the asymptotic relation (5.32) against the wave number $\hat{k}$ with $E = 50$, $\rho = 1$ and $\nu = 0.25$ is presented in Fig. 5.5.

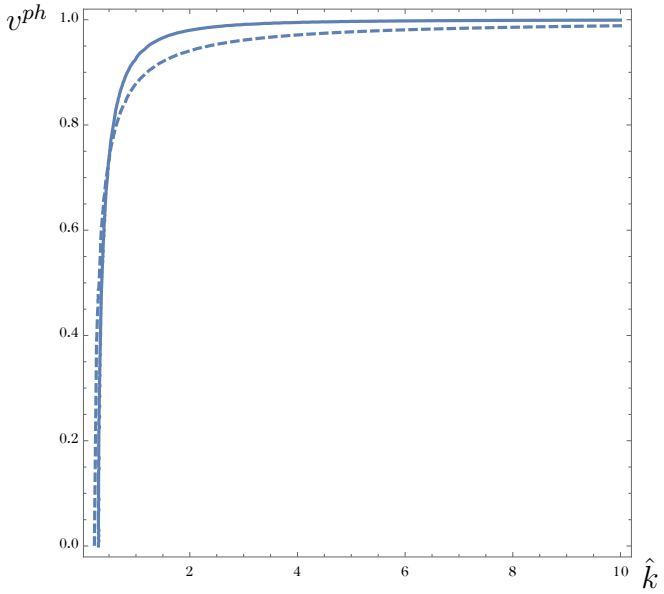

Figure 5.5: A comparison of leading asymptotic relation (dashed line) with exact secular equation (solid line).

5.4 Surface waves on a coated elastic half-space with the effect of gravity

In this section, an asymptotic model for surface waves on an elastic half-space coated by a thin vertically inhomogeneous layer, incorporated with the effect of gravity, is derived.

5.4.1 Problem statement

Consider an isotropic elastic half-space, occupying the domain $-\infty < x_1, x_2 < \infty$ and $x_3 \geq 0$, coated by a thin vertically layer of thickness h described by $-\infty < x_1, x_2 < \infty$ and $-h \leq x_3 \leq 0$, subject to prescribed surface loading along with the influence of gravity, see Fig. 5.6.

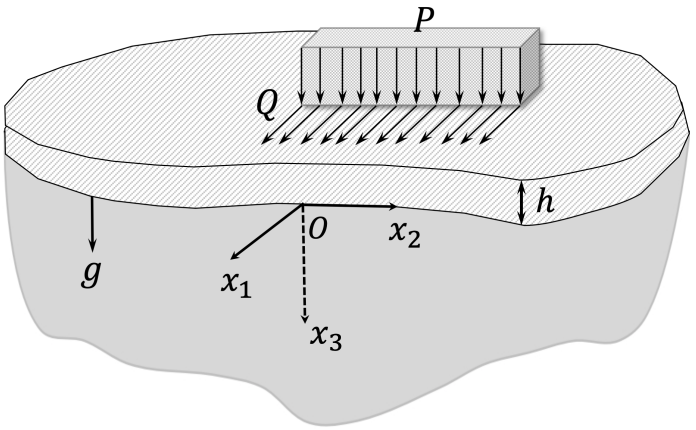

Figure 5.6: A coated elastic half-space under the gravity effect.

The imposed boundary conditions at the surface $x_3 = -h$ are formulated as

$$\sigma_{i3}^{(c)} = -Q, \qquad \text{and} \qquad \sigma_{33}^{(c)} = -P, \qquad i = 1, 2, \tag{5.33}$$

where as before, $P = P(x_1, x_2, t)$ and $Q = Q(x_1, x_2, t)$ are prescribed vertical and tangential surface loads, respectively.

The continuity conditions at the interface $x_3 = 0$ are given as in (3.3).

5.4.2 Effective boundary conditions

Let us introduce the small parameter ϵ in (1.70), along with the scaling (3.4) and the dimensionless quantities (3.5). Here, we set the dimensionless of tangential load Q as in (1.72). Then, the equation of motion (5.1) may be immediately rewritten as

$$\begin{aligned} &\sigma^*_{ii,\xi_i} + \sigma^*_{ji,\xi_j} + \sigma^*_{3i,\eta} + \frac{gL}{c_{2c}^2}\, u^*_{3,\xi_i} = \rho_*\, u^*_{i,\tau_0\tau_0}, \\ &\sigma^*_{33,\eta} + \epsilon\left(\sigma^*_{i3,\xi_i} + \sigma^*_{j3,\xi_j}\right) - \frac{gL}{c_{2c}^2}\left(u^*_{i,\xi_i} + u^*_{j,\xi_j}\right) = \rho_*\, u^*_{3,\tau_0\tau_0}, \end{aligned} \tag{5.34}$$

where $c_{2c}^2 = \rho_c \,/\, \mu_0$.

The constitutive relations (1.7) are also rewritten as in (3.7) and (3.8), as well as, the boundary conditions (5.33) and (3.3) take the form

$$\begin{aligned} &\sigma_{i3}^{*}=-q^{*}, \qquad \sigma_{33}^{*}=-p^{*} \qquad \text{at} \qquad \eta=-1, \\ &\text{and} \qquad u_{k}^{*}=v_{k}^{*} \qquad \text{at} \qquad \eta=0, \end{aligned} \tag{5.35}$$

where $i=1,2$ and $k=1,2,3$.

Next, we expand the displacement and stress as asymptotic series linked by the small parameter ϵ as in (3.10). At leading order, we have

$$\begin{aligned} &\sigma_{ii,\xi_i}^{(0)}+\sigma_{ij,\xi_j}^{(0)}+\sigma_{i3,\eta}^{(0)}+\frac{gL}{c_{2c}^{2}}\,u_{3,\xi_i}^{(0)}=\rho_{*}\,u_{i,\tau_0\tau_0}^{(0)}, \\ &\sigma_{33,\eta}^{(0)}-\frac{gL}{c_{2c}^{2}}\left(u_{i,\xi_i}^{(0)}+u_{j,\xi_j}^{(0)}\right)=\rho_{*}\,u_{3,\tau_0\tau_0}^{(0)}, \\ &\sigma_{ij}^{(0)}=\kappa_{2}^{2}\left(u_{i,\xi_j}^{(0)}+u_{j,\xi_i}^{(0)}\right), \\ &\sigma_{ii}^{(0)}=4\kappa_{2}^{2}\left(1-\kappa_{c}^{-2}\right)\,u_{i,\xi_i}^{(0)}+2\kappa_{2}^{2}\left(1-2\kappa_{c}^{-2}\right)u_{j,\xi_j}^{(0)}, \\ &u_{k,\eta}^{(0)}=0, \end{aligned} \tag{5.36}$$

subject to boundary conditions

$$\begin{aligned} &\sigma_{i3}^{*}=-q^{*}, \qquad \sigma_{33}^{*}=-p^{*} \qquad \text{at} \qquad \eta=-1, \\ &\text{and} \qquad u_{k}^{*}=v_{k}^{*} \qquad \text{at} \qquad \eta=0. \end{aligned} \tag{5.37}$$

Thus, the solutions of $\sigma_{k3}^{(0)}$ $(k=1,2,3)$ are found as

$$\sigma_{33}^{(0)}=v_{3,\tau_0\tau_0}^{*}\int_{-1}^{\eta}\rho_{*}\left(z\right)dz+gL\int_{-1}^{\eta}c_{2c}^{-2}\left(z\right)dz\,\left(v_{i,\xi_i}^{*}+v_{j,\xi_j}^{*}\right)-p^{*}, \tag{5.38}$$

and

$$\sigma_{i3}^{(0)} = \left(\int_{-1}^{\eta} \rho_* (z)\, dz \right) v^*_{i,\tau_0\tau_0} - 4 \left(\int_{-1}^{\eta} \kappa_2^2 (z) \left(1 - \kappa_c^{-2}(z)\right) dz \right) v^*_{i,\xi_i\xi_i}$$

$$- \left(\int_{-1}^{\eta} \kappa_2^2 (z)\, dz \right) v^*_{i,\xi_j\xi_j} - \left(\int_{-1}^{\eta} \kappa_2^2 (z) \left(3 - 4\kappa_c^{-2}(z)\right) dz \right) v^*_{j,\xi_i\xi_j}$$

$$-gL \left(\int_{-1}^{\eta} c_{2c}^{-2} (z)\, dz \right) v^*_{3,\xi_i} - q^*, \tag{5.39}$$

where $i \neq j = 1, 2$.

In terms of original dimension form, the expressions for the stresses at the interface $x_3 = 0$ may be obtained as

$$\begin{aligned} \sigma_{i3} &= h \left(\tilde{\rho}\, u_{i,tt} - \tilde{\delta}\, u_{i,ii} - \tilde{\mu}\, u_{i,jj} - \left(\tilde{\delta} - \tilde{\mu} \right) u_{j,ij} - \tilde{\rho}\, g\, u_{3,i} \right) - Q_i, \\ \sigma_{33} &= h\, \tilde{\rho} \left(u_{3,tt} + g \left(u_{i,i} + u_{j,j} \right) \right) - P, \quad (i \neq j = 1, 2), \end{aligned} \tag{5.40}$$

where, as before, Q_1 and Q_2 denote the components of prescribed in-plane surface force in the x_1 and x_2 directions, respectively, δ defined in (3.16), and all quantities with tilde are expressed by the mean value of functions in (3.17).

For plane-strain problem, the latter effective boundary conditions can be diminished as

$$\begin{aligned} \sigma_{13} &= h \left(\tilde{\rho}\, u_{1,tt} - \tilde{\delta}\, u_{1,11} - \tilde{\rho}\, g\, u_{3,1} \right) - Q, \\ \sigma_{33} &= h\, \tilde{\rho} \left(u_{3,tt} + g\, u_{1,1} \right) - P. \end{aligned} \tag{5.41}$$

5.4.3 Asymptotic model for surface waves

With the effective boundary conditions (5.41) derived, an asymptotic model for surface wave may now be constructed, generalising the previous results in Chapter 3 to incorporate the effect of gravity. Consequently, the associated boundary condition for a homogeneous isotropic substrate are rewritten at $x_3 = 0$ as

$$\begin{aligned} \mu\,(u_{1,3} + u_{3,1}) &= h\left(\tilde{\rho}\,u_{1,tt} - \tilde{\delta}\,u_{1,11} - \tilde{\rho} g\,u_{3,1}\right) - Q, \\ \lambda(u_{1,1} + u_{3,3}) + (\lambda + 2\mu)\,u_{3,3} &= h\,\tilde{\rho}\,(u_{3,tt} + g\,u_{1,1}) - P. \end{aligned} \tag{5.42}$$

Employing the Helmholtz decomposition (1.22) into (5.3) and (5.42), we obtain wave equations (5.4) subject to boundary conditions at $x_3 = 0$

$$\begin{aligned} \mu\,(2\phi_{,13} + \psi_{,11} - \psi_{,33}) = h\,\Big[\tilde{\rho}\,(\phi_{,1tt} - \psi_{,3tt}) - \tilde{\delta}\,(\phi_{,111} - \psi_{,113}) \\ -\tilde{\rho} g\,(\phi_{,13} + \psi_{,11})\Big] - Q, \end{aligned}$$

$$\mu\left(\left(\kappa^2 - 2\right)\phi_{,11} + \kappa^2\,\phi_{,33} + 2\psi_{,13}\right) = h\,\tilde{\rho}\,[\phi_{,3tt} + \psi_{,1tt} + g\,(\phi_{,11} - \psi_{,13})] - P. \tag{5.43}$$

Let us introduce the slow-time perturbation scheme (1.91) along with notation

$$G = \frac{\varepsilon}{\epsilon}, \qquad \text{and} \qquad \varepsilon = \frac{gL}{c_2^2}. \tag{5.44}$$

Here we have two small parameters ε and ϵ associated with the effect of gravity and thickness of coating. In the following derivation we are assuming them to be of the same order, so $G = O(1)$.

Then, the equations (5.4) are rearranged in terms of the new scaling

$$\phi_{,\gamma\gamma} + \alpha_R^2\,\phi_{,\xi\xi} + 2\epsilon\left(1-\alpha_R^2\right)\phi_{,\xi\tau} - \epsilon^2\left(1-\alpha_R^2\right)\phi_{,\tau\tau} = -\epsilon\,\kappa^{-2}\,G\,\psi_{,\xi},$$

$$\psi_{,\gamma\gamma} + \beta_R^2\,\psi_{,\xi\xi} + 2\epsilon\left(1-\beta_R^2\right)\psi_{,\xi\tau} - \epsilon^2\left(1-\beta_R^2\right)\psi_{,\tau\tau} = \epsilon\,G\,\phi_{,\xi}, \tag{5.45}$$

subject to the following boundary conditions, restated as

$$2\phi_{,\xi\gamma} + \psi_{,\xi\xi} - \psi_{,\gamma\gamma} = \epsilon\left(\frac{c_R^2}{\tilde{c}_2^2} - \frac{\tilde{\delta}}{\mu}\right)\left(\phi_{,\xi\xi\xi} - \psi_{,\xi\xi\gamma}\right) - \epsilon^2\,\frac{c_2^2}{\tilde{c}_2^2}\,G\left(\phi_{,\xi\gamma} + \psi_{,\xi\xi}\right)$$

$$+\frac{c_R^2}{\tilde{c}_2^2}\left[2\,\epsilon^2\left(\psi_{,\xi\gamma\tau} - \phi_{,\xi\xi\tau}\right) + \epsilon^3\left(\phi_{,\xi\tau\tau} - \psi_{,\gamma\tau\tau}\right)\right] - \frac{L^2\,Q}{\mu},$$

$$\left(\kappa^2-2\right)\phi_{,\xi\xi} + \kappa^2\,\phi_{,\gamma\gamma} + 2\psi_{,\xi\gamma} = \epsilon\,\frac{c_R^2}{\tilde{c}_2^2}\left(\phi_{,\xi\xi\gamma} + \psi_{,\xi\xi\xi}\right) + \epsilon^2\frac{c_2^2}{\tilde{c}_2^2}\,G\left(\phi_{,\xi\xi} - \psi_{,\xi\gamma}\right) \tag{5.46}$$

$$+\frac{c_R^2}{\tilde{c}_2^2}\left[\epsilon^3\left(\phi_{,\gamma\tau\tau} + \psi_{,\xi\tau\tau}\right) - 2\epsilon^2\left(\phi_{,\xi\gamma\tau} + \psi_{,\xi\xi\tau}\right)\right] - \frac{L^2\,P}{\mu} \qquad \text{at} \qquad \gamma = 0,$$

where $\tilde{c}_2^2 = \mu\,/\,\tilde{\rho}$.

Now, we apply the asymptotic expansion as in (1.94). At next order, we deduce from (1.39), (1.100) and (5.45) that

$$\bar{\phi}^{(1,1)} = \frac{\left(1-\alpha_R^2\right)}{\alpha_R}\,\phi_{,\tau}^{(0)} + \frac{G\,\kappa^{-2}}{\left(1+\beta_R^2\right)}\,\bar{\phi}^{(0)},$$

$$\psi^{(1,1)} = \frac{1}{2\beta_R}\left(\frac{\left(1-\beta_R^4\right)}{\beta_R}\,\phi_{,\tau}^{(0)} + G\,\bar{\phi}^{(0)}\right). \tag{5.47}$$

At next order, the boundary conditions (5.46) with (5.47) become at $\gamma = 0$

$$2\alpha_R\,\phi^{(1,0)}_{,\xi\xi} + (1+\beta_R^2)\bar{\psi}^{(1,0)}_{,\xi\xi} + 2\left(\frac{1-\alpha_R^2}{\alpha_R} - \frac{2\,(1-\beta_R^2)\,\alpha_R}{1+\beta_R^2}\right)\phi^{(0)}_{,\xi\tau}$$

$$+2\,G\left(\frac{\kappa^{-2}}{1+\beta_R^2} - \frac{1}{2}\right)\bar{\phi}^{(0)}_{,\xi} - \left(\frac{c_R^2}{\tilde{c}_2^2} - \frac{\tilde{\delta}}{\mu}\right)\left(\frac{1-\beta_R^2}{2}\right)\bar{\phi}^{(0)}_{,\xi\xi\xi} = -\frac{L^2\,\mathcal{H}\,(Q)}{\mu},$$

(5.48)

$$-\left(1+\beta_R^2\right)\phi^{(1,0)}_{,\xi\xi} - 2\beta_R\,\bar{\psi}^{(1,0)}_{,\xi\xi} + 2\left(1-\beta_R^2\right)\left(\frac{2\alpha_R}{(1+\beta_R^2)\,\beta_R} - 1\right)\phi^{(0)}_{,\xi\tau}$$

$$+2G\left(\frac{1}{2\beta_R} - \frac{\alpha_R}{(1+\beta_R^2)}\right)\bar{\phi}^{(0)}_{,\xi} - \frac{c_R^2}{\tilde{c}_2^2}\,\alpha_R\left(\frac{1-\beta_R^2}{1+\beta_R^2}\right)\bar{\phi}^{(0)}_{,\xi\xi\xi} = -\frac{L^2\,P}{\mu}.$$

The solvability of the last system at $\gamma = 0$ leads to

$$\left[4\alpha_R\,\beta_R - \left(1+\beta_R^2\right)^2\right]\phi^{(1,0)}_{,\xi\xi} + 4\left[\left(1-\alpha_R^2\right)\frac{\beta_R}{\alpha_R} + \left(1-\beta_R^2\right)\frac{\alpha_R}{\beta_R} - \left(1-\beta_R^4\right)\right]\phi^{(0)}_{,\xi\tau}$$

$$+2\,G\left[\vartheta + \kappa^{-2}\,\vartheta^{-1} - (\alpha_R+\beta_R)\right]\bar{\phi}^{(0)}_{,\xi} - \frac{(1-\beta_R^2)}{\mu}\left[c_R^2\,\tilde{\rho}\,(\alpha_R+\beta_R) - \tilde{\delta}\beta_R\right]\bar{\phi}^{(0)}_{,\xi\xi\xi}$$

$$= -\frac{2L^2\beta_R}{\mu}\left[\vartheta\,P + \mathcal{H}\,(Q)\right].$$

(5.49)

The first term in (5.49) vanishes in the view of (1.30), thus we have at $\gamma = 0$

$$2\phi^{(0)}_{,\xi\tau} + G\,B_{_g}\,\bar{\phi}^{(0)}_{,\xi} - b_c\,\bar{\phi}^{(0)}_{,\xi\xi\xi} = -\frac{\beta_R}{\mu B_{_I}}\left[\vartheta\,P + \mathcal{H}\,(Q)\right], \tag{5.50}$$

where $B_{_I}$, B_g and b_c defined in (1.54), (5.27) and (3.37), respectively.

According to (1.106), (1.107) and (5.44), the equations (5.50) are rewritten in terms of the original dimensional variables (x_1, x_3, t) at $x_3 = 0$

$$\Box_R \phi + \frac{g}{c_2^2} B_g \, \bar{\phi}_{,1} - hb_c \, \bar{\phi}_{,111} = -\frac{\beta_R}{\mu B_I} \left[\vartheta \, P + \mathcal{H}\left(Q\right)\right]. \tag{5.51}$$

Therefore, we arrive at the leading order the elliptic equations (1.109), governing the decay over the interior $(x_3 \geq 0)$, subject to boundary conditions at $x_3 = 0$

$$\Box_R \phi - \frac{g \, B_g}{c_2^2 \, \alpha_R} \phi_{,3} + \frac{hb_c}{\alpha_R} \phi_{,113} = -\frac{\beta_R}{\mu B_I} \left[\vartheta \, P + \mathcal{H}\left(Q\right)\right], \tag{5.52}$$

along with (1.43). The equation (5.52) can be recast in terms of the associated pseudo-differential operator at $x_3 = 0$ as

$$\Box_R \phi + \frac{g}{c_2^2} B_g \sqrt{-\partial_{11}} \, \phi - hb_c \sqrt{-\partial_{11}} \, \phi_{,11} = -\frac{\beta_R}{\mu B_I} \left[\vartheta \, P + \mathcal{H}\left(Q\right)\right], \tag{5.53}$$

or rewritten through the Hilbert transform

$$\Box_R \phi + \frac{g}{c_2^2} B_g \, \mathcal{H} \, \phi_{,1} - hb_c \, \mathcal{H} \phi_{,111} = -\frac{\beta_R}{\mu B_I} \left[\vartheta \, P + \mathcal{H}\left(Q\right)\right]. \tag{5.54}$$

Note that the latter model can be extended to the case of a vertically load acting on a thin vertically inhomogeneous layer coated elastic half-space, resulting in the elliptic equations (3.42), governing the decay over the interior $(x_3 \geq 0)$, subject to boundary conditions at $x_3 = 0$

$$\Delta \, \phi - \frac{1}{c_R^2} \phi_{,tt} + \frac{g}{c_2^2} B_g \sqrt{-\Delta} \, \phi - hb_c \sqrt{-\Delta} \;\; \Delta \, \phi = -\frac{1 + \beta_R^2}{2 \mu B_I} P, \tag{5.55}$$

along with (3.44) and (3.45).

The range of validity of the developed theory is given by $\frac{g}{c_2^2\,\hat{k}} \ll 1$ and also $\hat{k}h \ll 1$, from which $\frac{gh}{c_2^2} \ll 1$.

5.4.4 Approximate dispersion relation

The derived equation enables an approximation of the exact dispersion relation. Naturally, we deduce from (5.53) that

$$v^{ph} = \frac{c}{c_R} = \sqrt{1 - \left(\frac{g\, B_g}{|\,\hat{k}\,|\; c_2^2} + b_c \,|\, \hat{k} \,|\, h + ... \right)}. \tag{5.56}$$

It may be observed that in the absence of the coating ($h = 0$), the relation (5.56) reduces to (5.32).

For a homogeneous coating layer, the relation between ν^{ph} and $\hat{k}h$ with $h = 1$, $E_0/E = 1$, $\rho_0 \,/\, \rho = 1$ and $\nu_0 = \nu = 0.25$ is shown as

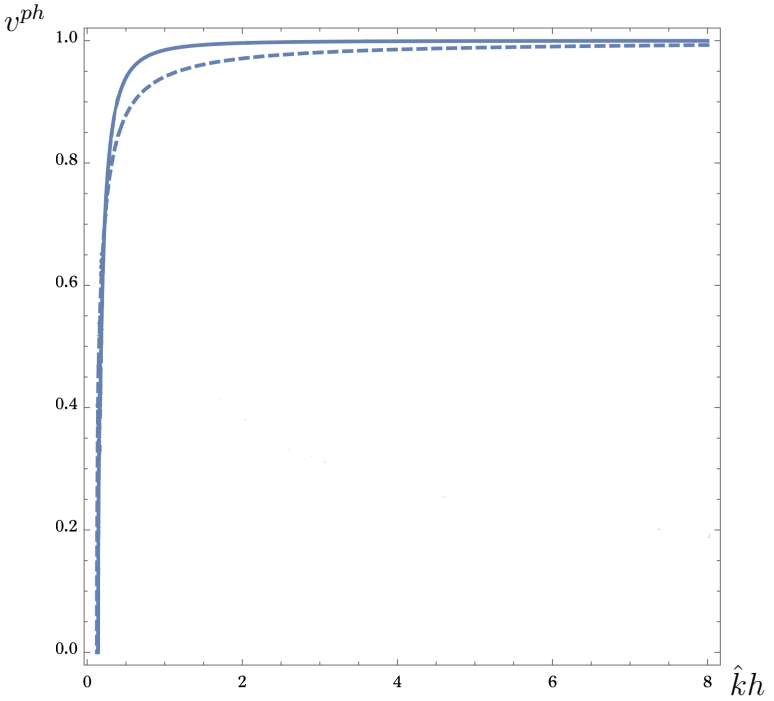

Figure 5.7: A comparison of the exact dispersion equation (5.15) (solid line) against the asymptotic relation (5.56) (dashed line).

In conclusion, the exact dispersion equation for a coated half-space under the gravity effect has been obtained. The explicit model for surface waves on a vertically inhomogeneous elastic layer coated and an uncoated elastic half-space have also been derived in gravity cases. The asymptotic formulation contains the wave equation, which is singularly perturbed by a pseudo-differential operator associating with the gravitational field. Several illustrative numerical examples of the approximate and exact dispersion relations of the surface waves have been presented.

Conclusion

In this thesis, explicit formulations for elastic surface waves induced by surface stresses have been derived.

First, the asymptotic model for surface wave on a coated elastic half-space has been developed. The previous results for isotropic half-space coated with a thin isotropic layer, subject to vertical surface stress considered in Dai et al. [2010], have been extended substantially, to account for anisotropy of layer and half-space, and also for vertical inhomogeneity of the coating. For all those scenarios, the asymptotic integration of the equations of elasticity through thickness of the layer was preformed, leading to the effective boundary conditions, replacing the effect of the coating. The resulting model contains an elliptic equation describing decay away from the surface, and a singularly perturbed hyperbolic equation on the interface between the layer and the half-space.

Secondly, the effect of gravitational force has been embedded within the developed methodology. The weak coupling between the wave potentials in the short-wave limit was noted, allowing a perturbation scheme leading a variation of a hyberbolic-elliptic model for surface wave under the effect of gravity.

In case of the coated half-space, investigation started from surface wave field induced by prescribed stresses on the surface of the coated orthotropic half-space was carried out. The formulation was obtained in terms of an auxiliary plane harmonic function, first appearing in the representation of the eigensolution in Prikazchikov [2013]. The displacements were expressed in terms of this auxiliary function and its harmonic conjugate. The resulting asymptotic model contains an elliptic equation for this function governing decay over the interior, as well as a pseudo-differential equation on the interface. Particular cases, when either coating or substrate are isotropic, were also examined.

Another development achieved in this thesis is related to a scenario of a vertically inhomogeneous coating on an isotropic substrate, including a particular case of multi-layered coating. In addition, an interesting special case of zero group velocity, when the wave seems to "not notice" the coating, has been pointed out.

The derived formulations for coated half-space were implemented for a number of dynamic loadings including the impact loading, as well as the moving loads. For the latter, explicit approximate solutions have been obtained. For example, for the case of a moving point load, the range of problem parameters associated with radiation of energy from the moving source was confirmed.

Another important outcome of this thesis is related to the derivation of explicit asymptotic model for the Rayleigh wave with account of the influence of gravity. First, a homogeneous half-space was treated. The exact dispersion relation was derived, along with its approximation, followed by the case of a substrate coated

by a thin inhomogeneous layer. Several illustrative numerical examples were also presented.

Finally, possible further developments within this approach involve consideration of more advanced materials of the thin layer, including nonlinear, nematic, as well as porous, viscous and soft materials, including aerogels, see e.g. Zakharov [2012], Gusakov and Vatul'yan [2018], Patil et al. [2017], Rege et al. [2019].

Appendix A

The related non-zero components of the matrix $\boldsymbol{A}$ are given by

$$
\begin{aligned}
&A_{11} = i\alpha_c\, e^{-\hat{k}h\alpha_c}, && A_{12} = -i\alpha_c\, e^{\hat{k}h\alpha_c}, && A_{13} = -\gamma_c^2\, e^{-\hat{k}h\beta_c},\\
&A_{14} = -\gamma_c^2\, e^{\hat{k}h\beta_c}, && A_{21} = \gamma_c^2\, e^{-\hat{k}h\alpha_c}, && A_{22} = \gamma_c^2 e^{\hat{k}h\alpha_c},\\
&A_{23} = i\beta_c\, e^{-\hat{k}h\beta_c}, && A_{24} = -i\beta_c\, e^{\hat{k}h\beta_c}, && A_{34} = -A_{33} = \beta_c,\\
&A_{41} = -A_{42} = \alpha_c, && A_{56} = -A_{65} = \hat{\mu}\,\gamma_s^2, && A_{36} = -\beta_s,\\
&A_{45} = \alpha_s, && A_{55} = i\hat{\mu}\,\alpha_s, && A_{66} = -i\hat{\mu}\,\beta_s,
\end{aligned}
\tag{A.1}
$$

and

$$
A_{31} = A_{32} = -A_{46} = -A_{35} = A_{43} = A_{44} = i, \qquad A_{15} = A_{16} = A_{25} = A_{26} = 0,
$$

$$
A_{51} = -A_{52} = i\alpha_c, \qquad -A_{53} = -A_{54} = A_{61} = A_{62} = \gamma_c^2, \qquad A_{64} = -A_{63} = i\beta_c,
$$

Appendix B

The 6×6 matrix $\mathbf{T}$ is given as

$$\mathbf{T} = \begin{pmatrix} A_{1c}\, e^{-kh\hat{\lambda}_{1c}} & B_{1c}\, e^{kh\hat{\lambda}_{1c}} & A_{2c}\, e^{-kh\hat{\lambda}_{2c}} & B_{2c}\, e^{kh\hat{\lambda}_{2c}} & 0 & 0 \\ C_{1c}\, e^{-kh\hat{\lambda}_{1c}} & D_{1c}\, e^{kh\hat{\lambda}_{1c}} & C_{2c}\, e^{-kh\hat{\lambda}_{2c}} & D_{2c}\, e^{kh\hat{\lambda}_{2c}} & 0 & 0 \\ E_{1c} & F_{1c} & E_{2c} & F_{2c} & -F_{1s} & -F_{2s} \\ H_{1c} & L_{1c} & H_{2c} & L_{2c} & -L_{1s} & -L_{2s} \\ A_{1c} & B_{1c} & A_{2c} & B_{2c} & -\hat{\mu}\ B_{1s} & -\hat{\mu}\, B_{2s} \\ C_{1c} & D_{1c} & C_{2c} & D_{2c} & -\hat{\mu}\, D_{1s} & -\hat{\mu}\, D_{2s} \end{pmatrix}, \quad \text{(B.1)}$$

where

$$A_{jc} = 2i\,\hat{\lambda}_{jc} - \gamma_{jc}\left(1 + \hat{\lambda}_{jc}^2\right), \qquad B_{jq} = -\left(2i\,\lambda_{jq} + \gamma_{jq}\left(1 + \lambda_{jq}^2\right)\right),$$

$$C_{jc} = i\left(1 - \hat{\lambda}_{jc}^2\right)\kappa_c^2 - 2\left(i - \gamma_{jc}\,\hat{\lambda}_{jc}\right), \qquad D_{jq} = i\left(1 - \hat{\lambda}_{jq}^2\right)\kappa_q^2 - 2\left(i + \gamma_{jq}\,\hat{\lambda}_{jq}\right),$$

$$E_{jc} = i - \gamma_{jc}\,\hat{\lambda}_{jc}, \qquad F_{jq} = i + \gamma_{jq}\,\hat{\lambda}_{jq}, \qquad H_{jc} = \hat{\lambda}_{jc} + i\,\gamma_{jc}, \qquad L_{jq} = -\hat{\lambda}_{jq} + i\,\gamma_{jq},$$

with $\hat{\mu} = \mu_0\,/\mu$, $j = 1, 2$ and $q = c, s$.

Bibliography

M. Abramowitz and I.A. Stegun. Handbook of mathematical functions with formulas, graphs, and mathematical table. In *US Department of Commerce*. National Bureau of Standards Applied Mathematics series 55, 1965.

J.D. Achenbach. Explicit solutions for carrier waves supporting surface waves and plate waves. *Wave Motion*, 28(1):89–97, 1998.

J.D. Achenbach. *Wave propagation in elastic solids*. Elsevier, 2012.

J.D. Achenbach and S.P. Keshava. Free waves in a plate supported by a semi-infinite continuum. *Journal of Applied Mechanics*, 34(2):397–404, 1967.

S.D. Adams, R.V. Craster, and D.P. Williams. Rayleigh waves guided by topography. *Proceedings of the Royal Society A: Mathematical, Physical and Engineering Sciences*, 463(2078):531–550, 2007.

M. Ahmad, E. Nolde, and A.V. Pichugin. Explicit asymptotic modelling of transient Love waves propagated along a thin coating. *Zeitschrift für angewandte Mathematik und Physik*, 62(1):173–181, 2011.

A.G. Alenitsyn. Rayleigh waves in an inhomogeneous elastic half-space of waveguide type. *Journal of Applied Mathematics and Mechanics*, 31(2):244–251, 1967.

S. Althobaiti, V. Bratov, A. Mubaraki, and D. Prikazchikov. Moving load on an elastic half-space coated with a thin vertically inhomogeneous layert. *Proceedings of XI International Conference on Structural Dynamics, EURODYN*, 2:2601–2611, 2020.

A.S. Alzaidi, J. Kaplunov, and L. Prikazchikova. The edge bending wave on a plate reinforced by a beam. *The Journal of the Acoustical Society of America*, 146(2): 1061–1064, 2019a.

A.S. Alzaidi, J. Kaplunov, and L. Prikazchikova. Elastic bending wave on the edge of a semi-infinite plate reinforced by a strip plate. *Mathematics and Mechanics of Solids*, 24(10):3319–3330, 2019b.

I. Argatov and A. Iantchenko. Rayleigh surface waves in functionally graded materials—long-wave limit. *The Quarterly Journal of Mechanics and Applied Mathematics*, 72(2):197–211, 2019.

I. Argatov and G. Mishuris. *Indentation testing of biological materials*. Springer, Cham, 2018.

I.I. Argatov and F.J. Sabina. Small-scale indentation of an elastic coated half-space: the effect of compliant substrate. *International Journal of Engineering Science*, 104:87–96, 2016.

M. Aßmus, K. Naumenko, and H. Altenbach. A multiscale projection approach for the coupled global–local structural analysis of photovoltaic modules. *Composite Structures*, 158:340–358, 2016.

Z. Ba and J. Liang. Fundamental solutions of a multi-layered transversely isotropic saturated half-space subjected to moving point forces and pore pressure. *Engineering Analysis with Boundary Elements*, 76:40–58, 2017.

V. Babich and A. Kiselev. *Elastic Waves: High Frequency Theory*. Chapman and Hall/CRC, 2018.

M.C.M. Bakker, M.D. Verweij, B.J. Kooij, and H.A. Dieterman. The traveling point load revisited. *Wave Motion*, 29(2):119–135, 1999.

O. Balogun and J.D. Achenbach. Surface waves on a half space with depth-dependent properties. *The Journal of the Acoustical Society of America*, 132(3):1336–1345, 2012.

D.M. Barnett and J. Lothe. Consideration of the existence of surface wave (Rayleigh wave) solutions in anisotropic elastic crystals. *Journal of Physics F: Metal Physics*, 4(5):671, 1974.

V.L. Berdichevsky. An asymptotic theory of sandwich plates. *International Journal of Engineering Science*, 48(3):383–404, 2010.

L. Bergmann and H. Henry. Ultrasonics and their scientific and technical applications. 1938.

M.A. Biot. The influence of initial stress on elastic waves. *Journal of Applied Physics*, 11(8):522–530, 1940.

M.A. Biot. *Mechanics of incremental deformations*. Wiley, New York, 1965.

F.M. Borodich. The Hertz-type and adhesive contact problems for depth-sensing indentation. *Advances in Applied Mechanics*, 47:225–366, 2014.

S. Bose. *High temperature coatings*. Butterworth-Heinemann, 2017.

P. Bövik. A comparison between the Tiersten model and O(h) boundary conditions for elastic surface waves guided by thin layers. *Journal of Applied Mechanics*, 63 (1):162–1679, 1996.

M.F. Brigatti and A. Mottana. *Layered mineral structures and their Application in Advanced Technologies*, volume 11. The Mineralogical Society of Great Britain and Ireland, 2011.

T.I. Bromwich. On the influence of gravity on elastic waves, and, in particular on the vibrations of an elastic globe. *Proceedings of the London Mathematical Society*, 1 (1):98–165, 1898.

Z. Cai and Y. Fu. On the imperfection sensitivity of a coated elastic half-space. *Proceedings of the Royal Society of London. Series A: Mathematical, Physical and Engineering Sciences*, 455(1989):3285–3309, 1999.

C. Campbell. *Surface Acoustic Wave Devices for Mobile and Wireless Communications, Four-Volume Set*. Academic press, 1998.

Y. Cao, H. Xia, and Z. Li. A semi-analytical/fem model for predicting ground vibrations induced by high-speed train through continuous girder bridge. *Journal of Mechanical Science and Technology*, 26(8):2485–2496, 2012.

P. Chadwick. The existence of pure surface modes in elastic materials with orthorhombic symmetry. *Journal of Sound and Vibration*, 47(1):39–52, 1976a.

P. Chadwick. Surface and interfacial waves of arbitrary form in isotropic elastic media. *Journal of Elasticity*, 6(1):73–80, 1976b.

P. Chadwick and D.A. Jarvis. Surface waves in a pre-stressed elastic body. *Proceedings of the Royal Society of London. A. Mathematical and Physical Sciences*, 366(1727): 517–536, 1979.

P. Chadwick and G.D. Smith. Foundations of the theory of surface waves in anisotropic elastic materials. In *Advances in Applied Mechanics*, volume 17, pages 303–376. Elsevier, 1977.

G.J. Chaplain, J.M. De Ponti, G. Aguzzi, A. Colombi, and R.V. Craster. Topological rainbow trapping for elastic energy harvesting in graded ssh systems. *Physical Review Applied*, 14:054045, 2020.

D.K. Chattopadhyay and K.V.S.N. Raju. Structural engineering of polyurethane coatings for high performance applications. *Progress in Polymer Science*, 32(3): 352–418, 2007.

R. Chebakov, J. Kaplunov, and G.A. Rogerson. A non-local asymptotic theory for thin elastic plates. *Proceedings of the Royal Society A: Mathematical, Physical and Engineering Sciences*, 473(2203):20170249, 2017.

K.D. Cherednichenko and S. Cooper. On the existence of high-frequency boundary resonances in layered elastic media. *Proceedings of the Royal Society A: Mathematical, Physical and Engineering Sciences*, 471(2178):20140878, 2015.

Y.S. Cho. Non-destructive testing of high strength concrete using spectral analysis of surface waves. *NDT & E International*, 36(4):229–235, 2003.

J. Cole. Stresses produced in a half-plane by moving loads. *Journal of Applied Mechanics*, 25:433–436, 1958.

A. Colombi, V. Ageeva, R.J. Smith, A. Clare, R. Patel, M. Clark, D. Colquitt, P. Roux, S. Guenneau, and R.V. Craster. Enhanced sensing and conversion of ultrasonic Rayleigh waves by elastic metasurfaces. *Scientific Reports*, 7(1):1–9, 2017.

D.J. Colquitt, A. Colombi, R.V. Craster, P. Roux, and S.R.L. Guenneau. Seismic metasurfaces: Sub-wavelength resonators and Rayleigh wave interaction. *Journal of the Mechanics and Physics of Solids*, 99:379–393, 2017.

H.H. Dai, J. Kaplunov, and D.A. Prikazchikov. A long-wave model for the surface elastic wave in a coated half-space. *Proceedings of the Royal Society A: Mathematical, Physical and Engineering Sciences*, 466(2122):3097–3116, 2010.

P.K. Datta. *Surface Engineering: Engineering applications*, volume 2. Royal Society of Chemistry, 1993.

A.T de Hoop. The moving-load problem in soil dynamics – the vertical displacement approximation. *Wave Motion*, 36:335–346, 2002.

J.M. De Ponti, A. Colombi, R. Ardito, F. Braghin, A. Corigliano, and R.V. Craster. Graded elastic metasurface for enhanced energy harvesting. *New Journal of Physics*, 22(1):013013, 2020.

M. Destrade. The explicit secular equation for surface acoustic waves in monoclinic elastic crystals. *The Journal of the Acoustical Society of America*, 109(4):1398–1402, 2001a.

M. Destrade. Surface waves in orthotropic incompressible materials. *The Journal of the Acoustical Society of America*, 110(2):837–840, 2001b.

Z. Dimitrovová. Semi-analytical solution for a problem of a uniformly moving oscillator on an infinite beam on a two-parameter visco-elastic foundation. *Journal of Sound and Vibration*, 438:257–290, 2019.

M.A. Dowaikh and R.W. Ogden. On surface waves and deformations in a pre-stressed incompressible elastic solid. *IMA Journal of Applied Mathematics*, 44(3):261–284, 1990.

N. Ege, B. Erbaş, and D.A. Prikazchikov. On the 3D Rayleigh wave field on an elastic half-space subject to tangential surface loads. *ZAMM-Journal of Applied Mathematics and Mechanics/Zeitschrift für Angewandte Mathematik und Mechanik*, 95 (12):1558–1565, 2015.

N. Ege, B. Erbaş, and J. Kaplunov. Asymptotic derivation of refined dynamic equations for a thin elastic annulus. *Mathematics and Mechanics of Solids*, 26(1): 118–132, 2021.

B. Erbaş, E. Yusufoğlu, and J. Kaplunov. A plane contact problem for an elastic orthotropic strip. *Journal of Engineering Mathematics*, 70(4):399–409, 2011.

B. Erbaş, J. Kaplunov, and D.A. Prikazchikov. The rayleigh wave field in mixed problems for a half-plane. *The IMA Journal of Applied Mathematics*, 78(5):1078–1086, 2013.

B. Erbaş, J. Kaplunov, D.A. Prikazchikov, and O. Şahin. The near-resonant regimes of a moving load in a three-dimensional problem for a coated elastic half-space. *Mathematics and Mechanics of Solids*, 22(1):89–100, 2017.

B. Erbaş, J. Kaplunov, E. Nolde, and M. Palsü. Composite wave models for elastic plates. *Proceedings of the Royal Society A: Mathematical, Physical and Engineering Sciences*, 474(2214):20180103, 2018.

B. Erbaş, J. Kaplunov, and M. Palsü. A composite hyperbolic equation for plate extension. *Mechanics Research Communications*, 99:64–67, 2019.

A. Erdelyi, W. Magnus, F. Oberhettinger, and F.G. Tricomi. *Tables of Integral Transforms*. McGraw-Hill, New York, 1954.

S.J. Feng, X.L. Zhang, L. Wang, Q.T. Zheng, F.L. Du, and Z.L. Wang. In situ experimental study on high speed train induced ground vibrations with the ballastless track. *Soil Dynamics and Earthquake Engineering*, 102:195–214, 2017.

L.B. Freund. Wave motion in an elastic solid due to a nonuniformly moving line load. *Quarterly of Applied Mathematics*, 30(3):271–281, 1972.

L.B. Freund. The response of an elastic solid to nonuniformly moving surface loads. *Journal of Applied Mechanics*, 40(3):699–704, 1973.

F.G. Friedlander. On the total reflection of plane waves. *The Quarterly Journal of Mechanics and Applied Mathematics*, 1(1):376–384, 1948.

D. Froio, E. Rizzi, F.M. Simões, and A.P. Da Costa. Universal analytical solution of the steady-state response of an infinite beam on a pasternak elastic foundation under moving load. *International Journal of Solids and Structures*, 132:245–263, 2018.

Y. Fu, J. Kaplunov, and D. Prikazchikov. Reduced model for the surface dynamics of a generally anisotropic elastic half-space. *Proceedings of the Royal Society A*, 476(2234):20190590, 2020.

Y.B. Fu and A. Mielke. A new identity for the surface–impedance matrix and its application to the determination of surface-wave speeds. *Proceedings of the Royal Society of London. Series A: Mathematical, Physical and Engineering Sciences*, 458(2026):2523–2543, 2002.

D.C. Gakenheimer and J. Miklowitz. Transient excitation of an elastic half space by a point load traveling on the surface. *Journal of Applied Mechanics*, 36:505–515, 1969.

H.G. Georgiadis and J.R. Barber. Steady-state transonic motion of a line load over an elastic half-space. the corrected cole/huth solution. *ASME Journal of Applied Mechanics*, 60(3):772–774, 1993.

H.G. Georgiadis and G. Lykotrafitis. A method based on the Radon transform for three-dimensional elastodynamic problems of moving loads. *Journal of Elasticity and the Physical Science of Solids*, 65(1-3):87–129, 2001.

E.V. Glushkov, N.V. Glushkova, S.I. Fomenko, and C. Zhang. Surface waves in materials with functionally gradient coatings. *Acoustical Physics*, 58(3):339–353, 2012.

E. Godoy, M. Durán, and J.C. Nédélec. On the existence of surface waves in an elastic half-space with impedance boundary conditions. *Wave Motion*, 49(6):585–594, 2012.

A.L. Goldenveizer. The principles of reducing three-dimensional problems of elasticity to two-dimensional problems of the theory of plates and shells. pages 306–311, 1966.

A.L. Goldenveizer. *Theory of thin elastic shells*, volume 2. Moscow: Nauka, 1976.

A.L. Goldenveizer. Asymptotic method in the theory of shells. *Theoretical and Applied Mechanics*, pages 91–104, 1980.

A.L. Goldenveizer, J.D. Kaplunov, and E.V. Nolde. On Timoshenko-Reissner type theories of plates and shells. *International Journal of Solids and Structures*, 30(5): 675–694, 1993.

R.V. Goldshtein. Rayleigh waves and resonance phenomena in elastic bodies. *Journal of Applied Mathematics and Mechanics*, 29(3):608–619, 1965.

V. Goncharov and L.M. Brekhovskikh. *Mechanics of Continua and Wave Dynamics*. Springer-Verlag, 1985.

K.F. Graff. *Wave motion in elastic solids*. Courier Corporation, 2012.

D. Gusakov and A. Vatul'yan. Dispersion properties of inhomogeneous poroelastic layer. *ZAMM-Journal of Applied Mathematics and Mechanics/Zeitschrift für Angewandte Mathematik und Mechanik*, 98(4):532–541, 2018.

R. Hauert. A review of modified DLC coatings for biological applications. *Diamond and Related Materials*, 12(3-7):583–589, 2003.

G. Hevin, O. Abraham, H.A. Pedersen, and M. Campillo. Characterization of surface cracks with Rayleigh waves: a numerical model. *NDT & E International*, 31(4): 289–297, 1998.

V.V. Kalinchuk and T.I. Belyankova. Dynamics of the surface of inhomogeneous media. *Moscow: Fizmatlit*, 2009.

I.V. Kamotskii and A.P. Kiselev. An energy approach to the proof of the existence of Rayleigh waves in an anisotropic elastic half-space. *Journal of Applied Mathematics and Mechanics*, 73(4):464–470, 2009.

J. Kaplunov and D.A. Prikazchikov. Explicit models for surface, interfacial and edge waves. *Dynamic localization phenomena in elasticity, Acoustics and Electromagnetism*, pages 73–114, 2013.

J. Kaplunov and D.A. Prikazchikov. Asymptotic theory for Rayleigh and Rayleigh-type waves. *Advances in Applied Mechanics*, 50:1–106, 2017.

J. Kaplunov, E. Nolde, and G.A. Rogerson. An asymptotic analysis of initial-value problems for thin elastic plates. *Proceedings of the Royal Society A: Mathematical, Physical and Engineering Sciences*, 462(2073):2541–2561, 2006a.

J. Kaplunov, A. Zakharov, and D. Prikazchikov. Explicit models for elastic and piezoelastic surface waves. *IMA Journal of Applied Mathematics*, 71(5):768–782, 2006b.

J. Kaplunov, E. Nolde, and D.A. Prikazchikov. A revisit to the moving load problem using an asymptotic model for the Rayleigh wave. *Wave Motion*, 47(7):440–451, 2010.

J. Kaplunov, D.A. Prikazchikov, B. Erbaş, and O. Şahin. On a 3D moving load problem for an elastic half space. *Wave Motion*, 50(8):1229–1238, 2013.

J. Kaplunov, L.I. Manevitch, and V.V. Smirnov. Vibrations of an elastic cylindrical shell near the lowest cut-off frequency. *Proceedings of the Royal Society A: Mathematical, Physical and Engineering Sciences*, 472(2189):20150753, 2016a.

J. Kaplunov, D.A. Prikazchikov, and G.A. Rogerson. Edge bending wave on a thin elastic plate resting on a Winkler foundation. *Proceedings of the Royal Society A: Mathematical, Physical and Engineering Sciences*, 472(2190):20160178, 2016b.

J. Kaplunov, D.A. Prikazchikov, and L.A. Prikazchikova. Dispersion of elastic waves in a strongly inhomogeneous three-layered plate. *International Journal of Solids and Structures*, 113:169–179, 2017.

J. Kaplunov, D. Prikazchikov, and L. Sultanova. Justification and refinement of winkler–fuss hypothesis. *Zeitschrift für angewandte Mathematik und Physik*, 69 (3):1–15, 2018.

J. Kaplunov, D. Prikazchikov, and L. Sultanova. Elastic contact of a stiff thin layer and a half-space. *Zeitschrift für angewandte Mathematik und Physik*, 70(1):22, 2019a.

J. Kaplunov, D. Prikazchikov, and L. Sultanova. On higher order effective boundary conditions for a coated elastic half-space. *Problems of Nonlinear Mechanics and Physics of Materials*, 94(1):449–462, 2019b.

J. Kaplunov, D. Prikazchikov, and L. Sultanova. Rayleigh-type waves on a coated elastic half-space with a clamped surface. *Philosophical Transactions of the Royal Society A*, 377(2156):20190111, 2019c.

J. Kaplunov, L. Prikazchikova, and M. Alkinidri. Antiplane shear of an asymmetric sandwich plate. *Continuum Mechanics and Thermodynamics*, pages 1–16, 2021.

J.D. Kaplunov. Long-wave vibrations of a thin walled body with fixed faces. *The Quarterly Journal of Mechanics and Applied Mathematics*, 48(3):311–327, 1995.

J.D. Kaplunov and E.V. Nolde. Long-Wave vibrations of a nearly incompressible isotropic plate with fixed faces. *The Quarterly Journal of Mechanics and Applied Mathematics*, 55(3):345–356, 2002.

J.D. Kaplunov, L.Y. Kossovitch, and E.V. Nolde. *Dynamics of thin walled elastic bodies*. Academic Press, 1998.

J.D. Kaplunov, E.V. Nolde, and G.A. Rogerson. A low-frequency model for dynamic motion in pre-stressed incompressible elastic structures. *Proceedings of the Royal Society of London. Series A: Mathematical, Physical and Engineering Sciences*, 456(2003):2589–2610, 2000.

J.D. Kaplunov, E.V. Nolde, and G.A. Rogerson. An asymptotically consistent model for long-wave high-frequency motion in a pre-stressed elastic plate. *Mathematics and Mechanics of Solids*, 7(6):581–606, 2002a.

J.D. Kaplunov, E.V. Nolde, and G.A. Rogerson. Short wave motion in a pre-stressed incompressible elastic plate. *IMA Journal of Applied Mathematics*, 67(4):383–399, 2002b.

Y.D. Kaplunov and L.Y. Kossovich. Asymptotic model of Rayleigh waves in the far-field zone in an elastic half-plane. *Doklady Physics*, 49(4):234–236, 2004.

L.A. Khajiyeva, D.A. Prikazchikov, and L.A. Prikazchikova. Hyperbolic-elliptic model for surface wave in a pre-stressed incompressible elastic half-space. *Mechanics Research Communications*, 92:49–53, 2018.

A.P. Kiselev. Rayleigh wave with a transverse structure. *Proceedings of the Royal Society of London. Series A: Mathematical, Physical and Engineering Sciences*, 460(2050):3059–3064, 2004.

A.P. Kiselev. General surface waves in layered anisotropic elastic structures. *Zapiski Nauchnykh Seminarov POMI*, 438:133–137, 2015.

A.P. Kiselev and D.E. Parker. Omni-directional Rayleigh, Stoneley and Schölte waves with general time dependence. *Proceedings of the Royal Society A: Mathematical, Physical and Engineering Sciences*, 466(2120):2241–2258, 2010.

S.L. Kramer. *Geotechnical earthquake engineering.* Pearson Education India, 1996.

V.V. Krylov. *Noise and vibration from high-speed trains.* Thomas Telford, 2001.

R. Kulchytsky-Zhyhailo and A.S. Bajkowski. Three-dimensional analytical elasticity solution for loaded functionally graded coated half-space. *Mechanics Research Communications*, 65:43–50, 2015.

E. Lanckau. Mechanics of continuous media. *Journal of Applied Mathematics and Mechanics*, 64(7):268–268, 1984.

M.I. Lashhab, G.A. Rogerson, and L.A. Prikazchikova. Small amplitude waves in a pre-stressed compressible elastic layer with one fixed and one free face. *Zeitschrift für angewandte Mathematik und Physik*, 66(5):2741–2757, 2015.

P.C.Y. Lee and N. Chang. Harmonic waves in elastic sandwich plates. *Journal of Elasticity*, 9(1):51–69, 1979.

M. Li, Q. Liu, Z. Jia, X. Xu, Y. Cheng, Y. Zheng, T. Xi, and S. Wei. Graphene oxide/hydroxyapatite composite coatings fabricated by electrophoretic nanotechnology for biological applications. *Carbon*, 67:185–197, 2014.

J. Lothe and D.M. Barnett. On the existence of surface-wave solutions for anisotropic elastic half-spaces with free surface. *Journal of Applied Physics*, 47(2):428–433, 1976.

P.G. Malischewsky and F. Scherbaum. Love's formula and H/V-ratio (ellipticity) of Rayleigh waves. *Wave Motion*, 40(1):57–67, 2004.

G.I. Mikhasev and H. Altenbach. *Thin-walled laminated structures*. Springer, 2019.

N.F. Morozov, P.E. Tovstik, and T.P. Tovstik. Bending vibrations of multilayered plates. *Doklady Physics*, 65(8):281–285, 2020.

A. Mubaraki, D. Prikazchikov, and A. Kudaibergenov. Explicit model for surface waves on an elastic half-space coated by a thin vertically inhomogeneous layer. *Proceedings of the 9th International Conference Dynamical Systems-Theory and Applications DSTA*, 2019.

S. Nath and P.R. Sengupta. Influence of gravity on propagation of waves in a medium in presence of a compressional source. *Sadhana*, 24(6):495–505, 1999.

A.J. Niklasson, S.K. Datta, and M.L. Dunn. On approximating guided waves in plates with thin anisotropic coatings by means of effective boundary conditions. *The Journal of the Acoustical Society of America*, 108(3):924–933, 2000.

A. Nobili and D.A. Prikazchikov. Explicit formulation for the Rayleigh wave field induced by surface stresses in an orthorhombic half-plane. *European Journal of Mechanics-A/Solids*, 70:86–94, 2018.

E. Nolde. Qualitative analysis of initial-value problems for a thin elastic strip. *IMA Journal of Applied Mathematics*, 72(3):348–375, 2007.

E. Nolde, A.V. Pichugin, and J. Kaplunov. An asymptotic higher-order theory for rectangular beams. *Proceedings of the Royal Society A: Mathematical, Physical and Engineering Sciences*, 474(2214):20180001, 2018.

E.V. Nolde, L.A. Prikazchikova, and G.A. Rogerson. Dispersion of small amplitude waves in a pre-stressed, compressible elastic plate. *Journal of Elasticity*, 75(1): 1–29, 2004.

N.P. Padture, M. Gell, and E.H. Jordan. Thermal barrier coatings for gas-turbine engine applications. *Science*, 296(5566):280–284, 2002.

A. Palermo, S. Krödel, A. Marzani, and C. Daraio. Engineered metabarrier as shield from seismic surface waves. *Scientific Reports*, 6(1):1–10, 2016.

D.F. Parker. The Stroh formalism for elastic surface waves of general profile. *Proceedings of the Royal Society A: Mathematical, Physical and Engineering Sciences*, 469(2160):20130301, 2013.

D.F. Parker and A.P. Kiselev. Rayleigh waves having generalised lateral dependence. *Quarterly Journal of Mechanics and Applied Mathematics*, 62(1):19–30, 2008.

S.P. Patil, A. Rege, M. Itskov, and B. Markert. Mechanics of nanostructured porous silica aerogel resulting from molecular dynamics simulations. *The Journal of Physical Chemistry B*, 121(22):5660–5668, 2017.

L. Pawlowski. *The science and engineering of thermal spray coatings*. John Wiley & Sons, 2008.

R.G. Payton. Transient motion of an elastic half-space due to a moving surface line load. *International Journal of Engineering Science*, 5(1):49–79, 1967.

C.V. Pham and A. Vu. Effective boundary condition method and approximate secular equations of Rayleigh waves in orthotropic half-spaces coated by a thin layer. *Journal of Mechanics of Materials and Structures*, 11(3):259–277, 2016.

A.V. Pichugin. Approximation of the Rayleigh wave speed. *people.brunel.ac.uk/ mastaap/draft06rayleigh.pdf.*, 2008.

A.V. Pichugin and G.A. Rogerson. An asymptotic membrane-like theory for long-wave motion in a pre-stressed elastic plate. *Proceedings of the Royal Society of*

London. Series A: Mathematical, Physical and Engineering Sciences, 458(2022): 1447–1468, 2002.

D.A. Prikazchikov. Rayleigh waves of arbitrary profile in anisotropic media. *Mechanics Research Communications*, 50:83–86, 2013.

D.A. Prikazchikov. Explicit model for surface waves in a pre-stressed, compressible elastic half-space. *International Journal of Mathematics and Physics*, 11(1):13–19, 2020.

D.A. Prikazchikov and G.A. Rogerson. On surface wave propagation in incompressible, transversely isotropic, pre-stressed elastic half-spaces. *International Journal of Engineering Science*, 42(10):967–986, 2004.

L. Prikazchikova, Y. Ece Ayd In, B. Erbaş, and J. Kaplunov. Asymptotic analysis of an anti-plane dynamic problem for a three-layered strongly inhomogeneous laminate. *Mathematics and Mechanics of Solids*, 25(1):3–16, 2020.

D.E. Quadrelli, R. Craster, M. Kadic, and F. Braghin. Elastic wave near-cloaking. *Extreme Mechanics Letters*, 44:101262, 2021.

L. Rayleigh. On waves propagated along the plane surface of an elastic solid. *Proceedings of the London Mathematical Society*, 1(1):4–11, 1885.

J.N. Reddy. *Mechanics of laminated composite plates and shells: theory and analysis*. CRC Press, 2003.

A. Rege, M. Hillgärtner, and M. Itskov. Mechanics of biopolymer aerogels based on microstructures generated from 2-d voronoi tessellations. *The Journal of Supercritical Fluids*, 151:24–29, 2019.

G.A. Rogerson and L.A. Prikazchikova. Generalisations of long wave theories for pre-stressed compressible elastic plates. *International Journal of Non-Linear Mechanics*, 44(5):520–529, 2009.

G.A. Rogerson and K.J. Sandiford. The effect of finite primary deformations on harmonic waves in layered elastic media. *International Journal of Solids and Structures*, 37(14):2059–2087, 2000.

D. Royer and E. Dieulesaint. *Elastic waves in solids II: generation, acousto-optic interaction, applications*. Springer Science & Business Media, 1999.

M.Y. Ryazantseva and F.K. Antonov. Harmonic running waves in sandwich plates. *International Journal of Engineering Science*, 59:184–192, 2012.

O. Şahin. Analysis of the Rayleigh wave field due to a tangential load applied on the surface of a coated elastic half-space. *Communications Faculty of Sciences University of Ankara Series A1 Mathematics and Statistics*, 69(1):158–171, 2020.

O. Şahin and N. Ege. Surface displacement field of a coated elastic half-space under the Influence of a moving distributional load. *Anadolu Üniversitesi Bilim Ve Teknoloji Dergisi-B Teorik Bilimler*, 5(1):77–90, 2017.

J.R. Schulenberger and C.H. Wilcox. The limiting absorption principle and spectral theory for steady-state wave propagation in inhomogeneous anisotropic media. *Archive for Rational Mechanics and Analysis*, 41(1):46–65, 1971.

M. Sethi, K.C. Gupta, R. Sharma, and D. Malik. Propagation of Rayleigh waves in nonhomogeneous elastic half-space of orthotropic material under initial compression and influence of gravity. *Mathematica Aeterna*, 2(10):901–910, 2012.

M.D. Sharma. Propagation of Rayleigh waves at the boundary of an orthotropic elastic solid: Influence of initial stress and gravity. *Journal of Vibration and Control*, 26(21-22):2070–2080, 2020.

A.L. Shuvalov and A.G. Every. On the long-wave onset of dispersion of the surface-wave velocity in coated solids. *Wave Motion*, 45(6):857–863, 2008.

W.S. Slaughter. *The linearized theory of elasticity*. Springer Science & Business Media, 2012.

S.L. Sobolev, P. Frank, and R. von Mises. Some problems in wave propagation. *Differential and Integral Equations of Mathematical Physics*, pages 468–617, 1937.

L. Sun, W. Xie, X. He, and T. Hayashikawa. Prediction and mitigation analysis of ground vibration caused by running high-speed trains on rigid-frame viaducts. *Earthquake Engineering and Engineering Vibration*, 15(1):31–47, 2016.

Z. Sun, C. Kasbergen, A. Skarpas, K. Anupam, K.N. van Dalen, and S.M. Erkens. Dynamic analysis of layered systems under a moving harmonic rectangular load based on the spectral element method. *International Journal of Solids and Structures*, 180:45–61, 2019.

H. Takeuchi and M. Saito. Seismic surface waves. *Methods in computational physics*, 11:217–295, 1972.

V.M. Tiainen. Amorphous carbon as a bio-mechanical coating—mechanical properties and biological applications. *Diamond and Related Materials*, 10(2):153–160, 2001.

H.F. Tiersten. Elastic surface waves guided by thin films. *Journal of Applied Physics*, 40(2):770–789, 1969.

T.C.T. Ting. Surface waves in an exponentially graded, general anisotropic elastic material under the influence of gravity. *Wave Motion*, 48(4):335–344, 2011.

S. Veprek and M.J. Veprek-Heijman. Industrial applications of superhard nanocomposite coatings. *Surface and Coatings Technology*, 202(21):5063–5073, 2008.

P.C. Vinh. Explicit secular equations of Rayleigh waves in elastic media under the influence of gravity and initial stress. *Applied Mathematics and Computation*, 215 (1):395–404, 2009.

P.C. Vinh and V.T.N. Anh. Rayleigh waves in an orthotropic half-space coated by a thin orthotropic layer with sliding contact. *International Journal of Engineering Science*, 75:154–164, 2014.

P.C. Vinh and V.T.N. Anh. An approximate secular equation of Rayleigh waves in an elastic half-space coated by a thin weakly inhomogeneous elastic layer. *Vietnam Journal of Mechanics*, 37(1):71–80, 2015.

P.C. Vinh and N.T.K. Linh. An approximate secular equation of Rayleigh waves propagating in an orthotropic elastic half-space coated by a thin orthotropic elastic layer. *Wave Motion*, 49(7):681–689, 2012.

P.C. Vinh and P.G. Malischewsky. An approach for obtaining approximate formulas for the Rayleigh wave velocity. *Wave Motion*, 44(7-8):549–562, 2007.

P.C. Vinh and R.W. Ogden. On formulas for the Rayleigh wave speed. *Wave Motion*, 39(3):191–197, 2004.

P.C. Vinh and G. Seriani. Explicit secular equations of Rayleigh waves in a non-homogeneous orthotropic elastic medium under the influence of gravity. *Wave Motion*, 46(7):427–434, 2009.

P.C. Vinh, V.T.N. Anh, and V.P. Thanh. Rayleigh waves in an isotropic elastic half-space coated by a thin isotropic elastic layer with smooth contact. *Wave Motion*, 51(3):496–504, 2014.

P.C. Vinh, T.T. Tuan, L.T. Hue, V.T.N. Anh, T.T.T. Dung, N.T.K. Linh, and P. Malischewsky. Exact formula for the horizontal-to-vertical displacement ratio of Rayleigh waves in layered orthotropic half-spaces. *The Journal of the Acoustical Society of America*, 146(2):1279–1289, 2019.

L.A. Wang, J. Zhao, and G. Wang. Dynamic response analysis of inhomogeneous saturated soil under moving loads. *Soil Mechanics and Foundation Engineering*, 57(3):211–218, 2020.

P.T. Wootton. *Control and suppression of elastic waves using periodic metasurfaces and bridges*. PhD thesis, Keele University, 2020.

P.T. Wootton, J. Kaplunov, and D.J. Colquitt. An asymptotic hyperbolic–elliptic model for flexural-seismic metasurfaces. *Proceedings of the Royal Society A*, 475 (2227):20190079, 2019.

P.T. Wootton, J. Kaplunov, and D. Prikazchikov. A second-order asymptotic model for Rayleigh waves on a linearly elastic half plane. *IMA Journal of Applied Mathematics*, 85(1):113–131, 2020.

L. You, K. Yan, T. Shi, J. Man, and N. Liu. Analytical solution for the effect of anisotropic layers/interlayers on an elastic multi-layered medium subjected to moving load. *International Journal of Solids and Structures*, 172:10–20, 2019.

L. You, K. Yan, J. Man, and T. Shi. 3d spectral element solution of multilayered half-space medium with harmonic moving load: Effect of layer, interlayer, and loading properties on dynamic response of medium. *International Journal of Geomechanics*, 20(12):04020227, 2020.

D.D. Zakharov. High order approximate low frequency theory of elastic anisotropic lining and coating. *The Journal of the Acoustical Society of America*, 119(4):1961–1970, 2006.

D.D. Zakharov. Effective high-order approximations of layered coatings and linings of anisotropic elastic, viscoelastic and nematic materials. *Journal of Applied Mathematics and Mechanics*, 74(3):286–296, 2010.

D.D. Zakharov. Surface and edge waves in solids with nematic coating. *Mathematics and Mechanics of Solids*, 17(1):67–80, 2012.

Q. Zhang and H. Liu. On the dynamic response of porous functionally graded microbeam under moving load. *International Journal of Engineering Science*, 153: 103317, 2020.

B. Zhen, J. Xu, and J. Sun. Analytical solutions for steady state responses of an infinite euler-bernoulli beam on a nonlinear viscoelastic foundation subjected to a harmonic moving load. *Journal of Sound and Vibration*, 476:115271, 2020.

B.A. Zhenning, J. Liang, V.W Lee, and H. Ji. 3d dynamic response of a multi-layered transversely isotropic half-space subjected to a moving point load along a horizontal straight line with constant speed. *International Journal of Solids and Structures*, 100:427–445, 2016.

W. Zhou, W. Chen, X. Shen, Y. Su, and E. Pan. On surface waves in a finitely deformed coated half-space. *International Journal of Solids and Structures*, 128: 50–66, 2017.